Characterization of CDK5RAP2 as a novel regulator in the Hippo signaling pathway

Inaugural-Dissertation

zur

Erlangung des Doktorgrades

der Mathematisch-Naturwissenschaftlichen Fakultät

der Universität zu Köln

vorgelegt von

Salil Kalarikkal Sukumaran

aus Kerala, India

Köln, 2014

Vorsitzender: Prof. Dr. H. Arndt

1. Berichterstatter: Prof. Dr. A. A. Noegel

2. Berichterstatter: Prof. Dr. P. Nürnberg

Tag der mündlichen Prüfung: 17 October 2014

This research work was carried out from October 2011 to August 2014 at the Centre for Biochemistry, Institute of Biochemistry I, Medical Faculty, University of Cologne, Cologne, Germany, under the supervision of Prof. Dr. Angelika A. Noegel.

Die vorliegende Arbeit wurde in der Zeit von October 2011 bis August 2014 unter der Anleitung von Prof. Dr. Angelika A. Noegel im Institut für Biochemie I der Medizinischen Fakultät der Universität zu Köln angefertigt.

Acknowledgements

I would first like to express my deepest gratitude and appreciation to Prof. Dr. Angelika Noegel for the opportunity given to me to carry out this research work in the Institute of Biochemistry I. Without her guidance, endless advices and persistent help, this study would not have been possible. I have been amazingly fortunate to have an advisor who gave me freedom to explore on my own and at the same time the guidance to recover when my steps faltered.

Mrs. Rosemarie Blau-Wasser's insightful comments and constructive criticisms at different stages of my research were thought provoking and they helped me focus my ideas. I am grateful to her for incorporating me into the *D. discoideum* field of studies and holding me to high research standards.

I also extend my heartfelt thanks to Prof. Dr. Michael Schleicher (LMU München) and Prof. Dr. Bernhard Schermer (CECAD, Köln) for their timely support in the provision of reagents during this study. Their presence was inevitable.

I also take the opportunity to thank Dr.Doris Birker and Prof. Carrien Niessen for the moral support, encouragement and kind considerations provided towards my PhD career. I would thankfully remember CECAD, Köln and UniKlinik, Köln for the funding and financial assistance during my PhD studies.

It is such a great honor to be part of an academic research organization, where the members are amenable. Thanking you for providing a very warm environment. To be specific, my appreciation also goes to all members of Lab. 14 and of the Institute of Biochemistry I which includes Napoleon (alias Napo), Maria Marco, Sarah, Sonja, Vivek, Ping Li, Atul and Ilknur. I cannot forget Mr. Berthold Gassen for all the great antibodies he provided during the course of this study. Mrs. Maria Stumpf is not left out for their technical support with the southern and phosphorylation experiments. Members of the other laboratories in the Biochemistry Institute are too numerous to mention who were in one way or the other of assistance to me during the research are also appreciated.

Most importantly, none of this would have been possible without the love and patience of my family. My immediate family, to whom this work is dedicated to, has been a constant source of love, support, concern and strength all these years. I want to thank members of my family especially my parents, my grandmother and my elder sister and her husband, who engineered

Table of contents

Abbreviations

cAMP	cyclic-Adenosinemonophosphate
Dd	*Dictyostelium discoideum*
DNA	Deoxyribonucleic acid
EDTA	Ethylenediaminetetraacetic acid
GST	Glutathion-S-Transferase
IPTG	Isopropyl-thio-galactoside
kDa	Kilo Dalton
min	Minute
mM	Millimolar
M	Molar
NIH	National Institutes for Health
PAGE	Polyacrylamide Gel electrophoresis
PCR	Polymerase chain reaction
PMSF	Phenylmethylsulfonyl fluoride
Q-RTPCR	Quantitative real time PCR
SDS	Sodium dodecyl sulphate
TAE	Tris-Acetate-EDTA-Buffer
Tris	Tris(hydroxymethyl)aminomethane

TRITC   Tetramethylrhodamine isothiocyanate

v/v   volume per volume

X-Gal   5-bromo-4-chloro-3-indolyl-β-D-Galactopyranoside

1. Introduction

The centrosome is the main microtubule organizing center (MTOC) and plays an important role in mitotic spindle orientation and genome stability (Bornens, 2012). It nucleates, anchors, and organizes microtubules. In animal cells it comprises a pair of centrioles and a surrounding pericentriolar matrix (PCM) (Fig. 1). The PCM is a key structure of the centrosome and is responsible for microtubule nucleation and anchoring. The major components of the PMC are large coiled coil proteins like pericentrin and proteins of the AKAP450 family that provide docking sites for γ-tubulin ring complexes and regulatory molecules. They allow the centrosome to function as MTOC and to carry out its regulatory functions during cell cycle transitions, cellular responses to stress, and organization of signal transduction pathways (Keryer et al., 2003; Doxsey et al., 2005).

Figure 1. An artistic view of the MTOC with its star pattern of microtubules radiating from the cylindrical centrioles to all parts of the cell. Source: Studiodaily, New York.

1.1 Centrosome and centriole biology

The centrosome was considered as the organ coordinating karyokinesis and cytokinesis. The absence of the centrosome in an unfertilized egg was seen as an efficient way to avoid parthenogenetic development (Bornens, 2012). The centrosome morphology varies largely in protozoa, algae, and fungi. In *Dictyostelium discoideum* it is a nucleus associated body consisting of a box-shaped core surrounded by the corona, an amorphous matrix functionally equivalent to the PCM (Ueda et al., 1999). The centrosome of animal cells is a cytoplasmic organelle formed around a core structure made of two microtubule-based cylinders of defined length and diameter, the centrioles, with a highly conserved nine fold radial symmetry (Bobinnec et al., 1998). The centriole pair comprises of a mature mother centriole and a young daughter centriole. It displays structural and functional asymmetry due to the generational difference between each member of the pair: The old, fully mature mother centriole is distinguished by two sets of nine appendages at its distal end whereas the young, immature, daughter centriole, assembled during the previous cell cycle, is about 80% the length of the mother centriole (Piel et al., 2000). Both centrioles are connected together by a linker comprising of various centrosomal proteins, the major ones being C-Nap1 and Rootletin. More recently, CDK5RAP2 was identified as a putative linker component which surrounds the centrioles (Graser et al., 2007).

Studies on early *C. elegans* embryos with genetic and RNA interference based approaches gave major insight into molecular mechanisms of centriole biogenesis (Leidel et al., 2005; Leidel and Gönczy, 2003; O'Connell et al., 2001). These studies revealed an ordered assembly pathway that involves the products of just five essential genes, termed *zyg-1* (Zygote defective-1), *spd-2* (Spindle defective-2), and three Spindle assembly genes *sas-4*, *sas-5*, and *sas-6* (Delattre et al., 2006; Pelletier et al., 2006). SAS-4, SAS-5, SAS-6, and SPD-2 are coiled-coil proteins, whereas ZYG-1 is a protein kinase. Shortly after fertilization of the

egg, SPD-2 is recruited to the paternal centrioles, which then allows the centriolar recruitment of ZYG-1. Next, a complex comprising SAS-5 and SAS-6 is recruited, which leads to the formation of a "central tube" that is closely associated with the original centriole. The central tube encompasses the highly conserved nine fold radial symmetry of the centriole/basal body (Kitagawa et al., 2011). In most species, the centriole is organized around a cartwheel that comprises a central hub of 25 nm in diameter from which nine spokes radiate outward and connect to nine microtubule blades (Strnad and Gönczy, 2008). The major molecular architect of the central hub of the cartwheel is found to be SAS-6, the oligomerisation properties of which help in self-assembling to form 9 radiating spokes (Kitagawa et al., 2011). Finally, SAS-4 facilitates the assembly of microtubules onto the periphery of this tube, resulting in the formation of a procentriole (Pelletier et al., 2006) (Fig. 2).
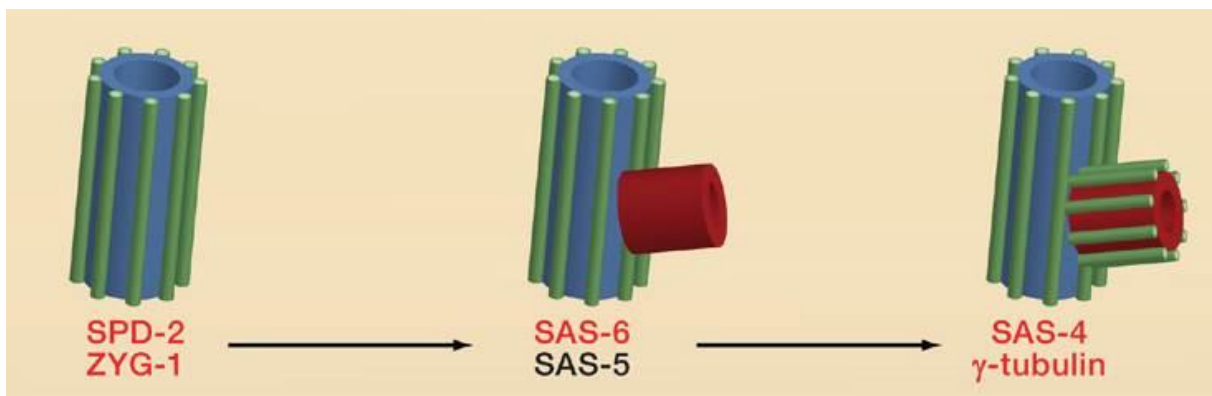
Figure 2. Centriole duplication in *C. elegans* embryos. SPD-2 recruits the protein kinase ZYG-1 to mother centrioles, which then recruits a complex of SAS-6 and SAS-5. This promotes the formation of a central tube (red) at right angles to the mother centriole. SAS-6 and SAS-5 then recruit SAS-4, which allows the centriolar microtubules (green) to associate with the central tube, thus forming the procentriole. The protein γ-tubulin is also required to convert the structure in to a procentriole. The proteins highlighted in red all have functional orthologs implicated in centriole duplication in other species (adapted from (Nigg and Raff, 2009).

Importantly, the significance of these findings is not limited to *C. elegans*. Although an ortholog of SAS-5 awaits definitive identification, SPD-2, SAS-4, and SAS-6 clearly have

orthologs in human cells termed Cep192 (Andersen et al., 2003), CPAP/HsSAS-4 (Hung et al., 2000), and HsSAS-6 (Leidel et al., 2005), respectively. Curiously, ZYG-1 does not have obvious structural orthologs outside of nematodes, but the available evidence suggests that PLK4 plays a functionally analogous role in human cells (Bettencourt-Dias et al., 2011; Habedanck et al., 2005).

In the last decade, the molecular composition of the isolated centrosome in the human and fly has revealed a number of proteins conserved across eukaryotes (Azimzadeh and Marshall, 2010; Carvalho-Santos et al., 2011). For the protein inventory of the *Dicytostelium* centrosome more than 70 new candidates have been identified (Reinders et al., 2006). In higher vertebrates, sequence database searches resulted in the identification of more than 2,000 peptides representing more than 500 proteins in the peak centrosome fraction (Andersen et al., 2003). Functional genomics in nematodes and flies has identified a small set of conserved proteins required for the initiation of centriole/basal body assembly and for centrosome reproduction.

1.2 Autosomal recessive primary microcephaly

The cellular regulation by centrosomes has been well studied. Increasing evidence indicates that this structure may be well designed for the organization of multiprotein scaffolds that can anchor a diversity of activities ranging from protein complexes involved in microtubule nucleation to multicomponent pathways in cellular regulation (Doxsey et al., 2005). The centrosome is an indispensable component of the cell-cycle machinery of eukaryotic cells, and perturbation of core centrosomal or centrosome-associated proteins is linked to cell-cycle misregulation and cancer (Badano et al., 2005). The structural complexity of the centrosome is reflected in its biochemical composition with a large number of proteins localized either in the centrioles or in the centrosomal matrix among which several are disease gene products

(Nigg and Raff, 2009; Kobayashi and Dynlacht, 2011). Aberrations in several centrosomal proteins are also reported in primary microcephaly (Table 1).

Locus name	Protein name	Localization
MCPH1	Microcephalin	Centrosome
MCPH2	WDR62	Centrosome
MCPH3	CDK5RAP2/Cep215	Centrosome
MCPH4	CASC5	Kinetochore
MCPH5	ASPM	Centrosome
MCPH6	CPAP/CENPJ	Centrosome
MCPH7	STIL	Centrosome
MCPH8	CEP135	Centrosome
MCPH9	CEP152	Centrosome
MCPH10	ZNF335	Nucleus
MCPH11	PHC1	Nucleus
MCPH12	CDK6	Centrosome
SCKL6	CEP63	Centrosome

Table 1. Genes implicated in MCPH (adapted from Nigg et al., 2014).

Autosomal recessive primary microcephaly, often shortened to MCPH which stands for "microcephaly primary hereditary", is a condition in which infants are born with a very small head and a small brain (Fig. 3). The term "microcephaly" comes from the Greek word for "small head". The MCPH-associated genes described to date have been implicated in cell division and cell cycle regulation and many of them have been localized to the centrosome (Kaindl, 2014).
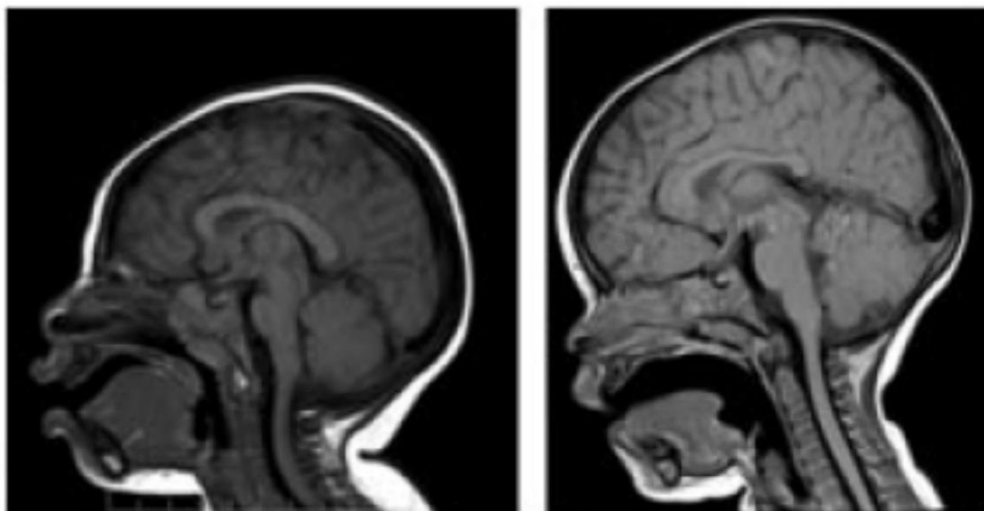
Figure 3. MRI images of a patient at 15 months (on the left) compared to a normal age and gender matched child (on the right) demonstrating cranio-facial disproportion characteristic of microcephaly (adapted from Pagnamenta et al., 2012).

MCPH is a rare neurodevelopmental disorder that results in severe microcephaly at birth with pronounced reduction in brain volume, particularly of the neocortex, simplified cortical gyration and intellectual disability (Issa et al., 2013b). Mutations in MCPH genes reduce the population of neurons in each of the six layers of the cerebral cortex during development, but there is little or no overt structural abnormalities other than reduced thickness of the cerebral cortex (Megraw et al., 2011). Patients with mutations in MCPH loci show moderate to severe microcephaly. Some of the notable phenotypes of microcephaly patients are decrease in size of head and brain volume (Bond et al., 2003, 2005), sensorineural hearing loss (Pagnamenta et al., 2012), short stature, seizures (Darvish et al., 2010) and mental retardation (Neitzel et al., 2002), but no motor deficit.

Mutations in the ASPM (Abnormal spindle-like microcephaly associated) gene is the most frequent cause of MCPH. Analysis of mouse and zebrafish mutants for *Aspm* demonstrates that Aspm is crucial for maintaining a cleavage plane orientation that allows symmetric, proliferative divisions of neuro-epithelial cells during brain development. Failure to do so leads to microcephaly disease condition (Pulvers et al., 2010; Fish et al., 2006; Novorol et al., 2013). Cdk5rap2[an/an] mutant mice (Hertwig's anemia mouse, in which an inversion of the exon 4 of Cdk5rap2 gene leading to the deletion of a large part of the gamma-tubulin ring complex binding domain) showed a dramatic reduction in brain size and thin superficial cerebral cortex layers and rarely survived beyond 1 week of age. The Cdk5rap2 mutants exhibited a significant decrease in the ratio of brain to body weight as compared with controls (Lizarraga et al., 2010). It has been reported that CDK5RAP2 shares homology at the amino terminus with several eukaryotic proteins, including *Schizosaccharomyces pombe* Mto1p (also known as Mbo1p and Mod20p) and Pcp1p, and *Drosophila melanogaster* centrosomin (Cnn), which

have been shown to function in the recruitment of γ-tubulin to MTOCs through interacting with γTuRCs (Fong et al., 2008). Mutation in the CDK5RAP2 homolog in *Drosophila*, Cnn, led to abnormalities in asymmetric division in the larval brain (Wakefield et al., 2001). Recently, cerebral organoid cultures with a mutation in Cdk5rap2 led to the observation of smaller embryoid bodies, which when subjected to neural induction failed to develop further (Lancaster et al., 2013). The centrosomal localization of the MCPH-associated proteins, particularly during the cell cycle, underlines the role of the centrosome in the etiology of this disease (Megraw et al., 2011).

1.3 Cyclin Dependent Kinase 5 regulatory subunit-associated protein 2 (CDK5RAP2)

The human *CDK5RAP2* gene is located on chromosome 9, has 38 exons spanning a region of 191 kb, and the deduced open reading frame encompasses 6130 bp encoding 1893 amino acids. So far four isoforms produced by alternative splicing have been reported: Isoform 1, the full-length form (UniProt ID: Q96SN8-1); Isoform 2, missing residues 702–733 at exon 19 (UniProt ID: Q96SN8-2); Isoform 3, missing residues 1009–1049 at exon 23 (UniProt ID: Q96SN8-3); Isoform 4, missing residues 1576–1654 at exon 32 (UniProt ID: Q96SN8-4) (Kraemer et al., 2011). To date, four different mutations have been identified in CDK5RAP2: a nonsense mutation in exon 4 (c.246T > A, p.Y82X), an A to G transition in intron 26 (c.4005-15A > G, p. R1334SfsX5) introducing a new splice acceptor site, a frame shift and a premature stop codon, a nonsense mutation in exon 8 (c.700G > T, p.E234X) and a nonsense mutation, c.4441C > T (p.Arg1481) introducing a premature stop codon (Bond et al., 2005; Hassan et al., 2007; Pagnamenta et al., 2012b; Issa et al., 2013b).
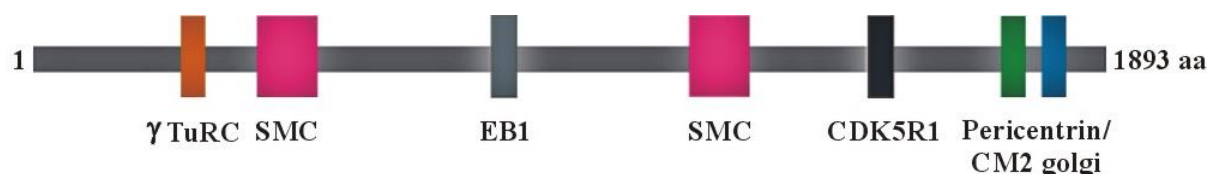
Figure 3. Schematic representation of the domain structure of CDK5RAP2. γTuRC: Gamma-Tubulin ring complex, SMC: Structural maintenance of chromosomes, EB1: End binding 1, CDK5R1: Cyclin dependent kinase 5 activator 1, CM2: Cnn Motif 2 (picture modified from Issa et al. 2013b).

The human CDK5RAP2 protein (NP_060719.4) contains a predicted N-terminal interaction site for the gamma tubulin ring complex (γTuRC) (Fong et al., 2008), two structural maintenance of chromosome (SMC) domains, a Ser-rich motif for interaction with plus-end tubulin binding protein EB1 (Fong et al., 2009), an interaction site for Cyclin dependent kinase 5 activator 1 (CDK5R1) (Wang et al., 2000) and Pericentrin (Buchman et al., 2010), and a CM2 (Cnn Motif 2) domain which is responsible for sequestering it to the centrosome and the Golgi apparatus which has a pericentrosomal location. The CM2-like sequence of CDK5RAP2 exhibits Ca^{2+}-independent calmodulin binding activity (Wang et al., 2010).

1.3.1 Physiological functions of CDK5RAP2

CDK5RAP2 is a pericentriolar structural component that functions in γTuRC attachment and therefore in the microtubule organizing function of the centrosome (Fong et al., 2008). The EB1 domain of CDK5RAP2 interacts with the growing microtubule tips and hence regulates microtubule dynamics (Fong et al., 2009). Furthermore, CDK5RAP2 also regulates mitotic spindle positioning, asymmetric centrosome inheritance, DNA damage signaling (Barr et al., 2010) and also has spindle checkpoint function (Zhang et al., 2009b). In addition, CDK5RAP2 is reported to restrict centriole replication by maintaining centriole engagement and cohesion (Barrera et al., 2010). Besides, CDK5RAP2 regulates chromosome segregation in neuronal progenitors (Lizarraga et al., 2010). In conjunction with further in vitro studies, CDK5RAP2 function specifically contributes to centrosome asymmetry (Conduit and Raff,

19

2010), centriole replication control and primary cilium formation (Barrera et al., 2010), kinetochore attachment to spindles and checkpoint control (Zhang et al., 2009b), binding to the dynactin complex (Lee and Rhee, 2010), cell-cycle regulation and cell-cycle exit (Buchman et al., 2010), microtubule plus-end dynamics (Fong et al., 2009), mitotic spindle formation, function and orientation (Lizarraga et al., 2010).

From the human phenotype and animal models, it has become clear that CDK5RAP2 has an influence on brain size regulation during fetal development (Issa et al., 2013a). Nonsense and splice mutations in *CDK5RAP2* result in truncated, non-functional proteins in microcephaly patients (Issa et al., 2013b). Some of the notable patient phenotypes resulting from CDK5RAP2 mutations are sensorineural hearing loss, intellectual disability and a reduced occipital frontal head circumference (Pagnamenta et al., 2012; Issa et al., 2013; Tan et al., 2014). Whether mutations in CDK5RAP2 and the decrease in neuronal cell density are associated with altered signal transduction pathways is not known.

1.4 Hippo signaling pathway

The Hippo signaling pathway is a tumor-suppressive pathway and is inactive at low cell density (Mori et al., 2014). It primarily affects the number of cells produced and has only minor effects on tissue patterning (Harvey et al., 2003) and is known as a key regulator of organ growth and tissue size in *Drosophila* and mouse (Udan et al., 2003; Lee et al., 2010; Lu et al., 2010; Halder and Johnson, 2011). At the center of the Hippo pathway is a core kinase cassette that consists of a pair of related serine/threonine kinases, mammalian STE20-like protein kinase 1 (MST1 and MST2) which are homologues of *D. melanogaster* Hippo (HPO), and large tumour suppressor 1 (LATS1) and LATS2 together with the adaptor proteins Salvador homologue 1 (SAV1) and MOB kinase activator 1A (MOB1A) and MOB1B (Harvey et al., 2003; Udan et al., 2003; Pantalacci et al., 2003; Tapon et al., 2002; Justice et al., 1995; Kango-Singh, 2002). These proteins limit tissue growth by facilitating LATS1- and

LATS2-dependent phosphorylation of the homologous oncoproteins Yes-associated protein (YAP) and Transcriptional co-activator with PDZ-binding motif (TAZ) (Huang et al., 2005) (Fig. 4).
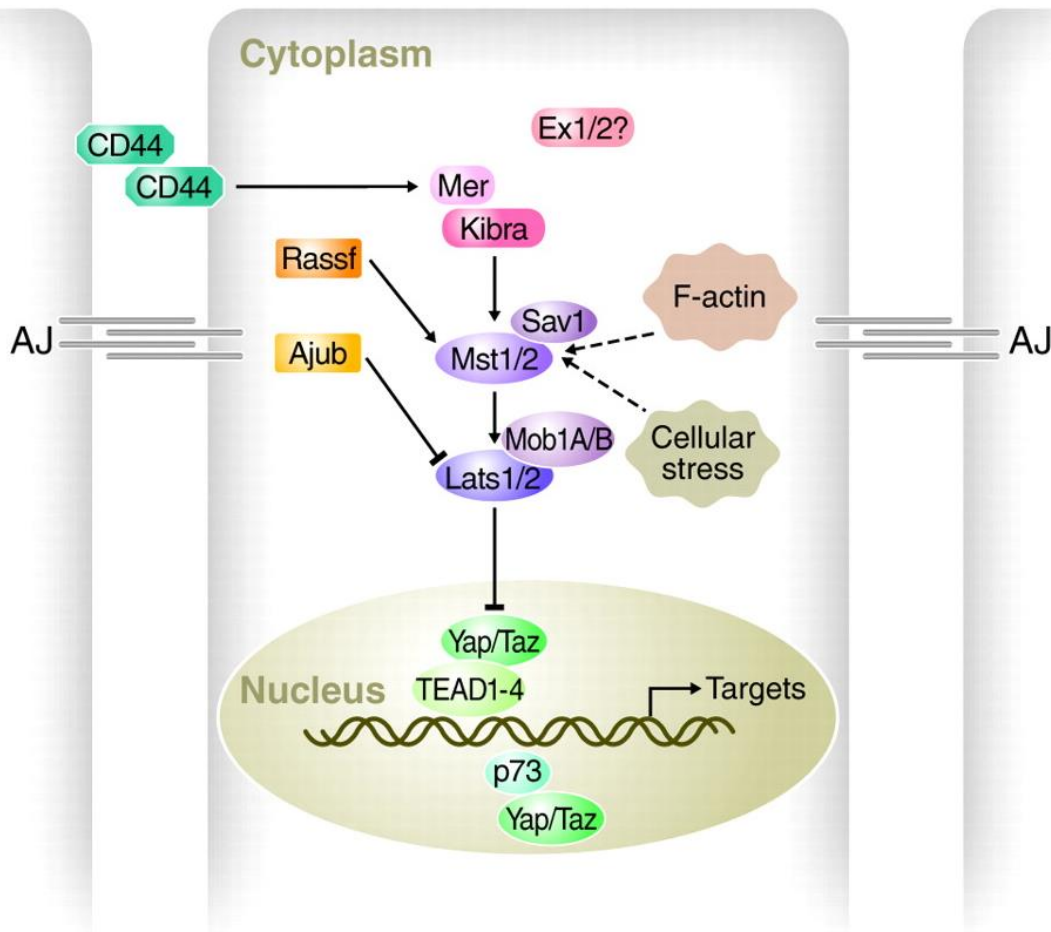
Figure 4. Schematic of the Hippo pathway in mammals. Cells (outlined in grey, nuclei in green) are shown with adherens junctions (AJ). Hippo pathway components in vertebrates are shown in various colors, with pointed and blunt arrowheads indicating activating and inhibitory interactions, respectively. Continuous lines indicate direct interactions, whereas dashed lines indicate unknown mechanisms (adapted from Halder and Johnson, 2011).

Phosphorylation of YAP and TAZ represses their activity by creating binding sites for the protein 14-3-3. The name 14-3-3 was initially coined by Moore and Perez in 1967 with regard to the particular elution and migration pattern of these proteins on DEAE-cellulose chromatography and starch-gel electrophoresis. The 14-3-3 proteins eluted in the 14th fraction of bovine brain homogenate and were found on positions 3.3 of subsequent electrophoresis

(Moore and Perez., 1967). The interaction of YAP/TAZ with 14-3-3 causes them to accumulate in the cytoplasm and that also stimulates their ubiquitin-mediated proteolysis (Zhao et al., 2007; Dong et al., 2007). YAP and TAZ and their *D. melanogaster* counterpart Yorkie (YKI) do not contain intrinsic DNA-binding domains but instead bind to the promoters of target genes through interaction with transcription factors. They promote tissue growth and cell viability by regulating the activity of different families of transcription factors, including Transcriptional enhancer factor domain (TEAD) and Similar to mothers against decapentaplegic (SMAD) family members (Hong et al., 2005). TEADs seem to be key mediators of growth and the tumorigenic potential of YAP, TAZ and YKI, but the genetic program that these factors regulate to drive tissue growth is not well defined (Hong et al., 2005).

The Hippo pathway is conserved throughout evolution and key kinase components have also been detected in *D. discoideum* (Rohlfs et al., 2007; Artemenko et al., 2012). In *Drosophila*, loss - of - function mutant clones for any of the genes *Warts*, *Salvador*, *Hippo* and *Mats* lead to a strong tissue overgrowth phenotype characterized by increased proliferation and diminished cell death.

1.4.1 Hippo signaling in mammalian organ size determination

In mammals, the first studies that connected Hippo signaling to organ size control employed a Yap overexpression strategy that mimicked pathway inactivation and showed that the induction of Yap expression in the adult mouse liver led to a dramatic three- to fourfold increase in liver mass as a result of increased cell numbers (Dong et al., 2007). Remarkably, when Yap overexpression was terminated, the liver rapidly reverted to its normal size, suggesting that intrinsic size control mechanisms were then activated, presumably to reduce cell numbers through an apoptotic process (Dong et al., 2007). These studies infer that Hippo signaling is crucial for regulating the size of the mammalian liver, and that it acts through a

mechanism that integrates global organ size control signals with the regulation of Yap. However, although the effect of Yap overexpression on liver size is dramatic, whether Hippo signaling is required to maintain liver size was not addressed by these studies. These findings show that Hippo signaling functions in regulating the size of the liver, despite this it appears that Hippo signaling, at least the one mediated by the Mst1 and Mst2 kinases, does not regulate the size or growth of other mammalian tissues to the same degree (Song et al., 2010).

1.4.2 Hippo signaling at the centrosome

The regulation of centrosomal biology by the Hippo components is presently a topic of intense research. The components of Hippo signaling pathway regulate the association of Nima-related Kinase 2 (NEK2) with the centrosome (Mardin et al., 2010). Nek2 is the direct substrate for phosphorylating the centrosomal linker proteins C-Nap1 (centrosomal Nek2-associated protein 1) and Rootletin which causes their dissociation from centrosomes and enables centrosome separation (Fry et al., 1998; Mayor et al., 2002; Bahe et al., 2005). It has also been demonstrated that Mst2 phosphorylates Nek2A, thereby recruiting Nek2A to centrosomes and promoting phosphorylation and displacement of centrosomal linker proteins. Additionally, it was shown that the hSav1–Mst1/Mst2–Nek2A pathway cooperates with forces provided by the kinesin motor Eg5 to allow centrosome separation and bipolar spindle formation (Mardin et al., 2010). Strikingly, certain Hippo pathway components, including the Lats and Mst1/Mst2 kinases and the scaffolding protein hSav1, localize to centrosomes (Guo et al., 2007). In addition, Mst1 was reported to control centrosome duplication (Hergovich et al., 2009). Another important member of the hippo pathway, hMOB1, also plays a role in centrosome duplication (Hergovich et al., 2009) and localises to the centrosomes (Wilmeth et al., 2010). LATS2 was also observed at the centrosome throughout cell cycle and was associated with Ajuba during mitosis which regulates spindle organization through recruitment of γ-tubulin to centrosomes (Abe et al., 2006).

1.5 *Dictyostelium discoideum* as a model organism

D. discoideum amoebae belong to the monophyletic group of mycetozoans that stands close to animals and fungi. *Dictyostelium* is a simple eukaryote that lives in the soil and feeds on bacteria by phagocytosis. The life cycle of *Dictyostelium* consists of growth and developmental phases. The individual cells divide by binary fission as long as food is present, however, when bacteria are exhausted, starvation triggers a process of chemotaxis driven by cyclic-AMP (cAMP) (Willard and Devreotes, 2006; Janetopoulos and Firtel, 2008). The cAMP signaling stimulates the single cell amoebae to aggregate to form multicellular structures leading to the development of fruiting body consisting of a stalk and a spore head filled with spores, and the release of the spores (Fig. 5).
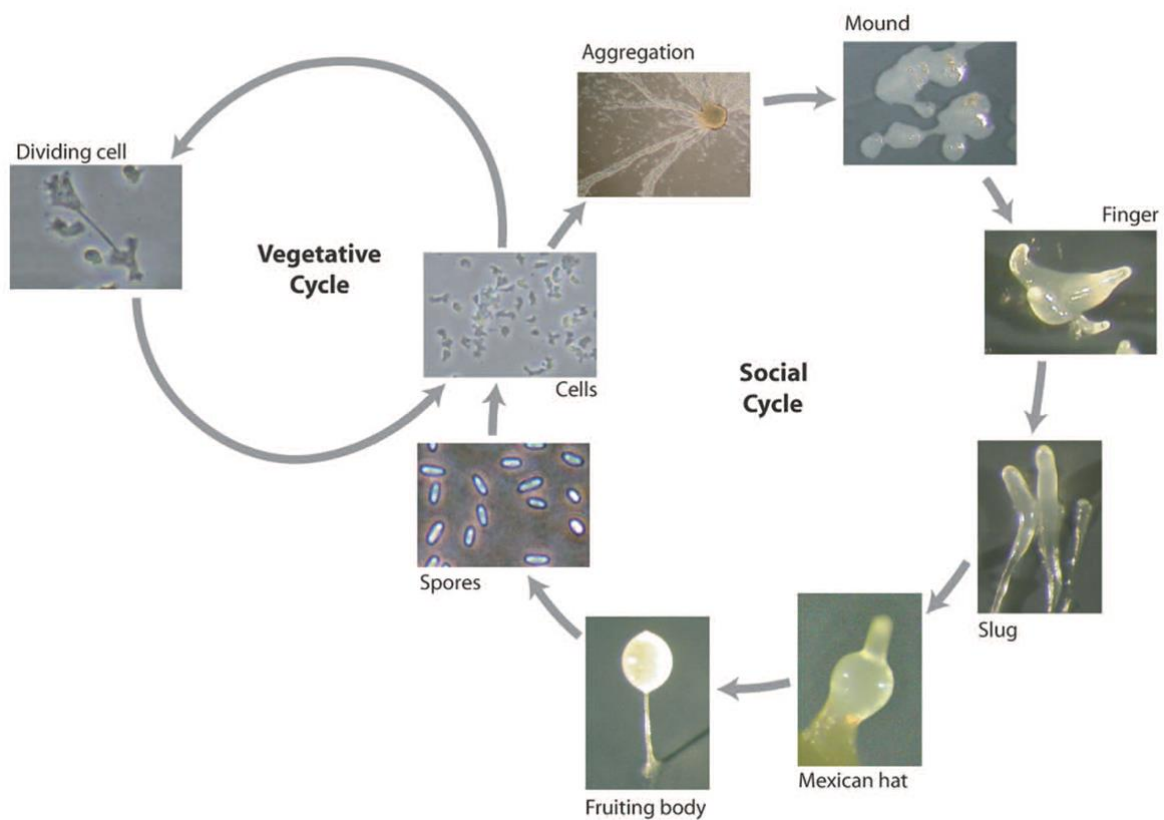
Figure 5. *D. discoideum* life cycle. Representative pictures of vegetative and developmental stages are shown (picture adapted from Calvo-Garrido et al., 2010).

In the wild, *Dictyostelium* amoeba feed on soil bacteria by phagocytosis but most laboratory strains are also able to grow in liquid axenic media by macropinocytosis. It is important to point out that cells are haploid throughout these vegetative and developmental cycles and this facilitates the generation of knockout strains (Calvo-Garrido et al., 2010). Despite its simplicity, *Dictyostelium* shows striking similarities with higher eukaryotes in many biological aspects including chemotaxis (Van Haastert and Veltman, 2007), developmental signaling pathways (Strmecki et al., 2005), the response to bacterial infections (Steinert and Heuner, 2005), the response to therapeutic drugs (Alexander et al., 2006) and programmed cell death including autophagic cell death (Giusti et al., 2009). *Dictyostelium* is an alternative model organism for centrosome research in addition to yeast and animal cells. With the elucidation of morphological changes and dynamics of centrosome duplication, the establishment of a centrosome isolation protocol, and the identification of many centrosomal components, there is a solid basis for understanding the biogenesis and function of this organelle (Gräf et al., 2004).

The *Dictyostelium* genome has been fully sequenced (Eichinger et al., 2005) and well-annotated data are publicly available (http://dictybase.org/). Moreover, it is amenable to a wide range of molecular genetic techniques including the generation of mutants by homologous recombination and random genetic screens, that have facilitated the comparative genomics to identify relevant genes conserved in the human genome (Torija et al., 2006). Thus, NIH has cited *Dictyostelium discoideum* as a non-mammalian model organism for biomedical research (http://www.nih.gov/science/models/).

1.6 Aim of this study.

The aim of this study is to characterise the *D.discoideum* CEP161 protein which we initially identified as a binding partner of CP250, a novel centrosomal protein with important roles in growth and development (Blau-Wasser et al., 2009). CEP161 was characterised based on following features:

1. Homology to proteins from other species

2. Subcellular localization.

3. Analysis of CEP161 in various physiological functions of the cell ranging from size, nuclear number, centrosome-nuclear distance and ratio, growth, development, motility to multicellular migration.

4. Its ability to interact with Dd Hippo related kinase-severin kinase.

The final part of the study was focused on the interaction of human CDK5RAP2 with MST1 and TAZ and hence to characterize the role of CDK5RAP2 in the Hippo signaling pathway.

2. Results

2.1 Identification and characterization of the pericentriolar matrix protein CEP161, the *D. discoideum* ortholog of CDK5RAP2

2.1.1 Identification of CEP161 as an interacting partner of CP250

We identified CEP161 as interaction partner of the centrosomal protein CP250 in immunoprecipitation experiments using GFP-CP250, a component of the pericentriolar matrix, followed by mass spectrometry analysis (Blau-Wasser et al., 2009). We then expressed different parts of CEP161 as GST fusion proteins to identify its binding site for CP250 and found that we could pull down GFP-CP250 from whole cell lysates with amino terminal sequences 1-763 (data not shown). A direct interaction of the proteins was shown by yeast-two-hybrid experiments in which the N-terminal sequences of CEP161 (residues 1-763) interacted with residues 1-1148 of CP250 (Fig. 6).

pAS CP250 1-1148	+	+	+
pACT CEP161 1-763	+	-	-
pACT CEP161 763-1114	-	+	-
pACT	-	-	+
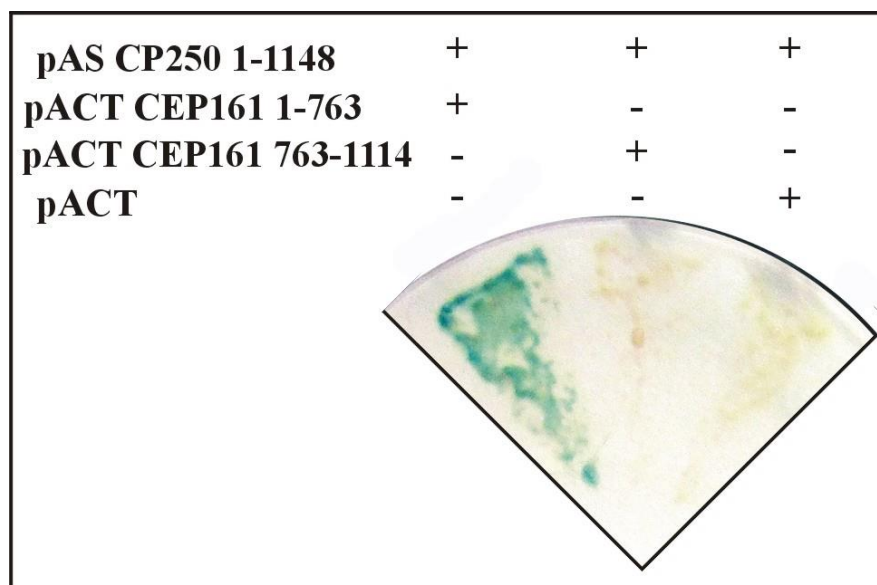
Figure 6. N-terminal part of CEP161 interacts with CP250. Yeast-2-hybrid analysis showing the direct interaction of pAS-CP250 (residues 1-1148) with pACT-CEP161 (residues 1-763), whereas pACT-CEP161 (residues 763-1114) did not show any interaction. The Y2H analysis for pAS-CP250 (residues 1-1148) with empty vector pACT was used as a negative control.

2.1.2 CEP161 domain and sequence alignment

The gene encoding CEP161 (DDB_G0282851) is located on chromosome 3 and has 2 exons. The open reading frame comprises 4146 base pairs and codes for a protein of 1381 aa with a molecular mass of 161,600. The protein was named CEP161 based on its molecular mass and location (see below). The BLAST prediction program revealed an N-terminal γ-Tubulin ring complex (γ-TuRc) domain (residues 99-174); the SMART prediction tool indicated the presence of four coiled-coil domains in the protein (Fig. 7A). The γ-TuRc domain (pfam07989) is present in several microtubule associated proteins which also include CDK5RAP2. The highest conservation is in a consensus ten amino acid motif as shown for the human, *Drosophila* and *D. discoideum* protein (Fig. 7B).

A

B

Figure 7. CEP161 domain and sequence alignment. A. CEP161 domain structure. B. CDK5RAP2 γ-TuRc domain sequence alignment and the protein accession numbers for the Human (Hs) (NP_060719), *Drosophila melanogaster* (Dm) (NP_725298.1) and *D. discoideum* protein (Dd) (DDB_G0282851). The numbers indicate the amino acid position of the γ-TuRc domain in the respective proteins. Colour code: Red background shows the residues which are strictly conserved in the column, yellow background shows the residues which are conserved within a group but not conserved from one group to the other.

2.1.3 CEP161 is a centrosomal protein.

To determine the subcellular localisation of CEP161, we generated monoclonal antibodies against a recombinant polypeptide (CEP161-D1, residues 1-763). mAb K83-632-4 showed in immunofluorescence studies a bright punctate staining near the nucleus suggestive of the centrosome (Fig. 8A). The centrosomal localization was confirmed by labeling GFP-CP250 knock-in cells where the antibody staining coincided with the GFP positive centrosome. GFP tagged CEP161 also was present in a single dot near the nucleus and was recognized by mAb K83-632-4 (Fig. 8B).

A
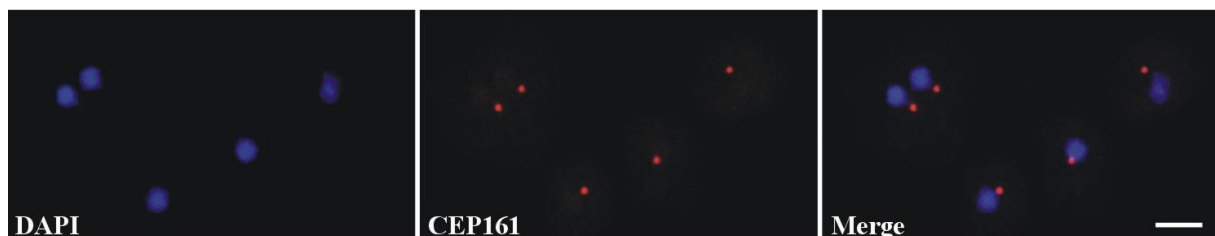
B
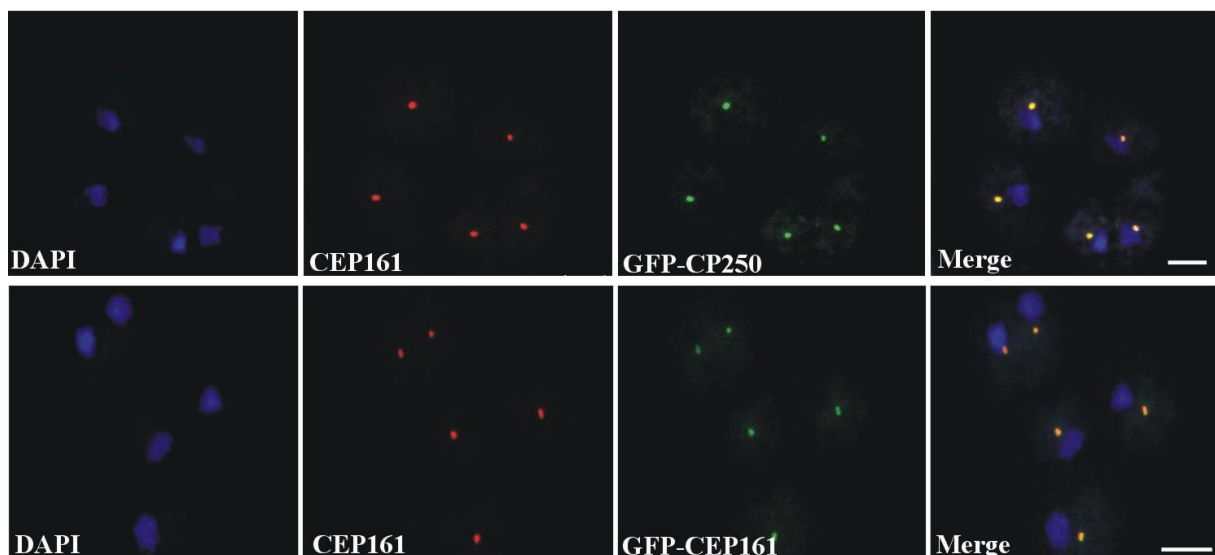
Figure 8: CEP161 as a novel centrosomal protein in _D. discoideum_. A. Localisation of CEP161 to the centrosomes in AX2 cells. The CEP161 genomic DNA sequence was cloned into pBsrN2 to produce CEP161 proteins with GFP located at the N-terminus. B. Cellular localisation of CEP161 to the centrosome in GFP-CP250 cells and in GFP-CEP161 cells.

CP250 was expressed as GFP-fusion rotein, CEP161 was detected with mAb K83-632-4, nuclei were stained with DAPI (Scale bar, 10 µm).

The centrosome and the Golgi apparatus co-localize in the vicinity of the nucleus. When we stained GFP-CEP161 cells with mAb190-340-8 for the Golgi marker comitin, we found CEP161 in the center of the Golgi apparatus (Fig. 9).
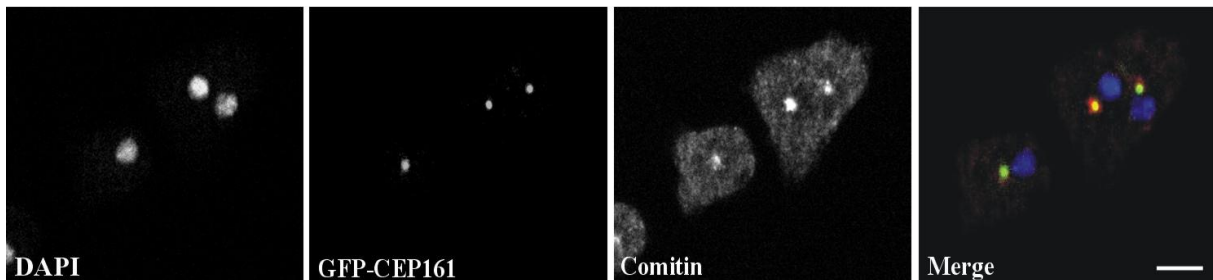
Figure 9: CEP161 localises to the Golgi-complex. CEP161 is a novel centrosomal protein in *D. discoideum* which also localises with the Golgi-complex as revealed by comitin staining with mAb 190-340-8, nuclei were stained with DAPI (Scale bar, 10 µm).

2.1.4 CEP161 constructs and truncated proteins

To identify the region of CEP161 that mediates the centrosome association of CEP161, we generated shortened proteins (GFP-CEP161-D1: designated D1, residues 1-1114; GFP-CEP161-D2: designated D2, residues 1-763; and GFP-CEP161-D3: designated D3, residues 763-1114) (Fig. 10A). Expression and molecular weights of the GFP tagged proteins were analysed by SDS-PAGE (Fig. 10B).

A
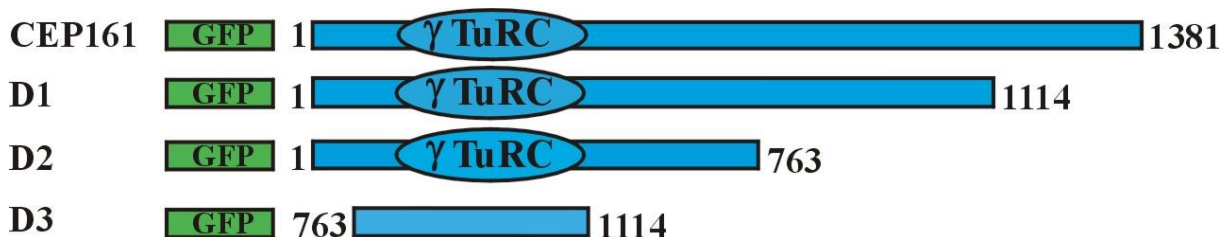
B
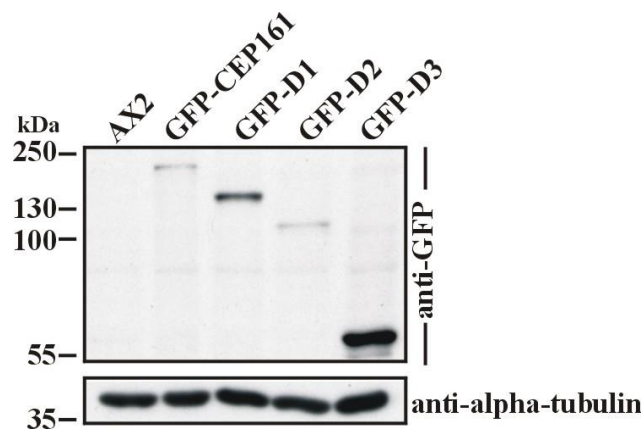
Figure 10. CEP161 constructs and protein expression. A. Overview of N-terminally GFP tagged CEP161 proteins. The position of the amino acids is given. B. Western blot for the GFP tagged proteins stably expressed in AX2 cells. Alpha-tubulin was used as the loading control. GFP fusion proteins were recognized by mAb K3-184-2, α-tubulin by YL1/2.

The expression levels varied for the GFP tagged proteins. GFP-CEP161 was present in lower amounts than endogenous CEP161 whereas GFP-D1 levels were 1.8 fold higher than those of CEP161 (Fig. 11A, B).

A
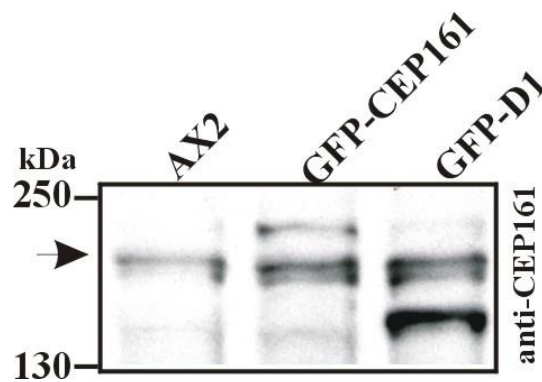
B
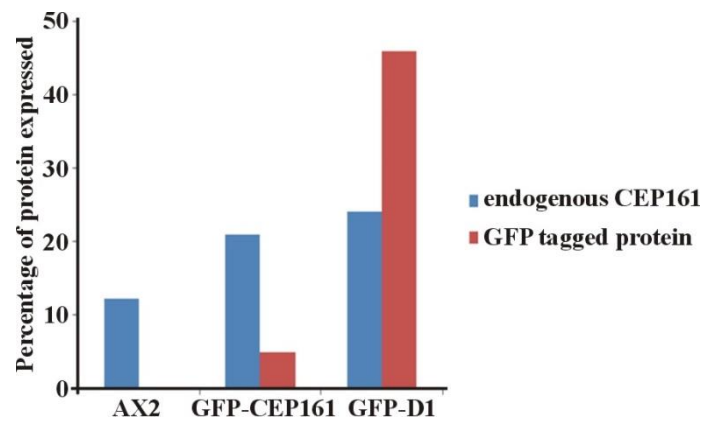
Figure 11. Quantification of CEP161. A. Western blot for endogenous CEP161 and GFP tagged proteins detected with CEP161 polyclonal antibodies. The arrow indicates the endogenous CEP161. B. Quantification of western blots for endogenous CEP161 and GFP tagged proteins.

2.1.5 Localisation of CEP161 truncated proteins

In immunofluorescence analysis the D1 and D2 proteins behaved like a centrosomal protein and appeared as a single dot near the nucleus. In contrast, the D3 protein was present throughout the nucleus although the prediction programs did not reveal nuclear localization signals or any DNA binding domain. We conclude that amino acids 1-763 are sufficient for localization of CEP161 to the centrosome (Fig. 12).
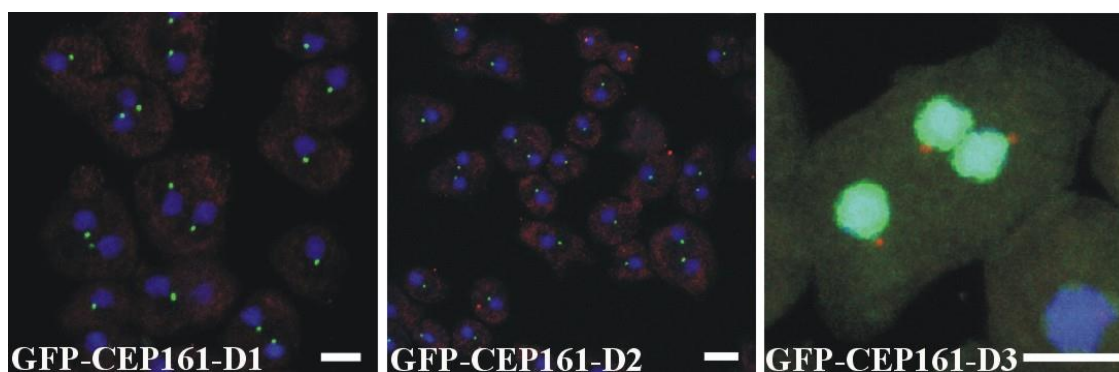
Figure 12. Subcellular localisation of GFP tagged proteins. For GFP-CEP161-D3 the centrosome was detected with mAb K68-332-3.Nuclei were stained with DAPI (Scale bar, 5 µm).

Based on its overall domain structure, the presence of the conserved γ-TuRc and the localization at the centrosome we presume that CEP161 is the *D. discoideum* ortholog of CDK5RAP2.

2.2 CEP161 mutant cells are viable, but impaired in growth and development

2.2.1 CEP161 regulates nuclear number and centrosome positioning

Isolation of a knockout mutant has not been successful. Therefore we overexpressed the GFP tagged versions of CEP161 full length and truncated proteins in AX2 cells in order to analyse the role of CEP161 for cell organization, growth and development. First we determined the nuclei number of the cells to understand the role of CEP161 in cell division and cell cycle. The D1, D2 and D3 cells were mostly mononucleated with their centrosome located very close to the nucleus in a distance of < 500 nm. By contrast, CEP161 affected the centrosome nucleus distance and approximately 40% of the CEP161 cells had the centrosome far away from the nucleus with a distance > 900 nm (Fig. 13A, B). We also observed that the nuclei-centrosome ratio was aberrant in a low percentage of the D1 and D2 expressors.

A
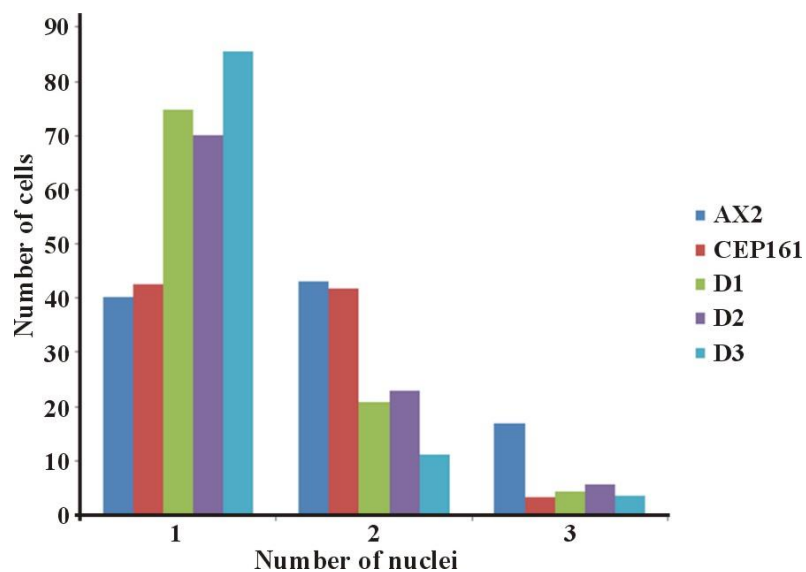
B
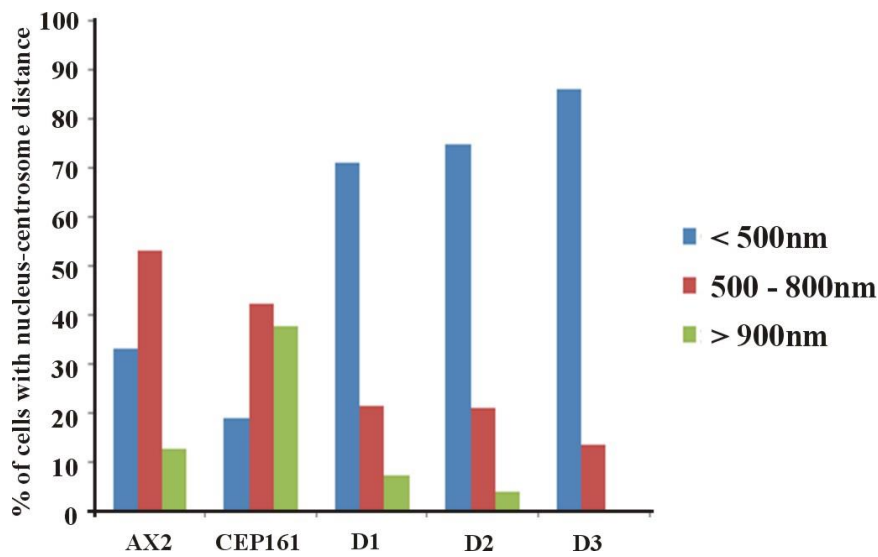
Figure 13. CEP161 regulates nuclear number and centrosomal position. A. Number of nuclei per cell. B. Percentage of cells with nucleus-centrosome distance as indicated. A total of 600 cells were counted for AX2 and mutant strains for each of the experiments shown in A, B.

2.2.2 The nuclear-centrosome ratio is altered in the mutants

Furthermore, 0.6% of the D1 cells had two centrosomes per nucleus. For D2 cells this number increased to 0.74%, and in 0.24% of the cells we observed 3 and more centrosomes per nucleus (Fig. 14A, B). This was not observed for all other strains.

A
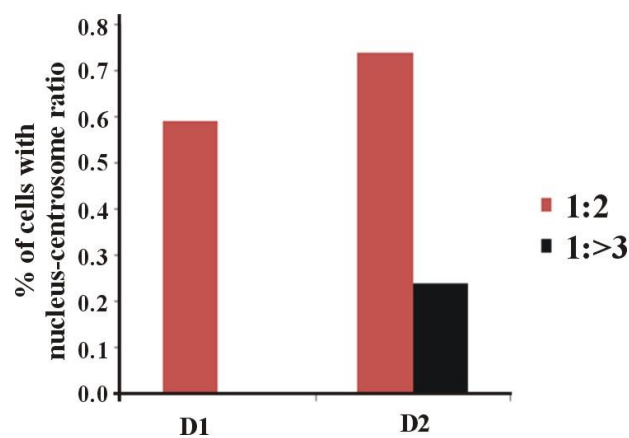
B
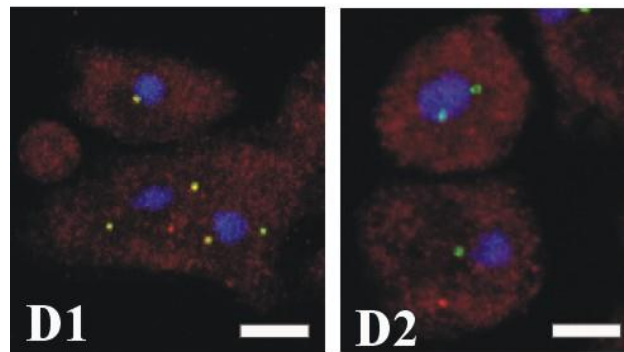
Figure 14: CEP161 regulates centrosomal number. A. Percentage of cells with nuclear-centrosome ratio. A total of 600 cells were counted for AX2 and mutant strains. D. Confocal images for D1 and D2 cells with abnormal distribution of nucleus-centrosome ratio. Nuclei were stained with DAPI, centrosomes were detected with the GFP signal of the GFP tagged D1 and D2 proteins. Scale bar, 5 µm.

2.2.3 CEP161 regulates cell size

Ectopic expression of CEP161 led to an increase in cell size with approximately 70% of the cells having a diameter greater than 12 µm. Interestingly, D1 (55%), D2 (52%) and D3 (70%) cells showed a decrease in the size of the cells and had a diameter below 10 µm (Fig. 15).
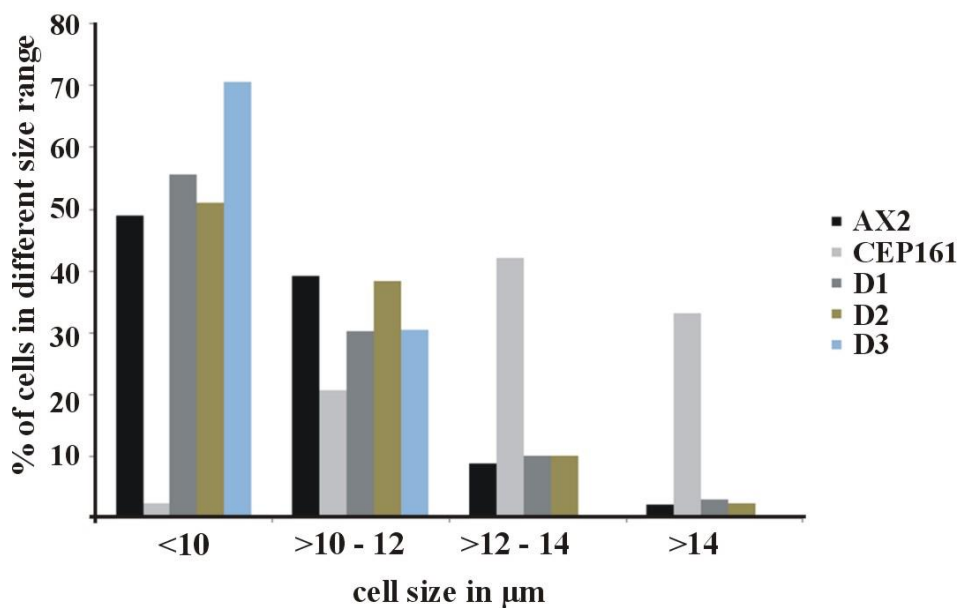
Figure 15. CEP161 regulates size. Cell size of the AX2 and CEP161 mutant strains in micrometers.

2.2.4 Role of CEP161 for growth

To examine the role of CEP161 for growth we assessed the phenotype of AX2 and CEP161 mutants on a bacteria lawn by measuring the increase in the diameter of the colony over time. Colony growth was significantly reduced for all mutants except for D3 which showed increased growth (Fig. 16A, B). Such a behavior could be due to reduced phagocytosis or to altered motility. Hence we assayed the phagocytic capability following yeast particle uptake. We found that fewer CEP161, D1 and D2 cells had ingested one or more yeast particles after 15 min than AX2 cells. D3 was similar to AX2 (Fig. 16C). In suspension culture the growth was reduced for the CEP161 and the D3 mutants, the D1 and D2 mutants showed a faster growth until day 5 after which there was a sharp decrease in the growth of the cells (Fig. 16D).

A
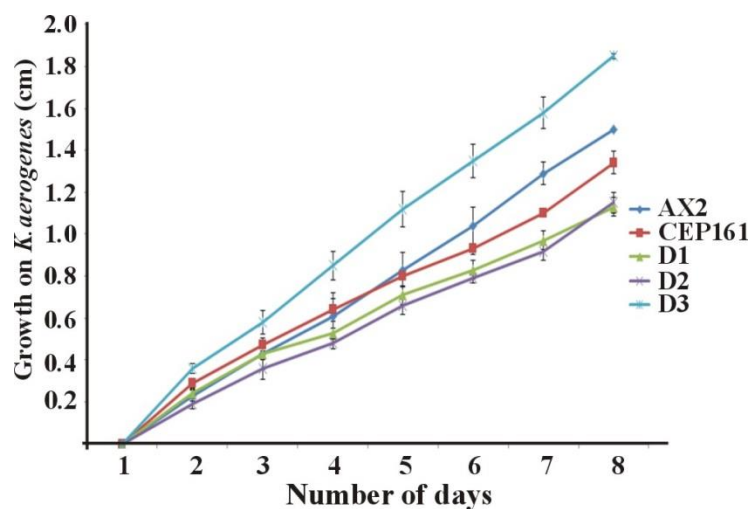
B
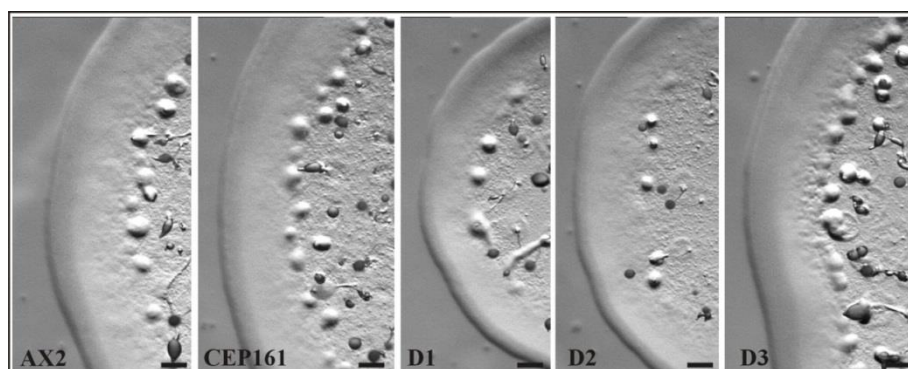
C
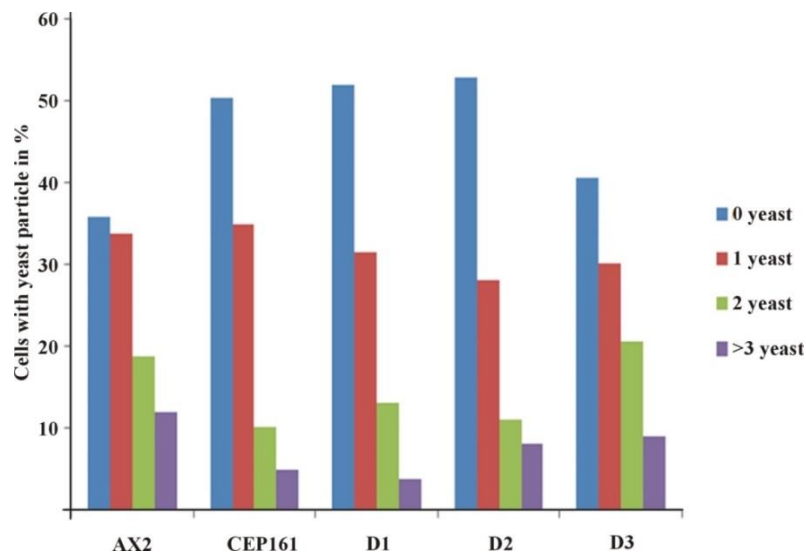
D
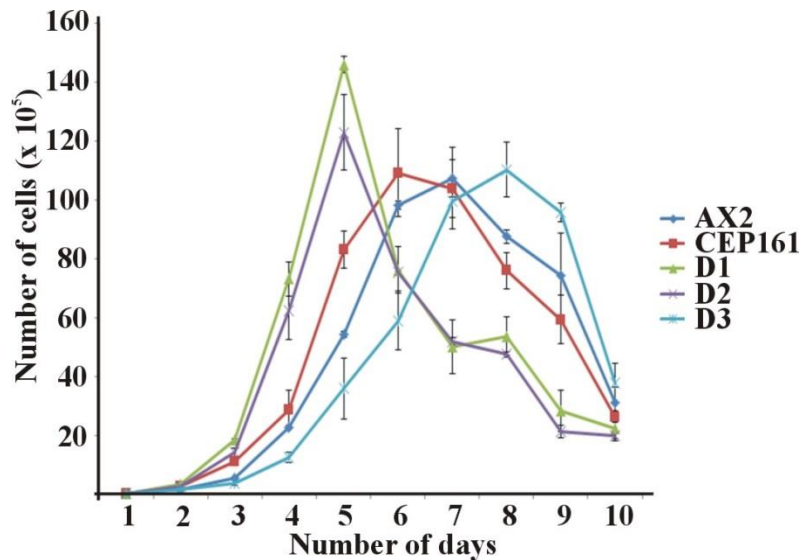
Figure 16: CEP161 affects growth. A. Growth on *K. aerogenes*. The increase of the plaque size was measured over days. B. Phenotype of AX2 and CEP161 mutants grown on a lawn of *Klebsiella*. The pictures were taken at day 6 after inoculation. C. Phagocytosis assay. TRITC labeled yeast were added to the cells. After 15 min incubation time the cells were fixed and the number of ingested yeast counted. D. Growth in shaking culture. The cell numbers were determined every 24 hours.

2.2.5 CEP161 affects development

When *D. discoideum* cells starve, they enter a developmental cycle that ends with the formation of fruiting bodies. The CEP161, D1 and D2 cells plated on phosphate agar aggregated and formed multicellular structures, the D3 cells could only form loose aggregates that did not develop into fruiting bodies. There was also marked increase in the size of the fruiting bodies for D1 and D2 mutants, both with regard to the length of the stalks and the size of the fruiting bodies, whereas the CEP161 fruiting bodies were not significantly different from those of AX2 (Fig. 17).
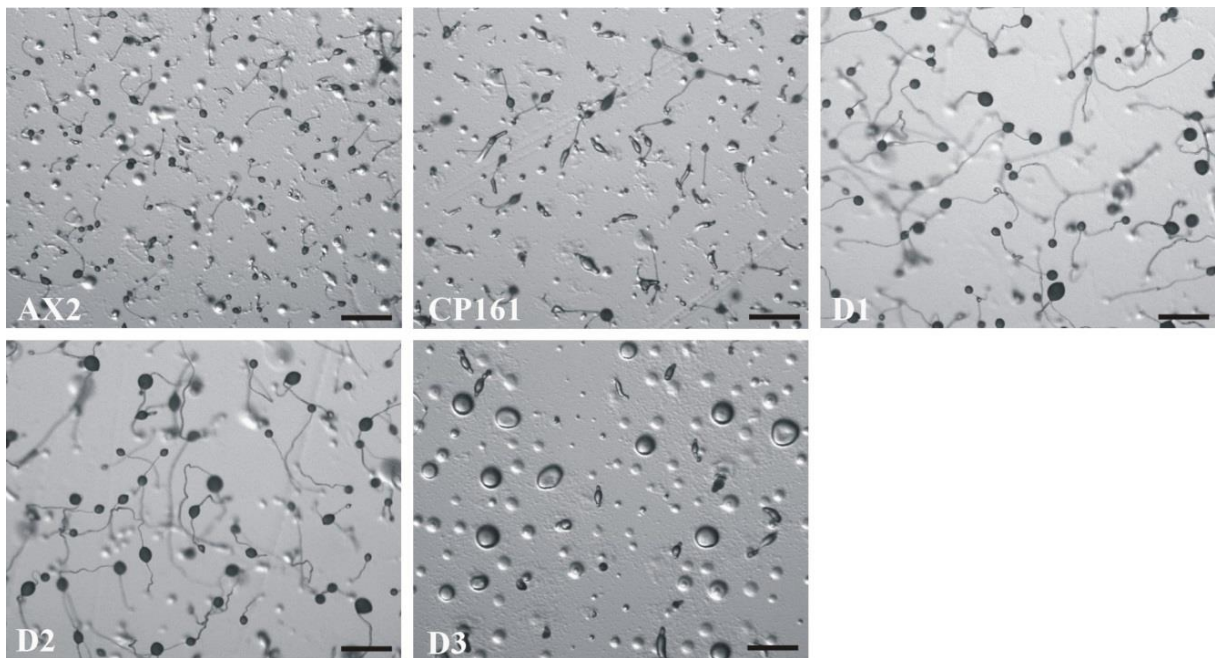
Figure 17. Development of wild type and mutant strains on phosphate agar plates. Pictures taken at 24 hours after starvation in phosphate agar plates. Scale bar 500 µm.

Development was also studied on a plastic surface with cells kept in Soerensen phosphate buffer. Under these conditions cells can form streams and aggregate. Further development does not take place. We observed that stream formation occurred slightly later for CEP161, D1 and D2 (9 h) as compared to AX2 (8 h). For the D3 cells we noted a severe delay in the streaming and aggregation behavior as they formed streams only after 28 hours (Fig. 18A). We then analyzed the expression levels of contact site A (csA) glycoprotein when cells were

starved in shaken suspension. csA gene expression is developmentally regulated and starts during aggregation reaching a peak at the tight aggregate stage. The protein is a cell adhesion molecule which enables cells to form EDTA stable cell-cell contacts during aggregation (Faix et al., 1990). In the experiment shown csA was detected in D1 at t6 and the amounts strongly increased at t8 and t10. In AX2, CEP161and D2 csA was present at t8 and the level increased at t10. In D3 csA was also seen at t8 and t10, however, the amounts were lower. At the t24 time point, when tight aggregates had formed in all strains, the csA signal was identical in all strains (Fig. 18B). We conclude that ectopic expression of CEP161 does not significantly alter development, whereas D1 and D2 lead to premature development and also to an increased size of the fruiting bodies and D3 has an inhibitory effect.

A
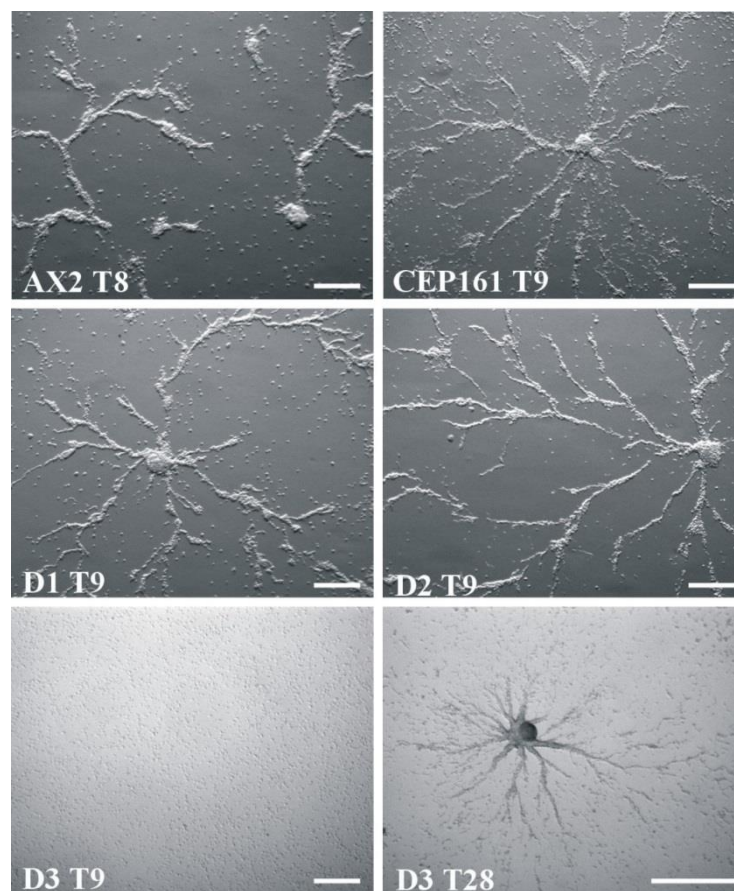
B
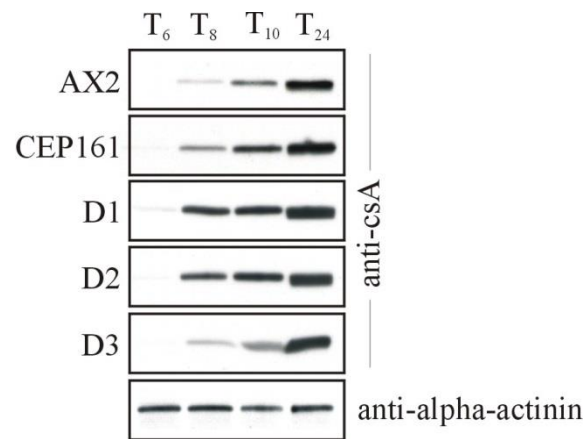
Figure 18. Streaming of AX2 and mutant cells. A. Stream formation on a plastic surface under phosphate buffer. The time points indicate the occurrence of stream formation. Scale bar, 250 μm. B. Time-dependent expression of csA. Cells were collected during development in shaking suspension at the indicated time points (in hours) and the lysates analyzed by SDS-PAGE and western blot. csA was detected by mAb33-294, mAb 47-16-1 detected α-actinin which was used as loading control. Since the α-actinin blot was similar for all strains, only the α-actinin blot for AX2 is shown.

Streaming and aggregation of the cells depends on the adhesion of the cells to the plastic substratum. Upon testing we observed that the mutants exhibited an altered adhesion and bound more strongly to the surface than AX2. This could account for the altered streaming behavior (Fig. 19).
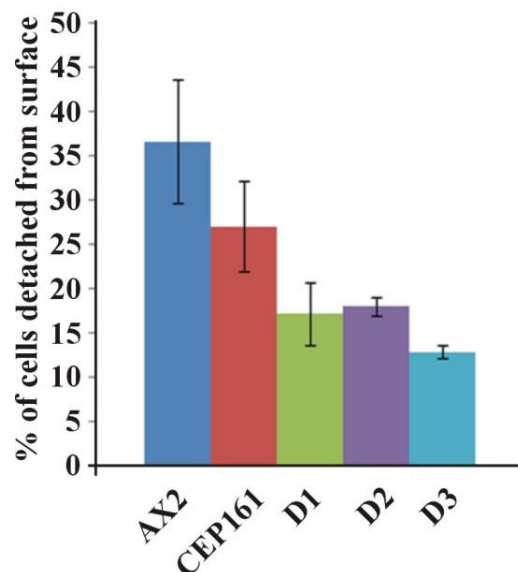
Figure 19. Cell-substrate adhesion. Percentage of cells detached from the surface in 24 well plates after shaking at 200 rpm for 1 hour.

2.2.6 CEP161 affects unicellular motility and polarity

Cell motility is an important feature during growth and development of *D. discoideum*. *Dictyostelium* cells exhibit an amoeboid type of cell motility. They deform very quickly and translocate via rapidly alternating cycles of pseudopod extension and pseudopod retraction in response to external signals which are dependent on changes in the actin cytoskeleton. To assess the role of CEP161 and mutant proteins for chemotactic motility during aggregation we analyzed the motile behaviour of aggregation competent cells and followed the motility of cells with time-lapse video microscopy. Mutant cells D1, D2 and D3 consistently displayed a reduced speed (~5-8 versus ~16 µm/min for AX2) (Fig. 20A and Table 2). AX2 cells were highly elongated and extend pseudopods mainly in the direction of the chemoattractant. The mutants displayed a change in morphology and had a more rounded shape in response to cAMP signaling (Fig. 20B). In the parameters analysed, directionality did not differ between AX2 and mutants CEP161, D1and D2 although D3 mutant showed a decrease, whereas the persistence was significantly reduced in the mutants D1, D2 and D3 (Table 2) suggesting that CEP161 of *D. discoideum* plays an important role in chemotaxis as it affects motility and polarity.

A
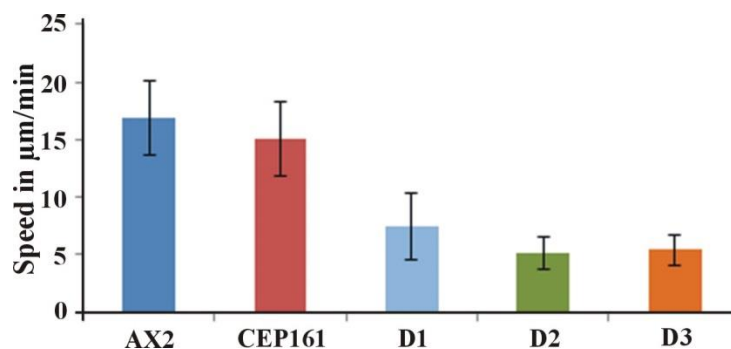
B
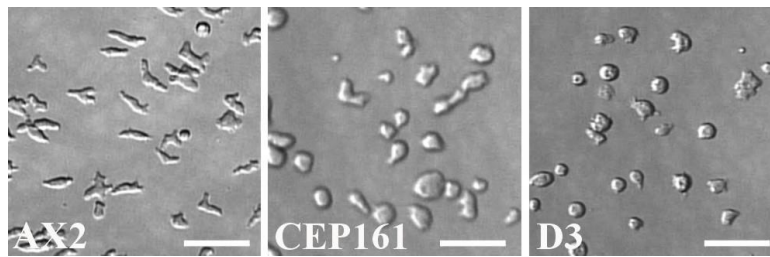
Figure 20. CEP161 affects cell motility and polarity. A. Chemotaxis assay. Analysis of speed during migration of aggregation-competent wild type and mutant cells towards the chemoattractant cAMP. B. Images showing migrating aggregation competent cells of AX2, CEP161 and D3 cells (scale bar, 50 μm).

Table 2

Parameter	AX2	CEP161	D1	D2	D3
Speed(μm/min)	16.9 +/- 6.2	15.0 +/- 3.2	7.5 +/- 2.9**	5.0 +/- 2.1**	5.4 +/- 1.3***
Persistence (μm/min-deg)	7.2 +/- 4.2	5.4 +/- 1.7**	2.8 +/- 1.3**	2.2 +/- 0.5**	1.8 +/- 0.8***
Directionality	0.75 +/- 0.20	0.6 +/- 0.21	0.7 +/- 0.20	0.6 +/- 0.21	0.5 +/- 0.18**

Table 2. **Analysis of chemotactic cell motility of AX2 and mutants**. Time-lapse image series were captured and stored on a computer hard drive at 30-second intervals. Images were taken at a magnification of 10X every 6 s. The DIAS software was used to trace individual cells along image series and calculate motility parameters. Speed refers to the speed of the cell's centroid movement along the total path; directionality indicates migration straightness; direction change refers to the number and frequency of turns; persistence is an estimation of movement in the direction of the path. Values are mean ± standard deviation of >30 cells from three or more independent experiments. The symbol * indicates the significance of the P-Value (*<0.5, **<0.01, ***<0.001).

2.2.7 CEP161 affects the directed migration of slugs

During multicellular development cells differentiate into prespore and prestalk cells in the aggregate, undergo a morphogenesis and can form a slug which can sense light and migrate in a straight path towards the light (Wallraff and Wallraff, 1997). Slugs are polar with a tip at the

anterior end consisting of prestalk cells, sensing the light that helps to control their migration and phototactic turning. AX2 and CEP161 slugs migrated in a nearly straight path towards the light source. D1, D2 and D3 deviated from this path and migrated in an angle towards light. Also, the path length appeared shorter in particular for D1 and D2 (Fig. 21A, B).

A
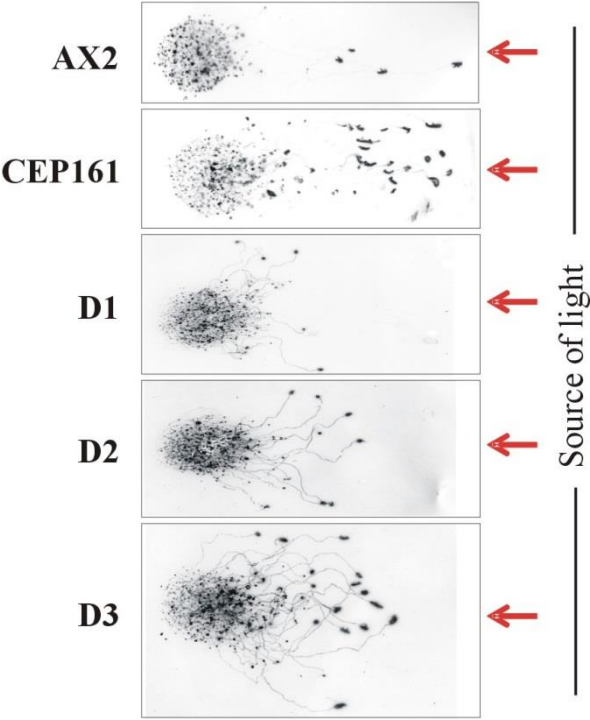
B
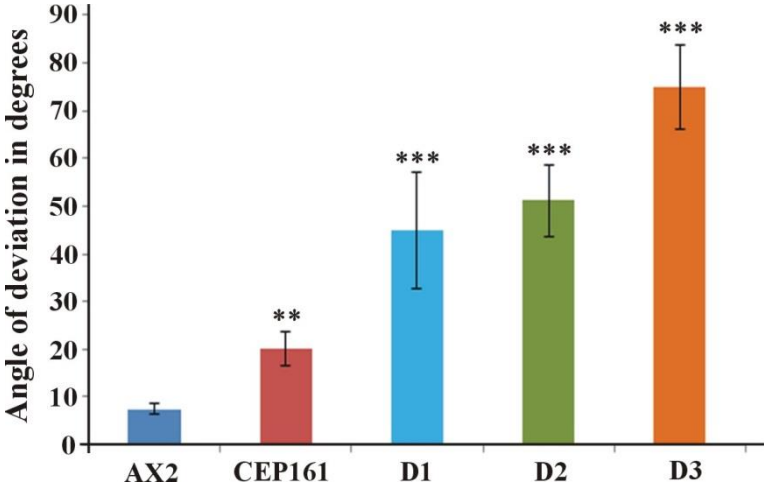
Figure 21. CEP161 affects the directed migration of slugs. A. Phototaxis assay. Slugs and slug trails were transferred to nitrocellulose filters and stained with amido black. The red

arrow indicates the source of light. B. Angle of deviation of the cells when migrating towards light. Number of slugs analysed n=4. The symbol * indicates the significance of the P-Value (*<0.5, **<0.01, ***<0.001).

2.3 Identification of CEP161 as an interacting partner of the Hippo homolog Hrk-Svk

To identify interaction partners of CEP161 we carried out immunoprecipitation experiments using cells expressing GFP tagged CEP161. The samples were analysed by SDS-PAGE and the bands were cut out and further analysed by mass spectrometry. The list of interaction partners of CEP161 from mass spectrometry data is shown in appendix I. Among the identified proteins we found severin kinase SvkA (DDB_G0286359) as a potential interacting partner. SvkA was described as a homolog of human MST3, MST4 and YSK1 kinases (Rohlfs et al., 2007). Our detailed sequence analysis showed that it is related to Hippo of *Drosophila* (25.1% identity, 35.7% similarity) and Hippo related Stk3 (MST1) of human (34.7% identity; 52.0% similarity). Particularly high homology was observed in the serine/threonine protein kinase domain of the proteins (Fig. 22).
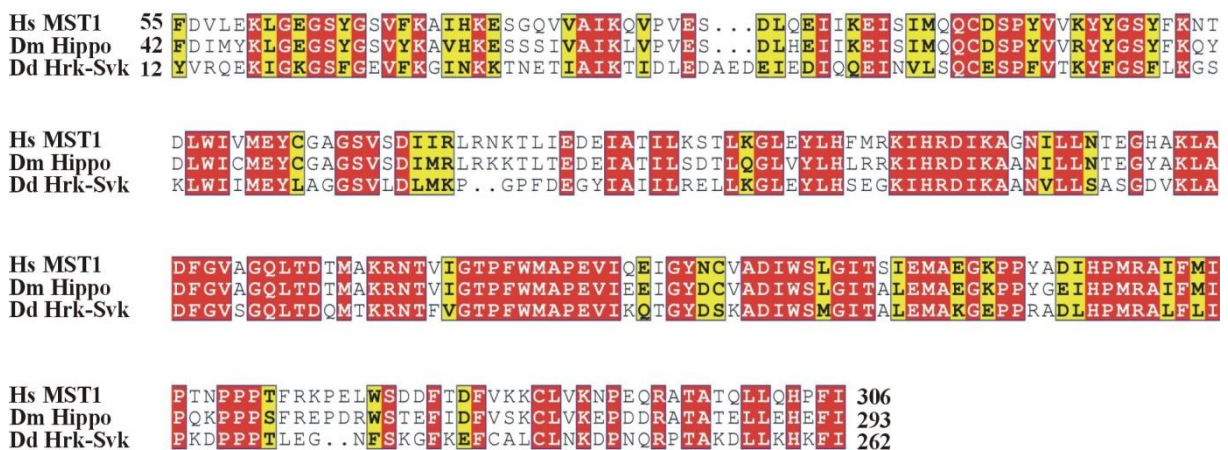
Figure 22. Sequence alignment for the serine/threonine protein kinase domain of human (Hs) MST2 (NP_006272.2), *Drosophila* (Dm) Hippo (NP_611427.1) and *Dictyostelium* (Dd) Hrk-Svk (DDB_G0286359). The numbers indicate the position of the STK domain in the respective proteins. Colour code: Red background shows the residues which are strictly conserved, yellow background shows similar residues.

Given the significance of SvkA to our study and its relation to Hippo, we have renamed it as Hippo related kinase-Svk (Hrk-Svk). To further establish Hrk-Svk as an interacting partner for CEP161, we performed GST pull down assays with GST-CEP161-D2 and GST-CEP161-D3 proteins. The D2 protein encompasses the γ-TuRC domain and a coiled coil domain, D3 encodes two coiled coil domains (Fig. 23A). Hrk-Svk interacted with the D2 and also the D3 proteins but not with GST. The precipitate was probed with Hrk-Svk polyclonal antibodies (Fig. 23B).

A
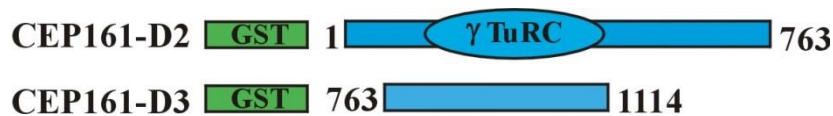
B
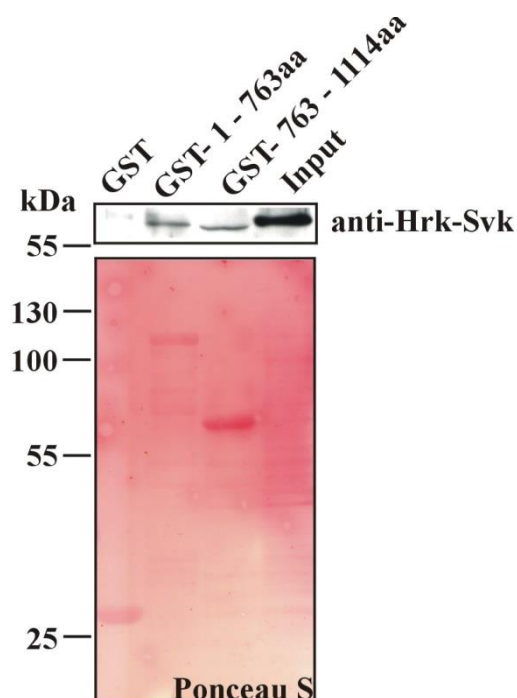
Figure 23. Interaction of CEP161 with Hrk-Svk. A. Schematic of the GST tagged CEP161 polypeptides. B. CEP161 interacts with Hrk-Svk in a pull down assay. The blot was probed with pAb for Hrk-Svk. The Ponceau S stained membrane is shown below.

The interaction was further investigated by using GST fusion proteins of Hrk-Svk for pulling down CEP161. Only the polypetide encompassing the serine threonine kinase domain (STKc) interacted with CEP161 locating the binding site in this domain (Fig. 24A, B).

A
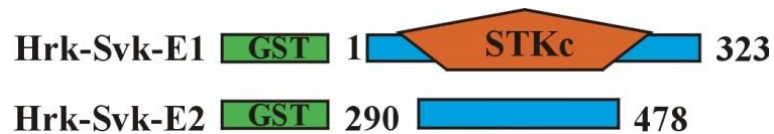
B
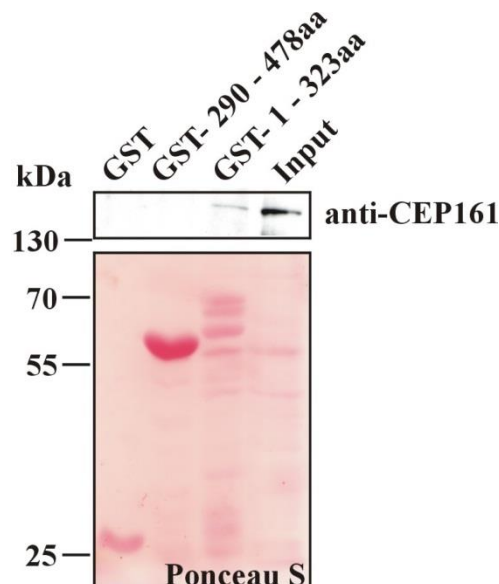
Figure 24. Interaction of CEP161 with the kinase domain of Hrk-Svk. A. Schematic of GST tagged constructs for Hvk-Svk polypeptides. B. Pull down assay showing the interaction of Hrk-Svk-E1 interacts with CEP161. The blot was probed with pAb CEP161.The Ponceau S stained membrane is shown below. GST-1-323 containing the kinase domain was very sensitive to proteolysis.

To investigate the localization of Hrk-Svk we expressed it as GFP tagged protein. Previously a cytosolic localization and enrichment at the centrosome was reported for GFP-Hrk-Svk (Rohlfs et al., 2007). When we stained GFP-Hrk-Svk expressing cells for CEP161 using mAb K83-632-4 we detected CEP161 staining in the center of the strongly GFP positive region

near the nucleus showing a yellow puncta in the overlay which indicates a colocalization (Fig. 25).
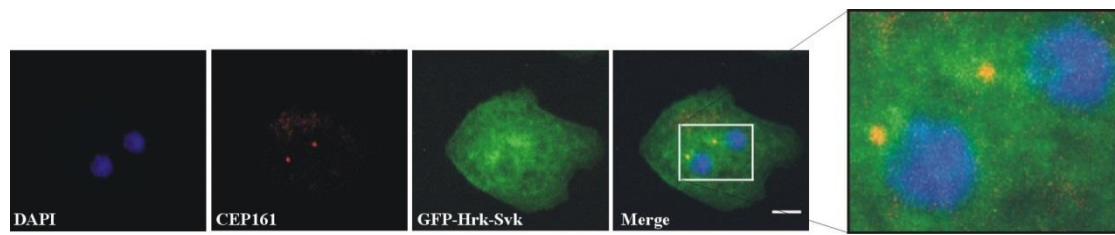
Figure 25. CEP161 colocalizes with GFP tagged Hrk-Svk in AX2 cells. CEP161 was detected with mAb K83-632-4. Nuclei were stained with DAPI. The boxed area is enlarged at the right. Scale bar, 5 µm.

2.4 Interaction of CDK5RAP2 with the mammalian Hippo homolog MST1

We extended our studies to the mammalian system to probe whether there is a similar interaction between components of the Hippo signaling pathway and CDK5RAP2. We used Myc tagged CDK5RAP2 and generated N-terminally truncated constructs C1 (residues 1-580) and C2 (residues 1-1271) also as Myc tagged polypeptides and expressed them in HeLa cells (Fig. 26).
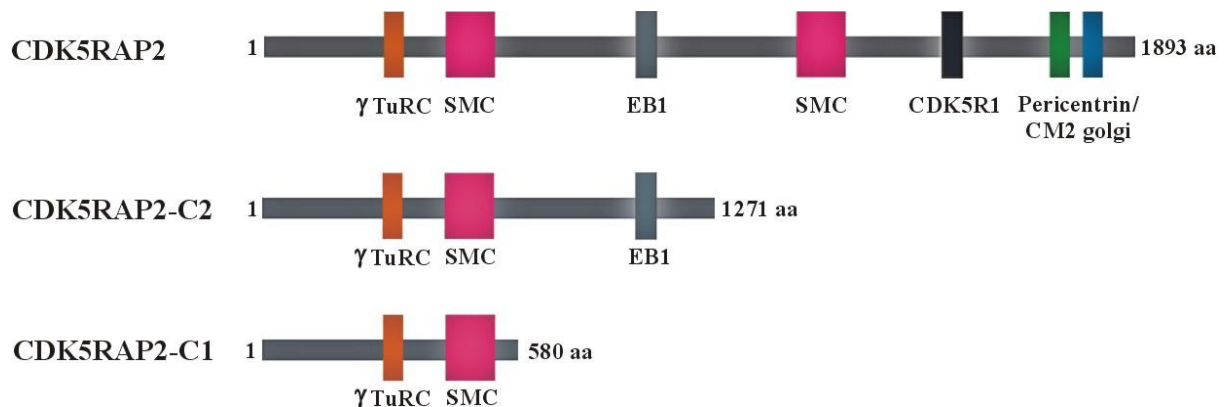
Figure 26. Schematic of Myc tagged constructs of CDK5RAP2. The amino acid residues and the domains are indicated.

2.4.1 The N-terminal part of CDK5RAP2 is sufficient for targeting to the centrosome

The Myc tagged constructs were expressed in HeLa cells and their localisation studied. Myc-CDK5RAP2 as well as the two truncated proteins was present in a dot near the nucleus which

colocalized with the centrosomal marker Pericentrin in immunofluorescence analysis (Fig. 27).
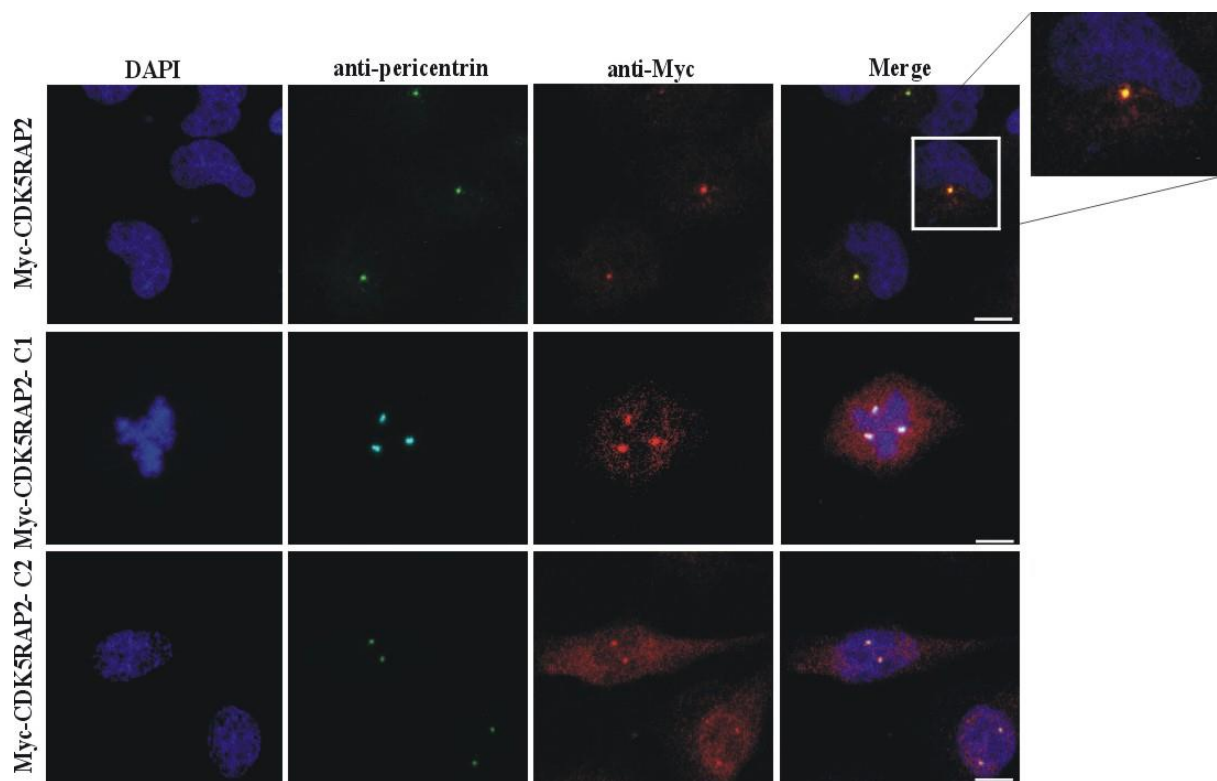
Figure 27. Immunofluorescence analysis of HeLa cells expressing Myc tagged CDK5RAP2 proteins. Myc was recognized by mAb 9E10, the centrosomal marker Pericentrin by pAb pericentrin, Nuclei was stained with DAPI. The boxed area is enlarged at the right. Scale bar, 10 µm.

The results suggest that the first 580 amino acids which contain the γ-TuRc domain of CDK5RAP2 are sufficient for targeting the centrosome. In some of the C1 and C2 expressing cells (0.8%) we noted an abnormal nucleus centrosome ratio (shown for Myc-CDK5RAP2-C1 with three centrosomes and Myc-CDK5RAP2-C2 with two centrosomes in Fig. 27) resembling the data obtained for DdCEP161-D1 and -D2 (Fig. 14A). The nucleus also often displayed an irregular shape in the cells expressing Myc-CDK5RAP2-C1 and -C2.

2.4.2 Overexpression of Myc tagged CDK5RAP2

Further experiments were carried out with HEK293T cells ectopically expressing Myc-CDK5RAP2. The amounts of the Myc tagged protein were 15-fold higher than the one of the endogenous CDK5RAP2 (Fig. 28A, B).

A
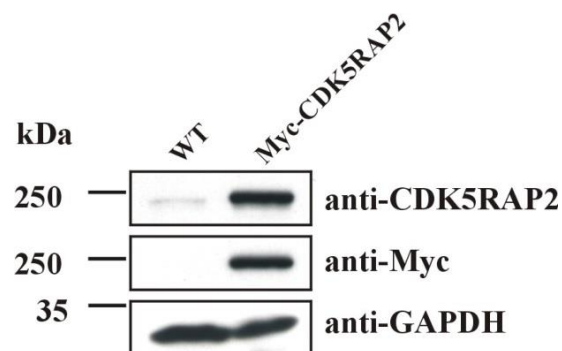
B
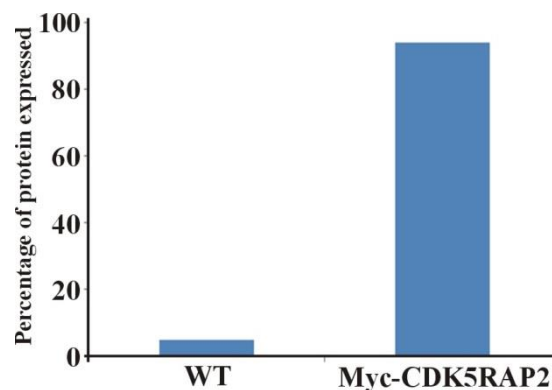
Figure 28. Expression of Myc-CDK5RAP2 in HEK293T cells. A. In the western blot, CDK5RAP2 was detected with pAb CDK5RAP2, Myc tagged protein with mAb 9E10, GAPDH with mAb GAPDH. B. Quantification of the Myc-CDK5RAP2 in wildtype and Myc-CDK5RAP2 transfected cells. Signals were analysed using ImageJ. For loading control we used GAPDH levels.

2.4.3 CDK5RAP2 interacts with the Hippo homolog MST1

The Hippo signaling pathway is highly conserved. Whereas most of the Hippo pathway components were identified in the fruit fly (*Drosophila melanogaster*) using mosaic genetic

screens, orthologs to these components have subsequently been found in mammals. The core component of the Hippo signaling is Hippo in *Drosophila* or MST1 in Humans. To understand the role of CDK5RAP2 in the Hippo signaling pathway, we tested whether CDK5RAP2 interacts with MST1, the ortholog of the *Dictyostelium* Hrk-Svk. We co-transfected HEK293T cells with Myc-CDK5RAP2 and GFP-MST1 and precipitated GFP-MST1 using GFP-trap beads. In the precipitate we detected Myc-CDK5RAP2. In immunoprecipitation experiments where we used Myc-CDK5RAP2-C1 and -C2, GFP-MST1 coprecipitated only with CDK5RAP2-C2 indicating that the binding site is located between residues 580 and 1271 which encompass the EB1 domain (Fig. 29).
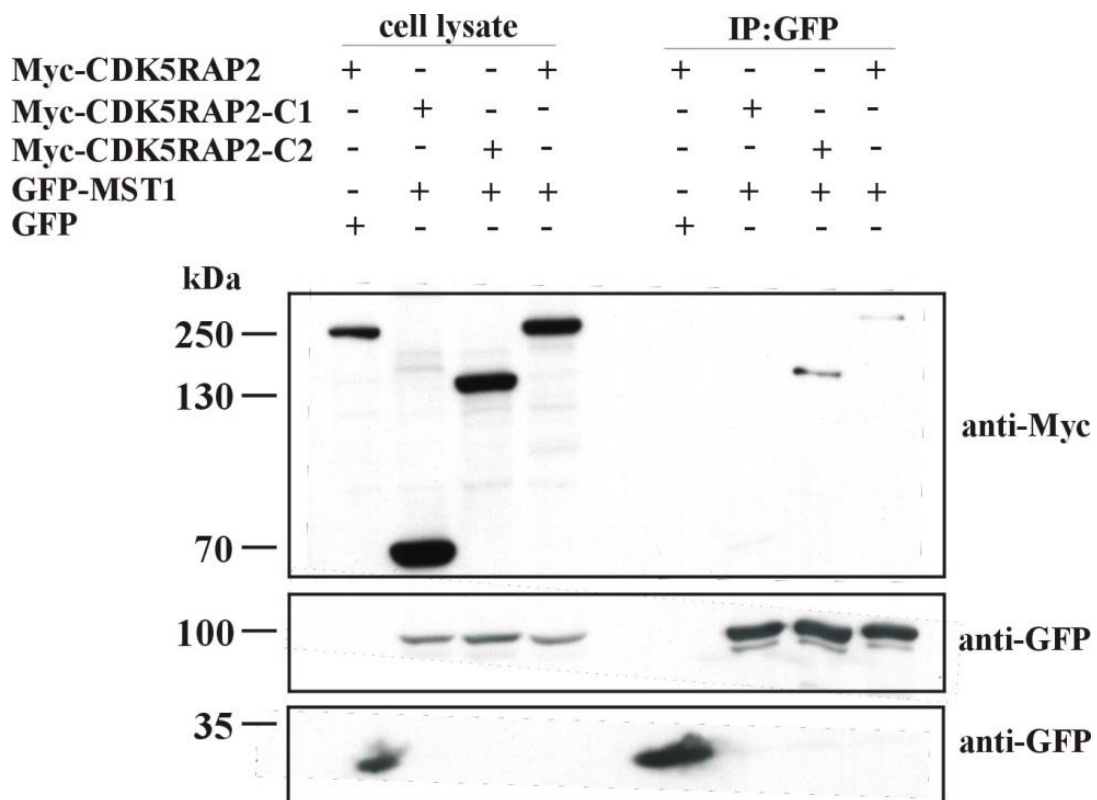
Figure 29. CDK5RAP2 interacts with MST1. HEK293T cells were transiently transfected with the GFP tagged MST1 and Myc tagged CDK5RAP2 and the GFP-fusion protein precipitated using GFP-trap beads. The precipitate (IP) was probed for the presence of Myc tagged CDK5RAP2 proteins. Analysis was with mAb 9E10 to detected Myc tagged proteins and mAb mAb K3-184-2 to detect GFP.

2.4.4 CDK5RAP2 colocalises with MST1

The interaction was further analysed by immunofluorescence analysis. HeLa cells transfected with Myc-CDK5RAP2 and GFP-MST1 were stained for the Myc tag with mAb 9E10 and Pericentrin as a centrosomal marker. GFP-MST1 was present in the cytosol and showed a dot like staining near the nucleus. This dot colocalized with the signal for Myc-CDK5RAP2 and was recognized by Pericentrin specific antibodies. The immunofluorescence analysis was also done with HeLa cells transfected with Myc-CDK5RAP2-C2 and GFP-MST1. A sharp puncta staining near the nucleus was observed for Myc staining. It colocalised with the GFP-MST1 signal which was further recognized by Pericentrin antibodies (Fig. 30A, B). We did not observe a co-localisation of the C1 protein with MST1 (data not shown).

A
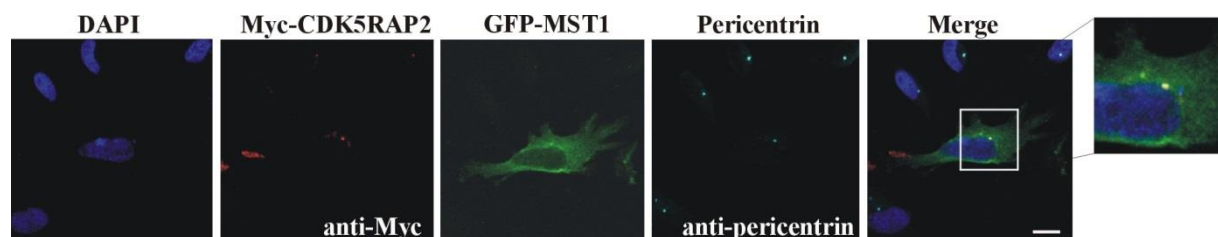
B
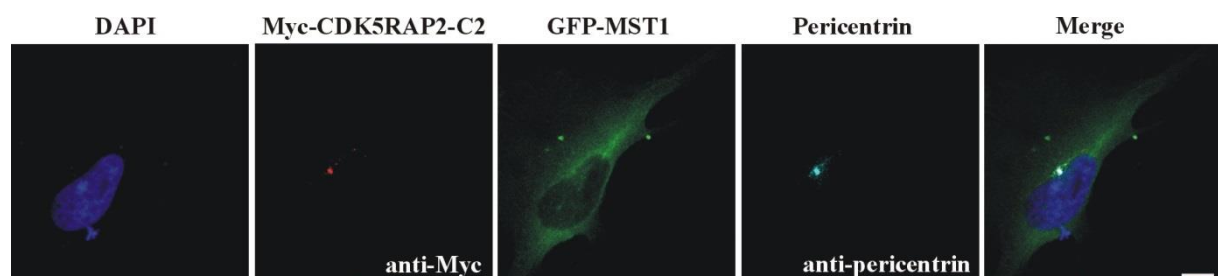
Figure 30. Immunofluorescence analysis to show the localization of CDK5RAP2 and MST1. A. Colocalisation of Myc-CDK5RAP2 with GFP-MST1 in HeLa cells. The inset shows a magnified image of CDK5RAP2 colocalising with MST1 at the centrosome. The boxed area is enlarged at the right. B Colocalisation of Myc-CDK5RAP2-C2 with GFP-MST1 in HeLa cells. Myc was detected with mAb 9E10, Pericentrin with pAb anti-pericentrin. Size bar, 10 μm.

2.5 CDK5RAP2 is a novel regulator of Hippo signaling

Next we examined the functional consequences of the MST1-CDK5RAP2 interaction on Hippo signaling using an established GAL4-TEAD luciferase reporter system, the repression of which reflects activity of the Hippo pathway (Lei et al., 2008; Tian et al., 2010). For the luciferase reporter assay, HEK293T cells were seeded in 24-well plates. A mixture of 5× upstream activating sequence (UAS)-luciferase reporter, Renilla, and the indicated plasmids were cotransfected. Twenty-four hours after cells were transfected, they were lysed, and luciferase activity was measured using a dual-luciferase reporter assay system (catalog no. E1960; Promega) following the manufacturer's instructions. The luciferase activity was measured by a luminometer (model TD-20/20). Transfection efficiency was normalized to thymidine kinase-driven Renilla luciferase activity.

The exogenous TAZ increased GAL4-TEAD activity. The positive control of TAZ expression alone expectedly showed a dramatic increase in the luciferase activity, which was normalized to 100%. For negative control, TAZ and LATS was co-transfected, since LATS is a potent inhibitor of TAZ in the Hippo signaling pathway. Inhibition of TAZ by LATS led to a decrease in the relative luciferase activity to 80%. Coexpression of CDK5RAP2 with TAZ augmented TEAD4 transcriptional activity to 121% (P-Value < 0.05), in comparison with TAZ expression alone. The expression of CDK5RAP2 without TAZ was not sufficient to induce TEAD activation (Fig. 31). It behaved like the "no plasmid" control. Although CDK5RAP2 was only able to induce a minor activation of TAZ, it points to the fact that CDK5RAP2 could have an impact on the Hippo signaling pathway.
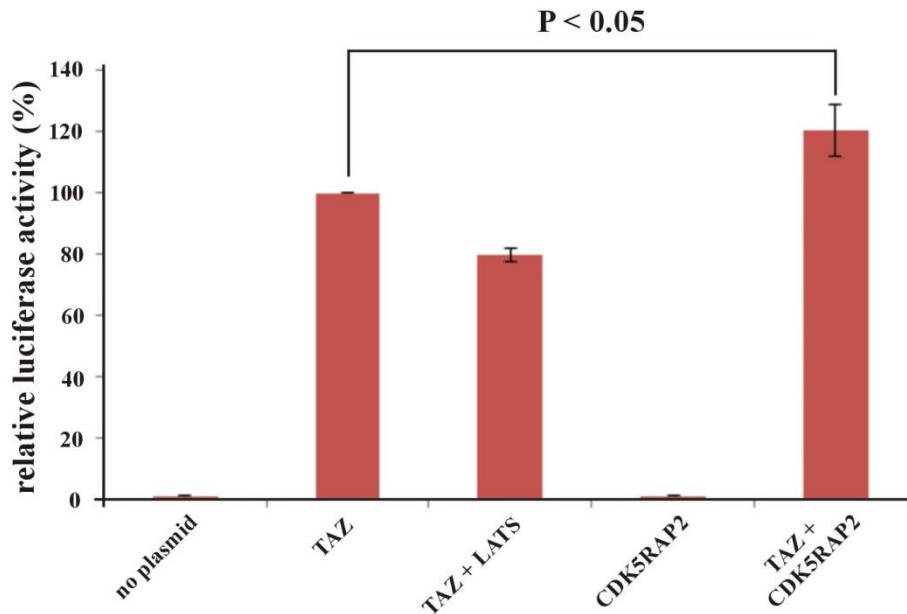
Figure 31. Luciferase assay. CDK5RAP2 regulates the activity of the transcriptional coactivators TAZ. Plasmids encoding the indicated proteins or empty pcDNA6 vector were cotransfected in HEK293T cells together with the TEAD reporter plasmids. Coexpression of CDK5RAP2 increased the TAZ-dependent signaling to 121% (n = 4; $P < 0.05$).

2.5.1 TAZ interacts with the N-terminal part of CDK5RAP2

To further understand the role of CDK5RAP2 in the Hippo signaling pathway, we analysed for a potential interaction of TAZ with CDK5RAP2 using Flag-trap beads. We also tested if the CDK5RAP2 truncated proteins C1 and C2 could also interact with TAZ, which would inturn help us to recognize the interacting residues of CDK5RAP2 with TAZ. The coimmunoprecipitation showed that Flag-TAZ bound to all three proteins indicating that the N-terminal part of Myc-CDK5RAP2 encompassing residues 1-580 is sufficient (Fig. 32). As negative control Flag-hnRNPF, which is a ribonuclear protein, was employed.
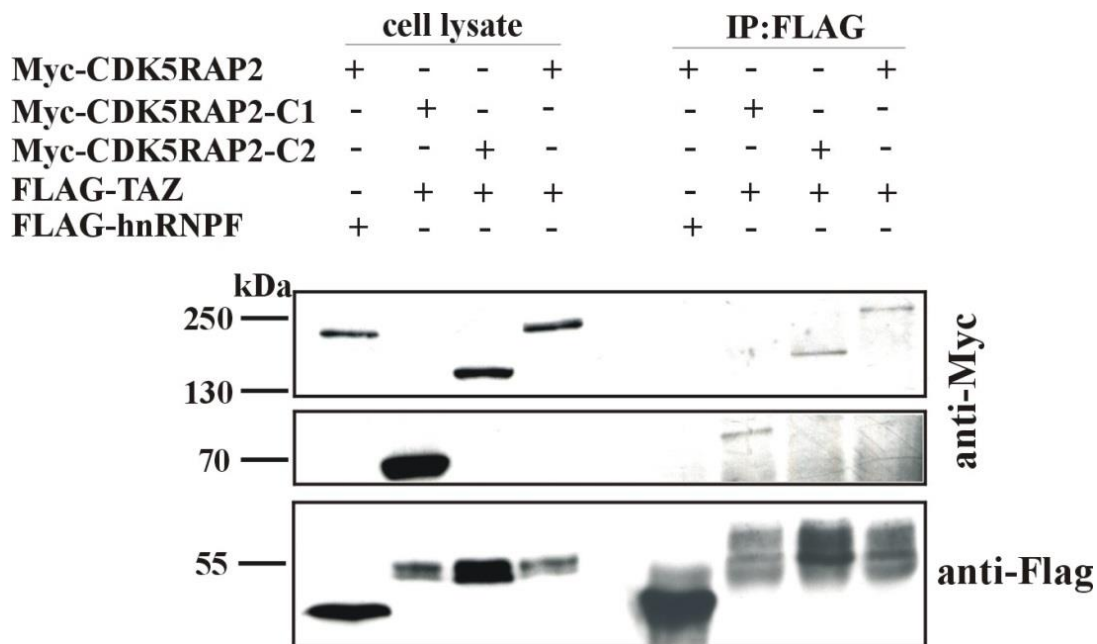
Figure 32. Co-immunoprecipitation assays to study the interaction of CDK5RAP2 with TAZ. Myc tagged CDK5RAP2 full length, and the C1 and the C2 proteins were tested. HEK293T cells were transiently cotransfected with GFP tagged MST1 and Myc tagged CDK5RAP2 proteins. After immunoprecipitation (IP) with GFP trap beads, the resulting blots were probed with mAb 9E10 to reveal Myc, mAb K3-184-2 to reveal GFP and pAb anti-Flag to reveal Flag.

2.5.2 Ectopic expression of CDK5RAP2 downregulates the expression of TAZ

Since there appeared to be an interaction of TAZ with CDK5RAP2, we wondered whether CDK5RAP2 has an impact on TAZ levels. We first quantified the amount of Flag-TAZ in whole cell lysates with wild type untransfected cells as the negative control and Flag-TAZ transfected cells as the positive control. We consistently observed a drastic reduction in the expression levels of TAZ upon cotransfection with plasmid DNA encoding Myc-CDK5RAP2 although the amounts of plasmid DNA were identical (Fig. 34A and B).

A
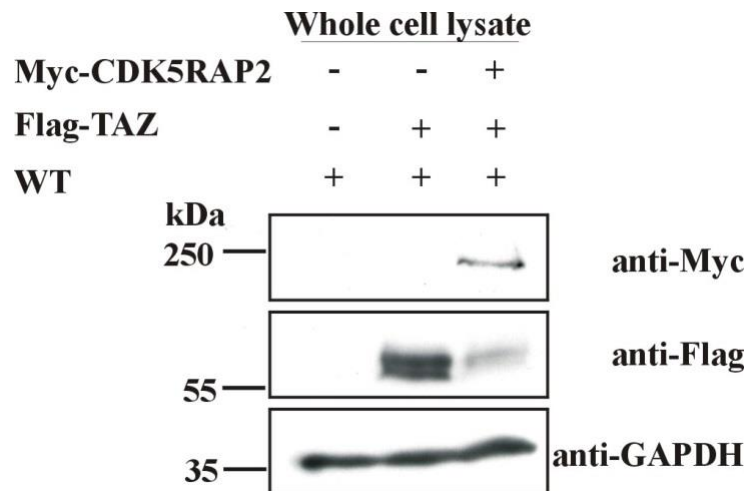
B
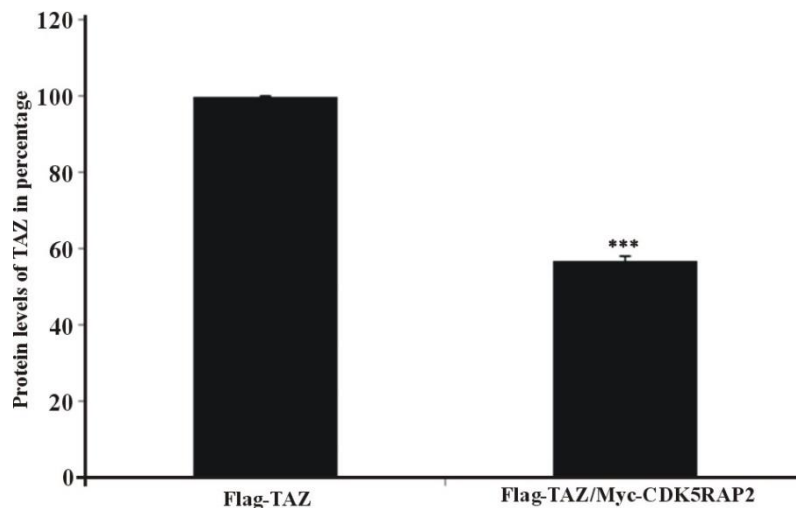
Figure 33. Ectopic expression of CDK5RAP2 affects the levelsof TAZ. A.Whole cell lysate for wild type (WT) HEK293T cells and HEK293T cells ectopically expressing Flag-TAZ, and cells ectopically expressing Flag-TAZ and Myc-CDK5RAP2. The blot was probed with pAb anti-Flag to reveal Flag, mAb 9E10 to reveal Myc and mAb GAPDH to reveal GAPDH . B. Quantification of Flag-TAZ from the whole cell lysate for HEK293T cells ectopically expressing Flag-TAZ, and cells ectopically expressing Flag-TAZ and Myc-CDK5RAP2. Signals were analysed using ImageJ. For loading control we used GAPDH levels. (P-value < 0.001).

In the Hippo signaling pathway, MST1 mediates the downstream phosphorylation events leading to the phosphorylation of TAZ on Ser-89, which creates a phosphoepitope that is rapidly engaged by 14-3-3, leading to inactivation and nuclear exclusion of TAZ (Lei et al., 2008). To directly investigate whether CDK5RAP2 influcences localisation of TAZ, we performed further fractionation experiments to reveal the cytoplasmic and nuclear levels of Flag-TAZ in cells ectopically expressing Myc-CDK5RAP2. In the cells transfected with Flag-TAZ, we observed cytoplasmic and nuclear distribution of TAZ. Upon ectopic expression of CDK5RAP2, we did not detect a difference in the ratio of the levels of Flag-TAZ in both compartments in comparison to the Flag-TAZ alone transfected cells showing that CDK5RAP2 does not influence the localisation of TAZ in the cells (Fig. 34). The decrease in the Flag-TAZ protein levels was also observed in whole cell lysates of the cells ectopically expressing Myc-CDK5RAP2 (Fig. 33).
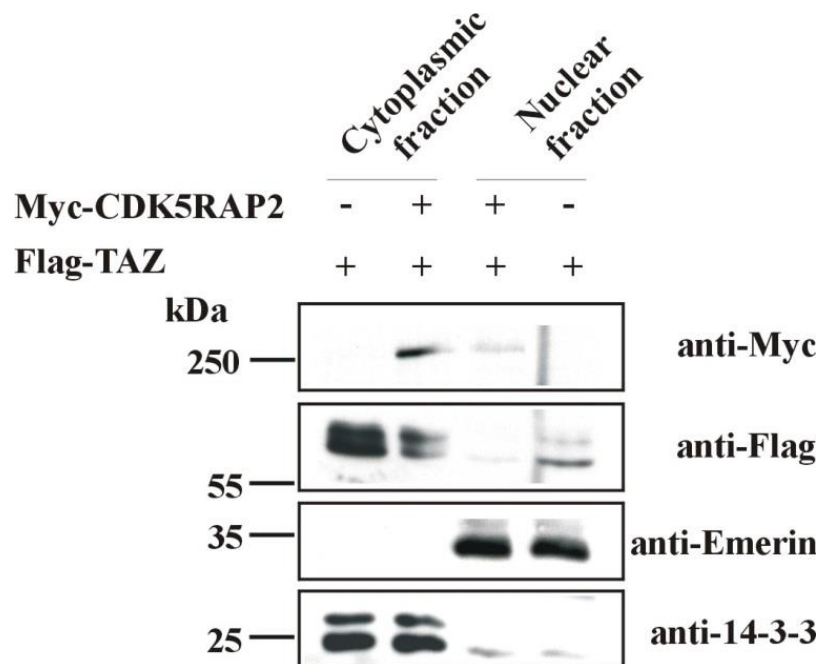
Figure 33. CDK5RAP2 does not influence the translocation of TAZ to the nucleus. Cell fractionation experiments of HEK293T cells expressing the indicated proteins. Please note the loading with the Myc-CDK5RAP2 fractions next to each other. 14-3-3 and emerin were used as cytosolic and nuclear marker proteins, respectively.

The substantial decrease in the protein levels of TAZ encouraged us to perform a quantitative-RTPCR (q-RTPCR) to examine the transcript abundance of TAZ. We used oligonucleotides (see Materials and Methods) which would recognize endogenous TAZ to amplify the transcripts in WT untransfected HEK293T cells and cells cotransfected with Myc-CDK5RAP2. We observed a decrease in the transcript levels of TAZ to ~80% of wild type level in cells ectopically expressing CDK5RAP2 (Fig. 35). The results indicate that CDK5RAP2 affects transcription of the *Taz* gene.
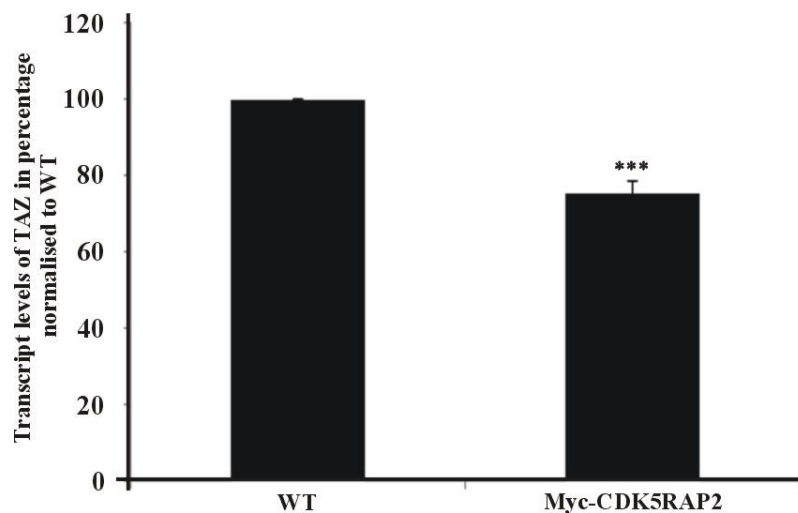
Figure 35. Effect of ectopically expressed Myc-CDK5RAP2 on endogenous TAZ mRNA levels. Quantitative RTPCR (q-RTPCR) to analyse the transcript abundance of endogenous TAZ in untransfected HEK293T cells (WT) and cells ectopically expressing Myc-CDK5RAP2 (P-value < 0.001).

2.5.3 CDK5RAP2 does not influence the interaction of TAZ with 14-3-3

In the cytoplasm, MST1 and LATS1 regulate the phosphorylation of TAZ at Ser-89. The phosphorylated motif of TAZ in turn interacts with 14-3-3 in the cytoplasm leading to the cytoplasmic retention of TAZ (Lei et al., 2008). In our coimmunoprecipitation assay we observed that TAZ interacts with the N-terminal part of CDK5RAP2. We further performed an interaction assay to identify if TAZ-CDK5RAP2 interaction affects the 14-3-3 binding affinity of TAZ. HEK293T cells were transfected with Flag-TAZ and then cotransfected with

Myc-CDK5RAP2. Flag-trap beads were used to precipitate Flag-TAZ and equal amounts of 14-3-3 protein were loaded on to the SDS-PAGE gel. The precipitate was probed for co-immunoprecipitated Flag-TAZ. Our assay did not show any significant difference in the interaction levels of TAZ and 14-3-3 between control and cells ectopically expressing CDK5RAP2. Thus it showed that CDK5RAP2 does not influence the interaction of TAZ and 14-3-3 proteins (Fig. 36).
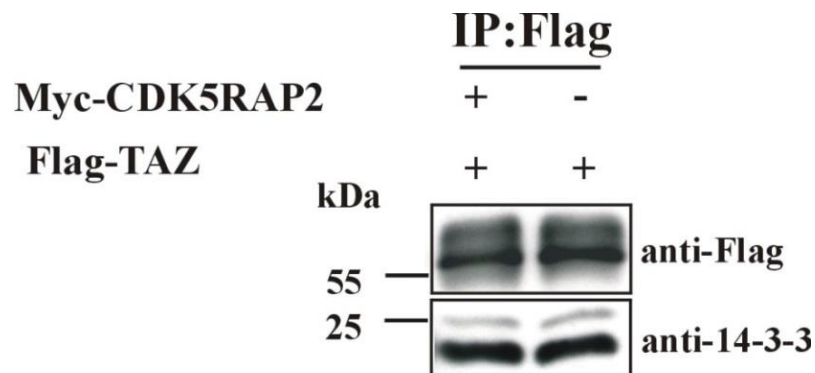
Figure 36. Interaction of TAZ with protein 14-3-3. Flag-trap beads were used to pull down Flag-TAZ from transfected HEK293T cells and the precipitate was probed with pAb specific for 14-3-3.

Appendix I: Mass spectrometry data of interactions partners for CEP161

Accession Number	Gene ID	Score	Interaction proved by
DDB0220454	act13	465.76	
DDB0230070	metK	65.66	
DDB0219924	hgsA	40.87	
DDB0191134	efaAII	38.85	
DDB0191133	abpA	38.78	
DDB0191154	p97	56.58	GST-CEP161-D3 pull down
DDB0191363	efbA	109.5	
DDB0191380	tuba	18.86	GST-CEP161-D3 pull down
DDB0191115	corA	46.58	
DDB0232994	psmd11	31.72	
DDB0233951	atp5B	68.33	
DDB0232968	psmC6	44.55	
DDB0238264	hsp-e2	95.03	
DDB0191262	ifdA	31.65	
DDB0267102	nap1	34.58	
DDB0232040	sptA	19.62	
DDB0215382	dscE	69.10	
DDB0201554	abpC	20.56	
DDB0231242	rpl5	20.55	
DDB0230070	metk	17.58	
DDB0229965	sarA	28.46	
DDB0235257	tufM	66.04	
DDB0214930	apm3	13.54	
DDB0191176	svka	34.28	GST-CEP161-D2 and -D3 pull down
DDB0215016	ddj1	39.16	
DDB0214937	gp130	34.20	
DDB0185207	vatB	22.31	
DDB0191169	tubB	33.19	
DDB0191103	ctxA	27.25	
DDB0233900	cp250	24.25	GST-CEP161-D3 pull down
DDB0191168	hapB	45.02	
DDB0191175	cadA	22.16	
DDB0219923	comA	25.03	

3. Discussion

CEP161 is a novel component of the *Dictyostelium* centrosome which has a gamma-Tubulin Ring Complex (γTuRC) domain and four predicted coiled coil domain and presumably forms an elongated molecule. These are the characteristics of a pericentriolar matrix protein. Using immunofluorescence analysis we identified CEP161 at the centrosome where it remained throughout the cell cycle (data not shown). For this association, the N-terminal part of the protein is responsible which harbors the γTuRC domain. The interaction site with its centrosomal binding partner CP250 is also located in this region.

We used mutant cells expressing various CEP161 polypeptides and studied their effect on cell size, growth, chemotactic motility and development, since these functions rely on an intact centrosome and a functioning microtubule system. The mutant cells had an altered size and a disadvantage when grown on a lawn of bacteria. This defective growth of mutants on the *Klebsiella* lawn was reflected by a reduced phagocytic activity of the mutant cells.

Further we observed changes in the motile behavior with respect to cell speed, motility and multicellular slug migration which points to the fact that CEP161 has important roles in cell polarity and directed migration. The motility defect could be partially attributed to the strong adhesion of the cells to the surface with reduced growth and development for the mutants. For a CP250 knockout mutant in which the interaction partner of CEP161 was completely missing we had observed similar defects in growth, development and motility (Blau-Wasser et al., 2009).

Ectopic expression of CEP161 also affected the localization of the centrosome. In ~80% of the cells it was located between 500-800 nm (~42%) and >900 nm (~40%) away from the nucleus, in wild type cells ~52% had a distance between 500-900 nm and only 12% a distance of >900 nm. Ectopic expression of the shortened D1, D2 and D3 proteins significantly

decreased the distance and the majority of the cells (>70%) had their centrosomes in the close vicinity of the nucleus (<500 nm). D1 and D2 expression led to an altered nucleus centrosome ratio. From our data it appears that the C-terminal residues 115-1381 of CEP161 have an impact on the regulation of the nucleus-centrosome distance and more general that the C-terminus is important for interactions with pathways that impact on cell physiology and centrosome biology.

A cross-talk among various signaling pathways has been implicated in growth and development of a cell (Huang et al., 2005; Zhao et al., 2010). We therefore set out to identify further partners of CEP161. In a proteomic analysis, we identified Hrk-Svk as interacting partner. Hrk-Svk is the homolog of *Drosophila melanogaster* Hippo and its serine/threonine kinase domain shows high similarity to Hippo homologs in higher organisms. Interestingly, some of the phenotypes like defects in development and directed slug movement that we observed upon ectopic expression of CEP161 and mutant proteins were also detected in Hrk-Svk mutants (Rohlfs et al., 2007). Hippo signaling is well characterised from *Drosophila* to humans, but the homologs/orthologs of the signaling members are not yet completely identified in lower organisms. In amoebozoans, the orthologs of TEAD and MOB1 and homolog of MST1 were identified, however no Warts/Lats or Yki/YAP homologs have been found (Sebé-Pedrós et al., 2012). Studies on another STE20 like protein, Kinase responsive to stress B (KrsB), revealed that it is an important regulator for cellular spreading, adhesion, chemotaxis and multicellular development (Artemenko et al., 2012). CEP161 controls various functions like growth, development, chemotaxis, adhesion and migration by possibly acting through the Hippo signaling pathway in *Dictyostelium*.

We could show that the interaction is conserved in mammalian cells as MST1, the Hrk-Svk homolog in humans, directly interacts with human CDK5RAP2. We further found that the amino acids 580–1271 of CDK5RAP2 are responsible for the interaction with MST1. These

amino acids are missing in several MCPH3 mutations which give rise to shortened proteins (Kraemer et al., 2011). Recently, it was reported that MST1 signaling controls centrosome duplication (Hergovich et al., 2009). Our data suggests that the centrosome duplication by MST1 could potentially be mediated through the interaction with CDK5RAP2, since we identified abnormal centrosome-nuclei ratio in Hela cells expressing CDK5RAP2-C1 and -C2 and the data is also consistent with results obtained for the *D. discoideum* cells expressing the CEP161-D1 and D2 proteins. We were also able to show for the first time that TAZ interacts with the N-terminal part of CDK5RAP2 (Fig. 35) and that the transcript and protein levels of TAZ were influenced by ectopically expressing CDK5RAP2. The interaction of CDK5RAP2 with TAZ does not affect the downstream interaction of TAZ with 14-3-3.

Our data for the first time implicates CDK5RAP2 in the control of cell size, growth and development and suggests that CDK5RAP2 could potentially be a novel regulator of the tumor suppressive Hippo pathway. Our findings further provide a possible explanation for the phenotype of small sized brain in microcephaly patients carrying loss-of-function mutations in CDK5RAP2. It is reported that loss of Mst1/2 or Lats1/2, or activation of YAP-TEAD in neural progenitor cells leads to a marked expansion of neural progenitors, partially due to upregulation of cell cycle re-entry and stemness genes, and a concomitant block to differentiation by suppressing key genes. Conversely, YAP loss of function results in increased cell death and precocious neural differentiation (Cao et al., 2008). Furthermore, bone marrow-derived mesenchymal stem cells depleted of TAZ show decreased osteogenesis (Hong et al., 2005). In addition, YAP and TAZ proteins are important in brain development (Lavado et al., 2013). In neuronal cells, loss of CDK5RAP2 might lead to insufficient TAZ-dependent proliferative signaling under certain conditions leading to reduced size of the brain. This idea is supported by the observation that there is a significant reduction in brain size in

MCPH patients with a mutation in *CDK5RAP2* leading to a non-functional protein (Bond et al., 2005).

Although further studies are needed to clarify the in vivo importance of the CDK5RAP2 mediated control of Hippo signaling, our findings may have important consequences. Normal organ development requires cellular proliferation to guarantee organ growth and tissue regeneration. One of the major downstream components of the Hippo signaling is TAZ, the activation of which leads to translocation to the nucleus to transcribe its target genes to promote cell proliferation, development and differentiation (Nishioka et al., 2009; Zhang et al., 2009a). Significantly, TAZ is overexpressed in many human tumors which include breast cancer samples and papillary thyroid carcinoma tissues (De Cristofaro et al., 2011), whereas attenuation of TAZ activity tends to have the opposite effect in the central nervous system (Lavado et al., 2013). In addition, Taz knock out mice were readily identified by their smaller size compared to their normal littermates (Tian et al., 2007). Furthermore, conditional knockout mouse of Mst1 and Mst2 in a variety tissues were generated and severe context-dependent phenotypes were observed with higher proliferation in liver and heart, but a reduced growth in pancreas (Zhou et al., 2009; Heallen et al., 2011; George ., 2012). Our data also show that CDK5RAP2 can control the activity of the Hippo pathway by regulating the transcript levels of TAZ, which is the master regulator of this pathway. The antagonistic regulation of TAZ by CDK5RAP2 suggests that it may act as a novel regulator of Hippo by controlling the proliferative signaling, which may be critical for growth and development of the brain. Our model shows that CDK5RAP2 could regulate the Hippo pathway at multiple sites. The EB1 domain of CDK5RAP2 interacts with MST1, whereas the N-terminal part which includes the γTuRC and SMC domain interacts with TAZ. However, CDK5RAP2 could possibly down regulate the transcription of the Taz gene by a non-canonical Hippo signaling pathway (Fig. 37).

Our *Dictyostelium* CEP161 and human CDK5RAP2 studies support the hypothesis that the Hippo pathway could be antagonistically regulated by CDK5RAP2, affecting proliferation, size, growth, development, polarity and migration. Thus, lack of CDKRAP2 in microcephaly patients may deregulate the activity of the Hippo signaling pathway, resulting in antiproliferative cellular signaling and thus, leading to reduced or insufficient growth. This might explain some aspects of the phenotype of MCPH. Understanding the degree to which this mechanism plays a role in MCPH in vivo will require further studies using animal models and patient cells.
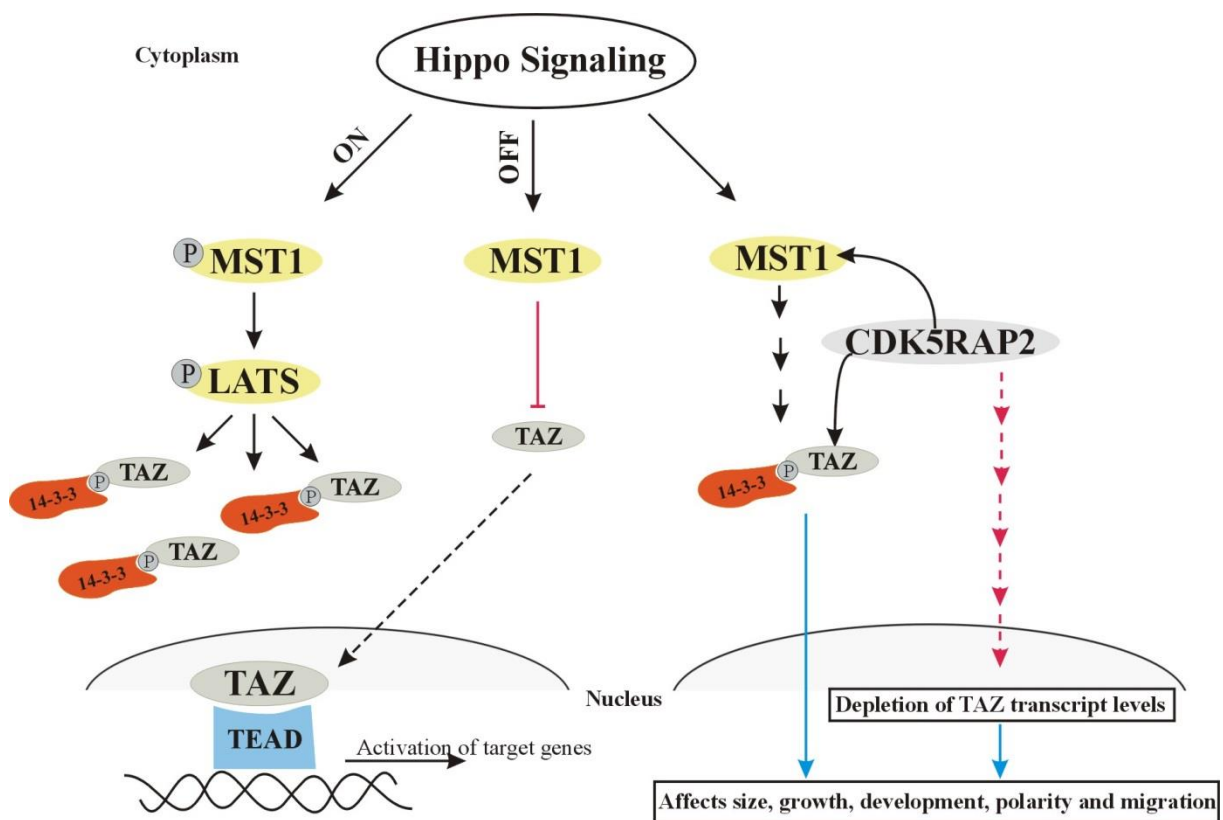
Figure 37. Model for CDK5RAP2 role as a novel regulator in the Hippo signaling pathway. CDK5RAP2 interacts with core Hippo components MST1 and TAZ and also downregulates the transcription levels of TAZ. CDK5RAP2 influence on Hippo pathway components in vertebrates is shown in various colors, with black pointed for direct

interactions and red blunt arrowheads indicating inhibitory interactions. CDK5RAP2 directly interacts with MST1 and TAZ. The interaction with TAZ does not influence its interaction with 14-3-3. Red dashed lines indicate unknown mechanisms of TAZ depletion in transcript levels by CDK5RAP2, whereas black dotted lines indicate translocation of TAZ to the nucleus. The blue pointed arrow indicates the functions affected. Abbreviations: MST1, Mammalian sterile 20 like 1; LATS, Large tumor suppressor; TAZ, transcriptional co-activator with PDZ- binding motif; TEAD, TEA domain protein.

4. Material and methods

Standard molecular biology techniques were performed as described in Sambrook et al., 1989. Light and heavy instruments used were properties of the Department. Standard laboratory materials and reagents were obtained from local suppliers.

4.1   Kits

NucleoSpin Extract 2 in 1	Macherey-Nagel
M-MLV reverse transcriptase RNase H Minus-kit	Promega
Quick Change Site-Directed Mutagenesis kit	Stratagene
pGEM-T easy Vector kit	Promega
Pure Yield Plasmid System	Promega

4.2   Enzymes, antibodies and antibiotics

4.2.1   *Enzymes for molecular biology:*

Taq-polymerase	Promega
T4 DNA ligase	Boehringer
Thrombin	GE Healthcare
Pfu DNA polymerase	Promega
GoTaq qPCR master mix	Promega
Alkaline phosphatase	Roche
Restriction endonuclease	New England Biolabs
Ribonuclease A	Sigma
Trypsin	Invitrogen

4.2.2 Primary antibodies

Mouse monoclonal anti- α-actinin mAb 47-16-8	(Schleicher *et al*., 1984)
Mouse monoclonal anti-csA mAb 33-294	(Berthold *et al*., 1985)
Mouse monoclonal anti-cap32 mAb 188-19-95	(Haus *et al*., 1993)
Mouse monoclonal anti-GFP mAb K3-184-2	(Noegel *et al*., 2004)
Mouse monoclonal anti-comitin mAb 190-340-8	(Weiner et al., 1993)
Mouse monoclonal anti-CEP161 mAb K83-632-4	This study
Mouse monoclonal anti-myc 9E10	Santa Curz Biotech
Mouse monoclonal anti-CP250 mAb K68-332-3	(Blau-Wasser et al., 2009)
Mouse- monoclonal anti-emerin (4G5)	Abcam
Mouse- monoclonal anti-GAPDH	Sigma
Rabbit polyclonal anti-GST	(Xiong *et al*., 2008)
Rabbit polyclonal anti-CDK5RAP2	Millipore
Rabbit polyclonal anti-14-3-3	Sigma
Rabbit polyclonal anti-Flag	Sigma
Rabbit polyclonal anti-CEP161	This study
Rat-anti-α-tubulin (YL1/2)	(Kilmartin et al., 1982)
Rabbit-anti-pericentrin	Abcam
Rabbit polyclonal anti-14-3-3	Santa Cruz Biotechnology
Rabbit polyclonal anti-Hrk-Svk	(Rohlfs et al., 2007)

4.2.3 Secondary antibodies

Anti-mouse IgG, Alexa488-conjugated	Sigma
Anti-mouse IgG, Alexa568-conjugated	Sigma
Anti-goat IgG, Alexa568-conjugated	Sigma
Anti-mouse IgG Alexa Fluor 488	Invitrogen

Anti-mouse IgG POD	Sigma
Anti-rabbit IgG POD	Sigma
Anti-rat IgG POD	Sigma

4.2.4 Antibiotics

Ampicillin	Sigma
Kanamycin	Sigma
Blasticidin S	Biomedicals
Dihydrostreptomycinsulphate	Sigma
Tetracyclin	Sigma
Gentamicin	Sigma
G418	Sigma
Penicillin/Streptomycin	Biochrom

4.3   Media and Buffers

All solutions and media used in the course of these experiments were prepared with deionized water from a pure water source in the laboratory. All other buffers and solutions which were not mentioned here are stated in the methods.

4.3.1 Buffers and Solutions

GST-fusion protein elution buffer, pH 7.2

50 mM Tris/HCl, pH 7.2

100 mM NaCl

10 mM reduced glutathione

0.2 % Tween-20

10 mM DTT

10 x NCP-buffer, pH 8.0

12.1 g Tris

87.0 g NaCl

5.0 ml Tween 20

2.0 g NaCl

Made up to 1 litre with deionised water, pH adjusted with HCl

50 x Tris/Acetate buffer (TAE), pH 8.0

242 g Tris

57.1 ml 16.6 M Glacial acetic acid

100 ml 0.5 M EDTA

Made up to 1 litre with deionized water

TBS lysis buffer, pH 7.2

50 mM Tris/HCl, pH 7.2

100 mM NaCl

TE-buffer, pH 8.0

10 mM Tris/HCl, pH 8.0

1 mM EDTA

4.3.2 Bacterial medium and agar plates

LB-medium (Sambroock *et al*., 1989)

10 g/l Bacto-Tryptone

5 g/l Yeast Extract

5 g/l NaCl

pH was adjusted to 7.0 with 5 M NaOH and the volume brought to 1 litre with deionised

water and then autoclaved.

<u>Ampicillin-LB-agar plates</u>

For the preparation of LB-agar plates, 0.9% (w/v) agar was added to LB-medium. After autoclaving and cooling to ~55°C, 100 mg/l ampicillin was added. Storage was at 4°C.

To prepare plates with ampicillin/IPTG/X-Gal, 10 µl of 1M IPTG and 50 µl of 20 mg/ml X-Gal was spread over the surface of LB-Amp-Plates and allowed to absorb for at least 30 minutes at 37°C prior to use.

4.3.3 Yeast medium

<u>YEPD-medium</u>

20 g Difco-Peptone

10 g Yeast Extract   Made up to 1 litre with deionized water and then autoclaved

<u>YEPD-agar plates</u>

20 g Difco-Peptone

10 g Yeast Extract

18 g Agar-Agar

Made up to 1 litre and then autoclaved

<u>100x L-Adenine solution</u>

200 mg of L-Adenine dissolved in 100 ml H$_2$O. Dissolution was aided with addition of drops of HCl and then sterile filtered.

<u>100x L-Tyrosine solution</u>

300 mg of L-Tyrosine dissolved in 100 ml H$_2$O. Dissolution was aided with addition of drops of NaOH and then sterile filtered.

<u>100x L-Histidine solution</u>

200 mg of L-Histidine dissolved in 100 ml H$_2$O and then sterile filtered.

<u>100x L-Leucine solution</u>

200 mg of L-Leucine dissolved in 100 ml H$_2$O and then sterile filtered.

100x L-Tryptophan solution

200 mg of L-Tryptophan dissolved in 100 ml H_2O and then sterile filtered.

100x L-Uracil solution

200 mg of L-Uracil dissolved in 100 ml H_2O. Dissolution was aided by slightly warming solution before it was sterile filtered.

50x Drop-out Solution

1,500 mg Isoleucine

7,500 mg Valine

1,000 mg Arginine

1,500 mg Lysine

1000 mg Methionine

2,500 mg Phenylalanine

10,000 mg Threonine

Filled up to 1 litre and then sterile filtered

20x Drop-out Solution

20 ml 50x Drop-out solution

10 ml 100x L-Uracil

10 ml 100x L-Tyrosine

10 ml 100x L-Adenine

1 M 3-Amino-1, 2, 4-triazol solution (3AT)

8.4 g 3-Amino-1, 2, 4-triazol dissolved in 100 ml deionised H_2O and then sterile filtered.

Composition of the Yeast Selection Plates and Selection Medium

	SD/-Leu/-Trp	SD/-Leu/-Trp/-His/+3AT
Yeast Nitrogen Base (g)	6.7	6.7

Agar-Agar (g)	20	20
Water (ml)	770	745
20% Glucose solution (ml)	100	100
20x Drop-out solution (ml)	50	50
100 x L-Histidine (ml)	10	
100 x L-Leucine (ml)	-	
100 x L-Tryptophan (ml)	-	
1M 3AT Solution (ml)		25

Yeast selection media were prepared but without the addition of the 20 g Agar to the preparations. To test for protein interactions, transformants on the SD /-Leu /-Trp plates were transferred to the SD /-Leu /-Trp /-His /+3AT plates. After 6-8 days, the colonies which grew were used to perform β-galactosidase activity staining.

4.4 Media and buffers for *Dictyostelium* cultures

<u>AX2-medium, pH 6.7 </u>(Claviez et al., 1982)

7.15 g Yeast extract

14.3 g Peptone

18.0 g Maltose

0.486 g KH_2PO_4

0.616 g Na_2HPO2 x H_2O

Made up with H_2O to 1 Liter

<u>Soerensen phosphate buffer, pH 6.0 </u>(Malchow et al., 1972)

2 mM Na_2HPO_4

14.6 mM KH_2PO_4

Phosphate-agar plates, pH 6.0

9 g agar made up with Soerensen phosphate buffer pH 6.0 to 1 Litre

Water agar plates

1% agar in Water

4.5 Bacteria, *D. discoideum*, and yeast strains

Bacteria

E.coli (XL1 blue) (Bullock et al., 1987)

E.coli (BL21) (Studier and Moffatt, 1986)

D. discoideum

AX2-214, also known as AX2 is a derivative of NC4 wild isolate (Raper, 1935) which can grow axenically.

Yeast strain

Saccharomyces cerevisiae Y190 (*His3* and *lacZ* reporter genes) (Johnston et al., 1991; Harper et al., 1993).

4.6 Oligonucleotides

Oligonucleotides used for PCR (Polymerase Chain Reaction) were purchased from Sigma-Genosys in Steinheim.

Cep161 1F   GGATCCATGAATGGATGGGGAGAAAGTGACG

Cep161 2320R   GGATCCGTAGATCTTCCTTCTCATCGAATAGC

Cep161 2293F   GGATCCTTGCTATTGGATGAGAAGGAAGATCTAC

Cep161 3342R   CCCGGGGATATCAGGATTTAAAGTTATTAAAGATGAAG

Cep161 3314F   GGATCCTCATCTTTAATAACTTTAAATCCTGATATC

Cep161 4143R   CCCGGGTTTTATTTGTTGTTTAAGTAAATTTAATTGTTTG

For site directed mutagenesis

Cep161 3295R   GAGCTAAAGAGATGGTCATGGTTCTTTTGGTTGTGG

Cep161 2290R   CCTTCTCATCCAATAGCAATTACTGTTGTTGTTGATTAGCC

For q-RTPCR

Taz 694F   AGAGAATGAGGGGAAAGGTGTT

Taz 1023R   CCGATCAGCACAGTGATTTTCT

4.7 *Dictyostelium* vector construction and transfection

For expression of CEP161 GFP fusion proteins in *Dictyostelium*, sequences encompassing amino acids 1-1114 corresponding to nucleotides 1-3340 (GFP-CEP161-D1), amino acids 1-763 corresponding to nucleotides 1-2290 (GFP-CEP161-D2) and amino acids 763-1114 corresponding to nucleotides 2290-3340 (GFP-CEP161-D3) were cloned into pBsr GFP N2 vector (Blau-Wasser et al., 2009). Expression was under the control of the constitutively active *D. discoideum* actin15 promoter. A PCR-mediated site-directed mutagenesis (QuikChange Site-Directed Mutagenesis Kit, Stratagene) was used to generate mutations in CEP161 to produce the GFP-CEP161-D1 and GFP-CEP161-D2 plasmids to yield truncated proteins. The mutations were confirmed by sequencing. The plasmids were introduced into AX2 cells by electroporation using a Biorad electroporator Gene Pulser Xcell (Biorad, München, Germany) according to the protocol supplied (Faix et al., 2004). Cells expressing GFP tagged proteins were identified by immunofluorescence analysis and western blotting.

4.8 Cloning of CEP161 genomic DNA and expression of recombinant proteins

For expression of recombinant CEP161-D2 (1-763aa) and -D3 (763-1114aa) as glutathione S transferase (GST) fusion proteins in *E. coli*, genomic DNAs were respectively cloned into pGEX-4T-1 vector (GE Healthcare Life Sciences). The Hrk-SvkA-E1 (1-323aa) and -E2 (290-478aa) constructs cloned in to pGEX-4T-1 vector were kindly provided by Prof. Michael Schleicher, Ludwig-Maximilians-University, München, Germany. *E. coli* strain XL1 Blue

was used for expression of the GST fusion proteins. Induction of protein expression was with 0.25 mM isopropyl β-D-thio-galactoside (IPTG) when an OD_{600} of 0.8 was reached. Cells were further cultured at 30°C for 3 hours. They were harvested, lysed in 50 mM Tris/HCl, pH 7.4, 100 mM NaCl, supplemented with Protease inhibitors (0.5 mM PMSF, 1mM Benzamidine and Complete (Roche) and 1mM DTT with an EmulsiFlex cell homogenizer (Avestin Europe GmbH, Mannheim, Germany). Lysates were separated into soluble and insoluble fractions by centrifugation at 18,000g. The fusion proteins from the soluble fraction were purified using GST-Sepharose beads (GE Healthcare).

4.9 Growth and development

Growth and development were done as described (Khurana et al., 2002). Cells were either grown on a lawn of *K. aerogenes* on SM agar plates, on a lawn of *E. coli* B12 on NA-agar or cultivated in shaking suspension (160 rpm) or in a submerged culture at 21-23°C in axenic medium (Harloff *et al*., 1989). Development was initiated by plating 5 x 10^7 cells which were washed twice with Soerensen phosphate buffer (17 mM Na^+/K^+ phosphate, pH 6.0) on phosphate agar plates and monitored. Development was also followed for cells starved in Soerensen phosphate buffer in shaken suspension (1 x 10^7 cells/ml; 160 rpm at 22°C) or in petri dishes. Mutants were maintained in the presence of appropriate antibiotics (3-5 µg/ml Blasticidin) (MP Biomedicals Inc., Eschwege, Germany). The following strains have been used; AX2-214 (wild type) (Noegel *et al*., 1985), AX2 expressing GFP tagged fusion proteins CEP161, D1, D2 and D3.

4.10 Generation of Antibodies

Mouse monoclonal antibodies were generated against CEP161-D2 (amino acids 1-763) as described (Xiong et al., 2008). For immunization of mice the GST-part was removed by thrombin cleavage. The identity of the CEP161 polypeptide was confirmed by mass

spectrometry. mAb K83-632-4 was used in this study. It recognized the bacterially produced recombinant protein and the endogenous protein in immunofluorescence. Rabbit polyclonal antibodies specific for CEP161 were generated against a GST fusion protein containing the amino acids 763-1114 (CEP161-D3). Polyclonal antibodies were generated by Pineda, Berlin, Germany. The pAb CEP161 recognized the recombinant and the endogenous protein in western blots of whole cell lysates. The polyclonal antibodies did not show a specific signal in immunofluorescence. For cleavage of the D3 protein from GST-Sepharose beads, the beads bound GST fusion proteins were washed 5 times with cleavage buffer (20 mM Tris/HCl, pH 7.4, 150 mM NaCl and 0.2 % Sarkosyl). Beads were then re-suspended in cleavage buffer and 3-5 U Prescission protease /mg fusion protein were added to the beads and incubated with little agitation at 4^0C overnight. As CEP161-D3 was released from the beads together with GST, we next performed an anion exchange chromatography step in order to separate the proteins. For this the protein solution was dialyzed against 20 mM Tris/HCl, pH 8.0, and 1 mM EDTA overnight before loading onto a DE-52 Sephadex column which had been calibrated with 50 mM Tris/HCl, pH 8.0, 1 mM EDTA. The protein was eluted with 1 M NaCl and the eluate dialyzed and analyzed by SDS-PAGE.

4.11 Immunofluorescence analysis for *D.discoideum* cells.

Immunofluorescence study was performed as previously described (Blau-Wasser *et al*., 2009). Briefly, cells were transferred onto coverslips in Petri dishes and fixed by ice-cold methanol (5 min, 20 °C). Cells were treated twice for 15 min (room temperature) with blocking solution (1x PBS containing 0.5% (wt/vol) BSA and 0.1% (vol/vol) fish gelatin). The appropriate antibodies were diluted in the blocking solution and applied on the cells for 1 h at room temperature; the excess of antibodies was removed by washing with the blocking solution before the 1 h incubation with the corresponding secondary antibodies. Analysis of fixed was done by laser scanning confocal microscopy using a Leica TCS SP5 microscope.

4.12 Pull down and immunoprecipitation assays for *D.discoideum*

For pull down and immunoprecipitation experiments, *D. discoideum* cells were lysed in 50 mM (10 mM for immunoprecipitation assay) Tris/HCl, pH 7.4, 150 mM NaCl, 0.5% NP40, supplemented with protease inhibitor cocktail (Sigma), 0.5 mM PMSF, 0.5 mM EDTA, and 1 mM Benzamidine by passing them through a 25G syringe (10-20 strokes) and incubated with agitation (1000 rpm) for 15 min at 4ºC (to ensure complete cell lysis) followed by a centrifugation step at 16,000 rpm for 10 min. The supernatants were either incubated with GST and GST-fusion proteins respectively or with GFP-trap beads (ChromoTek, Martinsried, Germany). After incubation for 3 h while GST beads were washed three times with wash buffer (50 mM Tris/HCl, pH 7.4, 150 mM NaCl, protease inhibitor cocktail, 0.5 mM PMSF, 0.5 mM EDTA, 1 mM Benzamidine), GFP-trap beads were washed with a different wash buffer (10 mM Tris/HCl pH 7.4, 50 mM NaCl, protease inhibitor cocktail, 0.5 mM PMSF, 0.5 mM EDTA, 1 mM Benzamidine). The beads were resuspended in SDS sample buffer, incubated at 95ºC for 5 min and the proteins separated by SDS-PAGE and analyzed by western blot.

4.13 Analysis of *D. discoideum* nuclear and centrosome abnormalities

The centrosome was stained with mAb K83-632-4 for CEP161; DNA of the fixed cells was stained with DAPI. Confocal microscopy images were taken and nuclei and centrosome number and the distance between centrosome and nucleus determined. The centrosome-nucleus distance was measured using the scale bar in the LAS-AF-LITE software for confocal microscopy imaging.

4.14 *D. discoideum* cell adhesion assay

To analyse cell-substrate adhesion a substrate detachment assay was carried out. A total of 1×10^6 cells in growth medium were added per well (24 well plates, Costar) and incubation

was for four hours at 22°C. Then the plates were shaken on a gyrotary shaker at 60, 120 and 200 rpm for one hour each. The number of detached cells was counted in a hemocytometer. The total number of cells was determined after resuspension of all cells and the percentage of detached cells calculated.

4.15 *D. discoideum* cell migration studies

This analysis was done as previously described (Blau-Wasser et al., 2009; Müller et al., 2013). Briefly, growing cells were plated in a chamber (ibidi GmbH-Martinsried, Germany) and random motility was followed. Images were recorded at intervals of 6 s using a Leica DM-IL inverse microscope (Deerfield, IL; 40x objective) and a conventional CCD video camera and analyzed using Dynamic Image Analysis Software (DIAS, Soll Technologies, Iowa City, IA). The DIAS software was used to trace individual cells along image series and automatically outlined the cell perimeters and converted them to replacement images from which the position of the cell centroid was determined. Speed and change of direction were computed from the centroid position. For processing images, Corel Draw version 11 and Adobe Photoshop were used.

4.16 Phototaxis assay

Phototaxis assays were essentially performed as described earlier (Khaire et al., 2007). For phototaxis, cells from shaking suspension culture were washed with Soerenson buffer and 5×10^5 cells were placed in the center of a water agar plate. The cells were allowed to adhere on to the agar surface and incubated in a dark chamber with a light source only at one end of the plate. Slugs were allowed to form and migrate towards light. After 48 h, slugs and slime trails were transferred onto nitrocellulose filters and stained with Amido Black. The filters exhibiting the stained slime trails were used to determine the distance travelled by the slugs

towards the source of light from the point of application. The angle of deviation of the slugs was measured with the software Kreiswinkelmesser.

4.17 Yeast Two-Hybrid Interaction

For the yeast two-hybrid screen, the full-length cDNAs of *D. discoideum* CP250 were cloned in frame into the yeast pAS2-1 vector (Clontech), resulting in fusion to the GAL4-DNA-BD (BD, binding domain). cDNA corresponding to 1- 763aa and 763 to 1114 aa of DdCEP161 was cloned into the yeast pACT2 vector (Clontech) resulting in a fusion to the GAL4-DNA-AD (AD, activation domain). Yeast Y190 strain which has *His3* and *lacZ* reporter genes was used for this assay.

Candidate colonies expressing interacting proteins were screened by plating on SD/-Leu/-Trp/-His/+3AT plates after which membrane colonies-lift β-galactosidase activity assay was performed according to the MATCHMAKER Y2H system manual. Briefly, colonies on SD/-Leu/-Trp/-His/+3AT selection plates were transferred to a Nitrocellulose membrane (Protran BA 85) by placing the membrane over colonies on selection plates for 20 min. The filter was carefully lifted off the agar plates and transferred (with colonies facing up) to a pool of liquid nitrogen for 10 sec. The frozen filter was then allowed to thaw at RT and placed on a Whatman filter paper presoaked in freshly prepared X-Gal solution (60 mM Na_2HPO_4, 40 mM NaH_2PO_4, 10 mM KCl, 1 mM $MgSO_4$, pH 7.0, 50 mM β-mercaptoethanol, X-Gal (1 mg/ml final concentration)) and incubated at 30^oC and checked between 1 to 6 h for the appearance of blue colonies.

4.18 Mammalian cell culture, constructs and transfection

HeLa (human epithelial carcinoma) and Hek293T (Human embryonic kidney) cell lines were grown in high glucose Dulbecco's Modified Eagle's Medium (DMEM, Sigma) supplemented

with 10% FBS, 2 mM glutamine, and 1% penicillin/streptomycin. All cells were grown in a humidified atmosphere containing 5% CO_2 at 37^0C.

Plasmidsfor mammalian cell transfection studies

Myc-CDK5RAP2	Addgene plasmid 41152
Myc-CDK5RAP2-C1 (1-580aa)	This study
Myc-CDK5RAP2-C2 (1-1271aa)	This study
GFP-MST1	B.Schermer (CECAD, Cologne, Germany)
Flag-TAZ	M. Yaffe (Massachusetts Institute of Technology, Boston, MA)
Lats	M. Yaffe (Massachusetts Institute of Technology, Boston, MA)
pGBD-Hyg-Luc and pGal4-TEAD	Biomyx, San Diego, USA

The cells were transfected using the reagent Polyethylenimine (PEI) Polysciences, Inc. (Catalogue No 23966-2). PEI condenses DNA into positively charged particles, which bind to anionic cell surface residues and are brought into the cell via endocytosis. For transfection, PEI and the DNA constructs are used in the ratio of 1:3. The mixture is incubated at room temperature in serum free DMEM media for 15 minutes and added directly on to the cells.

4.19 Immunofluorescence

Immunofluorescence was done as described (Taranum et al., 2012). The cells were grown on 12 mm coverslips and fixed with 3% paraformaldehyde (5 min, RT), followed by permeabilization with 0.5% Triton X-100 for 3 minutes (RT). Subsequently, the fixed cells were washed three times with 1x PBS and incubated for 15 minutes with blocking solution (1x PBG: PBS containing 5% BSA and 0.045% fish gelatine in 1x PBS, pH 7.4). After blocking, primary antibodies were diluted in PBG and incubated 1 h (RT) or overnight (4°C). The cells were washed three times for 5 minutes each, the samples were incubated with

appropriate secondary antibodies conjugated to Alexa 488/568 (1:1.000 diluted in PBG) for one hour at room temperature. Nuclear DNA was stained with 4',6-Diamidino-2'-phenylindole (DAPI, Sigma). Finally the coverslips were mounted on glass slides with gelvatol. Imaging was done by confocal laser scanning microscopy (Leica TCS-SP5). Images were processed using TCS-SP5 software.

3% Paraformaldehyde

3% PFA is dissolved in 1x PBS at 55^0C with stirring at room temperature for overnight.

10x PBG

10x PBS

5% BSA

0.45% Fish Gelatin

10x PBS

80 g NaCl

2 g KCl

14.4 g Na_2HPO_4

2.4 g KH_2PO_4

Adjust the pH to 7.4 with HCl and make up the volume to 1L with H_2O

4.20 Immunoprecipitation

For immunoprecipitation experiments, HEK293T cells were lysed in 10 mM Tris/HCl, pH 7.4, 50 mM NaCl, 0.5% NP40, protease inhibitor cocktail, 0.5 mM PMSF, 0.5 mM EDTA, 1 mM Benzamidine and incubated for 30 min at 4ºC (to ensure complete cell lysis) followed by a centrifugation step at 16,000 rpm for 10 min at 4ºC. The supernatants were either incubated with GFP-trap beads (ChromoTek, Martinsried, Germany) or with Flag-trap beads (Sigma, st.Louis, USA, Catalog Number A2220) for 2 hours at 4ºC. GFP-trap beads were washed with a different wash buffer (10 mM Tris/HCl pH 7.4, 50 mM NaCl, protease inhibitor cocktail,

0.5 mM PMSF, 0.5 mM EDTA, 1 mM Benzamidine). The beads were resuspended in SDS sample buffer, incubated at 95ºC for 5 min and the proteins separated by SDS-PAGE and analyzed by western blot.

4.21 Fractionation of cytoplasmic and nuclear proteins

HEK293T cells were transfected with Flag-TAZ and Myc-CDK5RAP2. The transfected cells were suspended in 1 ml hypotonic buffer (10 mM HEPES, pH 7.9, 1.5 mM MgCl$_2$, and 10 mM KCl, PIC) followed by centrifugation (1000 rpm, 20 s, 4°C). Pellets were again resuspended in 1 ml hypotonic buffer. Cell suspensions were lysed through a needle (0.4 mm) for 10 times and incubated on ice for 10 min. Nuclear and cytoplasmic fractions were separated by centrifugation (1000 rpm, 10 min, 4°C). Pellets (nuclear fraction) were washed with 1 ml PBS (1000 rpm, 6x10 min, 4°C). The samples were boiled in SDS sample buffer (95°C, 5 min) and analyzed by western blot.

4.22 Protein extraction from mammalian cells

Mammalian cells were trypsinised and washed with ice cold 1x phosphate buffered saline (PBS) plus protease inhibitor (DTT, Benzamidine and PMSF at 1 mM each). After centrifugation at 15,000 rpm at 4°C the pellet was resuspended in lysis buffer (50 mM Tris/HCl, pH 7.5, 50 mM NaCl, 1% Nonidet P-40, PIC and further protease inhibitors DTT, Benzamidine and PMSF. The sample was denatured in 5x SDS sample buffer at 95°C for 5 minutes. The samples were used for SDS-PAGE and western blot analyses.

5 x SDS-Sample buffer

5 x SDS loading buffer

2.5 ml 1M Tris/HCl, pH 6.8

4.0 ml 10% SDS

2.0 ml Glycerol

1.0 ml 14.3 M ß-Mercaptoethanol

200 µl 10% Bromophenol blue

4.23 Western blotting

For immunoblotting, equal amounts of total cell protein were separated by SDS-PAGE (12%, 3%-12% gradient gel). After the SDS-PAGE, sheets of Whatman filter papers and nitrocellulose membranes were pre-cut to the gel dimensions. The Whatman papers, sponges, membranes, and gels were immersed in transfer buffer for 5 min. For protein transfer, semi-dry (45 min, 12 Volt) or wet blotting (overnight, 15 Volt) transfer was used. Subsequently, the membrane was blocked with 12.5 ml 1% blocking solution under constant shaking for 1 h. After blocking, the membrane was incubated with primary antibody solution for either overnight (+4°C) or 1 h (RT). The membrane was washed three times with NCP for 15 min and incubatedwith the corresponding appropriate horseradish peroxidase coupled secondary antibodies (1:10.000) for 1 h, and the membrane was washed three times with NCP. Antigen-antibody complexes were detected by using the ECL western blotting detection solution. The protein bands were visualized using X-ray films. After imaging, the membrane was stripped with 0.2 M NaOH for 15 min. The stripped membrane was washed twice with NCP for 15 min. After washing the membrane, the membrane was blocked with blocking solution for 1 h at room temperature and used for antibody incubation.

Transfer buffer SDS-gels

48 mM Tris/HCl, pH 8.3

39 mM glycine

10% ethanol

Ponceau staining solution

2 g Ponceau S

100 ml 3% Trichloroacetic acid

0.04% Tween 20

ECL solution

2 ml 1 M Tris/HCl (pH 8.0)

200 μl Luminol (0.25 M in DMSO) 3-aminonaphthylhydrazide

89 μl (0.1 M in DMSO) p-coumaric acid

18 ml dH$_2$O

6.3 μl 30% H$_2$O$_2$

Blocking solution

4% milk-powder in TBS-T

4.24 Luciferase assay

The luciferase reporter plasmid (pGBD-Hyg-Luc) was transfected together with an activator plasmid (pGal4-TEAD), pGL4.74 (Promega) for normalization, and the indicated expression plasmids (TAZ, CDK5RAP2, Lats1, and the control empty pcDNA6) into HEK293T cells in a 96-well format using Lipofectamine LTX (Invitrogen) as a transfection reagent. The total amount of DNA was always adjusted with empty pcDNA6. Renilla luciferase and firefly luciferase activities were measured by using a reporter assay system (Dual Luciferase; Promega) in a luminometer (Mithras LB 940; Berthold) 24 h after transfection. For the Lats1 siRNA experiment, the indicated plasmids and siRNAs were cotransfected into HEK293T cells. The measurement was performed 48 h after transfection. Transfections and measurements were performed in triplicates for each single experiment, and each experiment was repeated at least three times. Error bars shown in the figures represent SEM. P-values were calculated using an unpaired Student's t test. Equal expression of the transfected proteins was confirmed by Western blot analysis.

4.25 RNA isolation and cDNA generation for quantitative RT-PCR analysis

For RT-PCR, total RNA was extracted for gene expression analysis using TRIzol (Invitrogen). Briefly, the cells were trypsinised and centrifuged in ice cold PBS (1200 rpm, 5 min). The pellet was suspended in 1 ml TRIzol (50-100 mg cells) and incubated for 5 min (RT). Subsequently, chloroform (for each ml of TRIzol 200 µl) was added, mixed and incubated at RT for 2-3 min followed by centrifugation (12,000 g, 15 min). The aqueous phase was precipitated with isopropanol (for each ml of solution 500 µl isopropanol) and incubated for 10 min (RT) and centrifuged (12,000 g, 10 min). The pellet was washed with 75% ethanol. After a centrifugation step, the pellet was dried and dissolved in RNAse-free water. Finally, the concentration and quality of the RNA was determined with the Agilent Bioanalyser (Agilent Technologies) and stored at -80°C.

cDNA was synthesized by reverse transcription of 5 µg RNA with oligo dT18 using Superscript II reverse transcriptase (Invitrogen) according to the manufacturer's guide. In brief, 1µg of total RNA was mixed with 2 µl of random primers (pdN6 50 µM, Stratagene) and filled up to 15 µl with nuclease free water. After incubation for 5 min at 70°C and cooling for 2 min on ice, 5 µl 5x reaction buffer (Promega), 1.25 µl dNTPs (10 mM, Stratagene), 1 µl RNase inhibitor (Rnasin 40 U/µl, Promega), 1.75 µl nuclease free water and 1 µl M-MLV-RT (200 U/µl) were added. The samples were incubated for 1 h at 37°C and stored at -20°C until use.

Each sample for real-time RT-PCR analysis contained 200 ng of cDNA, SYBR Green Master Mix and 0.4 µM of each primer. The PCR amplification and real-time fluorescence detection were performed with the Opticon III instrument (MJ Research) using the QuantitectTM SYBR1 green PCR kit (Qiagen). As quantification standard defined concentrations of annexinA7 cDNA (Döring et al., 1991) were used for amplification. PCR amplification was carried out according to the manufacturer's instruction and all PCR products were amplified in a linear cycle. GAPDH mRNA was employed as an internal standard, and each gene

expression was determined by RT-PCR and normalized against WT GAPDH mRNA levels. All PCR products were amplified in a linear cycle. Data are the mean +/-SD from three samples per group of four independent experiments.

4.26 Mass spectrometry analysis

The GFP-trap beads (Chromtek) were incubated with the lysate of the AX2 cells expressing GFP-CEP161 with the lysis buffer at 4^0C for 2 hours. AX2 cell lysate incubated with the GFP beads served as the negative control. The beads were washed with the wash buffer for two times. The beads were centrifuged 1000 rpm for 2 min and the supernatant discarded. The beads were boiled in 2x SDS buffer (2% SDS and 1M Tris/HCl, pH 6.8) at 95^0C for 5 min. The supernatant was taken for liquid chromatography-electrospray ionization-tandem mass spectrometry (LC-ESI-MS/MS) 2.5 h-Gradient analysis.

4.27 Miscellaneous experiments

4.27.1 *D.discoideum* cell size

Cell size was determined using cells that had been treated with 20 mM EDTA in Soerensen phosphate buffer in order to obtain perfectly round cells. Approximately 800 cells each for AX2 and the mutants were measured.

4.27.2 Protein sequence alignment

Protein sequences of CDK5RAP2 proteins from *H. sapiens* (Q96SN8), *D. melanogaster* (P54623) and *D. discoideum* (Q54RX7) and protein sequences of MST1 proteins from *H. sapiens* (Q13043), *D. melanogaster* (Q8T0S6) and *D. discoideum* Hrk-SvkA (O61122) were retrieved from Uniprot protein database and aligned using ClustalW program with Blosum 62 matrix. The aligned sequences were processed through EsPript for representation.

5. Summary

CEP161 is a novel component of the *Dictyostelium discoideum* centrosome and is the ortholog of mammalian CDK5RAP2. Mutations in CDK5RAP2 are associated with autosomal recessive primary microcephaly (MCPH), a neurodevelopmental disorder characterized by reduced head circumference, a reduction in the size of the cerebral cortex and a mild to moderate mental retardation. Here we show that the amino acids 1-763 of the 1381 amino acids of CEP161 protein are sufficient for centrosomal targeting and centrosome association. AX2 cells over-expressing truncated and full length CEP161 proteins have defects in growth and development. Furthermore, we identified the kinase SvkA (severinkinase A) as its interaction partner which is the *D. discoideum* Hippo related kinase designated here as Hrk-svk. Hrk-svk is the direct homolog of human MST1. Both proteins co-localize at the centrosome. We further demonstrate that this interaction is also conserved in mammals. We were able to show that CDK5RAP2 interacts with MST1 and TAZ and it also down-regulates the transcript levels of TAZ in HEK293T cells. Taken together, our data on *Dictyostelium* CEP161 and human CDK5RAP2 supports the hypothesis that CDK5RAP2 as a novel regulator of Hippo signaling pathway. We propose that CDK5RAP2 mutations may lead to a decrease in the number of neurons and the subsequent reduction of brain size by regulating the hippo signaling pathway.

Zusammenfassung

CEP161, eine neue Komponente des Zentrosoms von *Dictyostelium discoideum,* ist das Ortholog des humanen CDK5RAP2. Mutationen in CDK5RAP2 verursachen MCPH (autosomal recessive primary microcephaly), eine Erkrankung des Nervensystems, die durch reduzierten Kopfumfang, eine Reduktion in der Größe der Großhirnrinde und einer leichten bis mittelschweren geistigen Behinderung gekennzeichnet ist. In unserer Arbeit haben wir gezeigt, dass die Aminosäuren 1 bis 763 der 1381 Aminosäuren von CEP161 ausreichend sind für das zentrosomale Targeting und für die Verbindung zum Zentrosom. AX2-Zellen, die verkürztes und Volllängen CEP161 über-exprimierten, hatten Wachstums- und Entwicklungsdefekte. Darüber hinaus haben wir die Proteinkinase SvkA (severinkinase A) als Interaktionspartner von CEP161 identifiziert. SvkA ist die *D. discoideum* Hippo-verwandteproteinkinase, sie hier als Hrk-svk bezeichnet und ist das direkte Homolog der humanen MST1. Beide Proteine colokalisieren am Zentrosom und wir haben gezeigt, dass diese Interaktion auch beim Menschen konserviert ist. Weiterhin konnten wir zeigen, dass CDK5RAP2 mit MST1 und TAZ interagiert und TAZ in HEK293T-Zellen transkritionell abreguliert. Zusammenfassend unterstützen unsere Daten von *Dictyostelium* CEP161 und humanem CDK5RAP2 die Hypothese, dass CDK5RAP2 ein neuer Regulator des Hippo Signalübertragungswegs ist. Wir schlagen vor, dass CDK5RAP2 Mutationen zu einer Verringerung der Anzahl der Neuronen und damit zu einer Reduktion der Größe des Gehirns durch die Regulierung des Hippo Signalübertragungswegs führen.

6. Reference

Abe, Y., M. Ohsugi, K. Haraguchi, J. Fujimoto, and T. Yamamoto. 2006. LATS2-Ajuba complex regulates gamma-tubulin recruitment to centrosomes and spindle organization during mitosis. *FEBS Lett.* 580:782–788.

Alexander, S., J. Min, and H. Alexander. 2006. Dictyostelium discoideum to human cells: Pharmacogenetic studies demonstrate a role for sphingolipids in chemoresistance. *Biochim. Biophys. Acta - Gen. Subj.* 1760:301–309.

Andersen, J.S., C.J. Wilkinson, and T. Mayor. 2003. Proteomic characterization of the human centrosome by protein correlation profiling. 426: 570-574

Artemenko, Y., P. Batsios, J. Borleis, Z. Gagnon, J. Lee, and M. Rohlfs. 2012. Tumor suppressor Hippo / MST1 kinase mediates chemotaxis by regulating spreading and adhesion. *Proc. Natl. Acad. Sci. U S A.* 109:13632-13637.

Azimzadeh, J., and W.F. Marshall. 2010. Building the centriole. *Curr. Biol.* 20.

Badano, J.L., T.M. Teslovich, and N. Katsanis. 2005. The centrosome in human genetic disease. *Nat. Rev. Genet.* 6:194–205.

Bahe, S., Y.D. Stierhof, C.J. Wilkinson, F. Leiss, and E.A. Nigg. 2005. Rootletin forms centriole-associated filaments and functions in centrosome cohesion. *J. Cell Biol.* 171:27–33.

Barr, A.R., J. V Kilmartin, and F. Gergely. 2010. CDK5RAP2 functions in centrosome to spindle pole attachment and DNA damage response. *J. Cell Biol.* 189:23–39.

Barrera, J.A., L.R. Kao, R.E. Hammer, J. Seemann, J.L. Fuchs, and T.L. Megraw. 2010. CDK5RAP2 regulates centriole engagement and cohesion in mice. *Dev. Cell.* 18:913–26.

Bettencourt-Dias, M., F. Hildebrandt, D. Pellman, G. Woods, and S.A. Godinho. 2011. Centrosomes and cilia in human disease. *Trends Genet.* 27:307–15.

Blau-Wasser, R., U. Euteneuer, H. Xiong, B. Gassen, M. Schleicher, A.A. Noegel, U. Robert, and W. Johnson. 2009. CP250, a novel acidic coiled coil protein of the Dictyostelium centrosome, affects growth, chemotaxis and the nuclear envelope. *Mol. Biol. Cell.* 20:4348–4361.

Bobinnec, Y., A. Khodjakov, L.M. Mir, C.L. Rieder, B. Eddé, and M. Bornens. 1998. Centriole disassembly in vivo and its effect on centrosome structure and function in vertebrate cells. *J. Cell Biol.* 143:1575–1589.

Bond, J., E. Roberts, K. Springell, S.B. Lizarraga, S. Lizarraga, S. Scott, J. Higgins, D.J. Hampshire, E.E. Morrison, G.F. Leal, E.O. Silva, S.M.R. Costa, D. Baralle, M. Raponi,

G. Karbani, Y. Rashid, H. Jafri, C. Bennett, P. Corry, C.A. Walsh, and C.G. Woods. 2005. A centrosomal mechanism involving CDK5RAP2 and CENPJ controls brain size. *Nat. Genet.* 37:353–355.

Bond, J., S. Scott, D.J. Hampshire, K. Springell, P. Corry, M.J. Abramowicz, G.H. Mochida, R.C.M. Hennekam, E.R. Maher, J.P. Fryns, A. Alswaid, H. Jafri, Y. Rashid, A. Mubaidin, C.A. Walsh, E. Roberts, and C.G. Woods. 2003. Protein-truncating mutations in ASPM cause variable reduction in brain size. *Am. J. Hum. Genet.* 73:1170–1177.

Bornens, M. 2012. The centrosome in cells and organisms. *Science*. 335:422–426.

Buchman, J.J., H.C. Tseng, Y. Zhou, C.L. Frank, Z. Xie, and L.H. Tsai. 2010. Cdk5rap2 interacts with pericentrin to maintain the neural progenitor pool in the developing neocortex. *Neuron*. 66:386–402.

Bullock, W.O., J.M. Fernandez, and J.M. Short. 1987. XL1-Blue: A high efficiency plasmid transforming recA Escherichia coli strain with beta-galactosidase selection. *Biotechniques*. 5:376–379.

Calvo-Garrido, J., S. Carilla-Latorre, Y. Kubohara, N. Santos-Rodrigo, A. Mesquita, T. Soldati, P. Golstein, and R. Escalante. 2010. Autophagy in Dictyostelium: genes and pathways, cell death and infection. *Autophagy*. 6:686–701.

Cao, X., S.L. Pfaff, and F.H. Gage. 2008. YAP regulates neural progenitor cell number via the TEA domain transcription factor. *Genes Dev.* 22:3320–3334.

Carvalho-Santos, Z., J. Azimzadeh, J.B. Pereira-Leal, and M. Bettencourt-Dias. 2011. Evolution: Tracing the origins of centrioles, cilia, and flagella. *J. Cell Biol.* 194:165–175.

Claviez, M., K. Pagh, H. Maruta, W. Baltes, P. Fisher, and G. Gerisch. 1982. Electron microscopic mapping of monoclonal antibodies on the tail region of Dictyostelium myosin. *EMBO J.* 1:1017–1022.

Conduit, P.T., and J.W. Raff. 2010. Cnn dynamics drive centrosome size asymmetry to ensure daughter centriole retention in Drosophila neuroblasts. *Curr. Biol.* 20:2187–2192.

De Cristofaro, T., T. Di Palma, A. Ferraro, A. Corrado, V. Lucci, R. Franco, A. Fusco, and M. Zannini. 2011. TAZ/WWTR1 is overexpressed in papillary thyroid carcinoma. *Eur. J. Cancer*. 47:926–933.

Darvish, H., S. Esmaeeli-Nieh, G.B. Monajemi, M. Mohseni, S. Ghasemi-Firouzabadi, S.S. Abedini, I. Bahman, P. Jamali, S. Azimi, F. Mojahedi, A. Dehghan, Y. Shafeghati, A. Jankhah, M. Falah, M.J. Soltani Banavandi, M. Ghani, M. Ghani-Kakhi, M. Garshasbi, F. Rakhshani, A. Naghavi, A. Tzschach, H. Neitzel, H.H. Ropers, A.W. Kuss, F. Behjati, K. Kahrizi, and H. Najmabadi. 2010. A clinical and molecular genetic study of 112 Iranian families with primary microcephaly. *J. Med. Genet.* 47:823–828.

Delattre, M., C. Canard, and P. Gönczy. 2006. Sequential Protein Recruitment in C. elegans Centriole Formation. *Curr. Biol.* 16:1844–1849.

Dong, J., G. Feldmann, J. Huang, S. Wu, N. Zhang, S.A.Comerford, M.F. Gayyed, R. A Anders, A. Maitra, and D. Pan. 2007. Elucidation of a universal size-control mechanism in Drosophila and mammals. *Cell*. 130:1120–1133.

Döring, V., M. Schleicher, and A.A. Noegel. 1991. Dictyostelium annexin VII (synexin). cDNA sequence and isolation of a gene disruption mutant. *J. Biol. Chem.* 266:17509–17515.

Doxsey, S., D. McCollum, and W. Theurkauf. 2005. Centrosomes in cellular regulation. *Annu. Rev. Cell Dev. Biol.* 21:411–34.

Eichinger, L., J.A. Pachebat, G. Glöckner, M.A. Rajandream, R. Sucgang, M. Berriman, J. Song, R. Olsen, K. Szafranski, Q. Xu, B. Tunggal, S. Kummerfeld, M. Madera, B.A. Konfortov, F. Rivero, A.T. Bankier, R. Lehmann, N. Hamlin, R. Davies, P. Gaudet, P. Fey, K. Pilcher, G. Chen, D. Saunders, E. Sodergren, P. Davis, A. Kerhornou, X. Nie, N. Hall, C. Anjard, L. Hemphill, N. Bason, P. Farbrother, B. Desany, E. Just, T. Morio, R. Rost, C. Churcher, J. Cooper, S. Haydock, N. van Driessche, A. Cronin, I. Goodhead, D. Muzny, T. Mourier, A. Pain, M. Lu, D. Harper, R. Lindsay, H. Hauser, K. James, M. Quiles, M. Madan Babu, T. Saito, C. Buchrieser, A. Wardroper, M. Felder, M. Thangavelu, D. Johnson, A. Knights, H. Loulseged, K. Mungall, K. Oliver, C. Price, M.A. Quail, H. Urushihara, J. Hernandez, E. Rabbinowitsch, D. Steffen, M. Sanders, J. Ma, Y. Kohara, S. Sharp, M. Simmonds, S. Spiegler, A. Tivey, S. Sugano, B. White, D. Walker, J. Woodward, T. Winckler, Y. Tanaka, G. Shaulsky, M. Schleicher, G. Weinstock, A. Rosenthal, E.C. Cox, R.L. Chisholm, R. Gibbs, W.F. Loomis, M. Platzer, R.R. Kay, J. Williams, P.H. Dear, A.A. Noegel, B. Barrell, and A. Kuspa. 2005. The genome of the social amoeba Dictyostelium discoideum. *Nature*. 435:43–57.

Faix, J., G. Gerisch, and a a Noegel. 1990. Constitutive overexpression of the contact site A glycoprotein enables growth-phase cells of Dictyostelium discoideum to aggregate. *EMBO J.* 9:2709–2716.

Faix, J., L. Kreppel, G. Shaulsky, M. Schleicher, and A.R. Kimmel. 2004. A rapid and efficient method to generate multiple gene disruptions in Dictyostelium discoideum using a single selectable marker and the Cre-loxP system. *Nucleic Acids Res.* 32:e143–150.

Fish, J.L., Y. Kosodo, W. Enard, S. Pääbo, and W.B. Huttner. 2006. Aspm specifically maintains symmetric proliferative divisions of neuroepithelial cells. *Proc. Natl. Acad. Sci. U. S. A.* 103:10438–10443.

Fong, K.W., Y.K. Choi, J.B. Rattner, and R.Z. Qi. 2008. CDK5RAP2 is a pericentriolar protein that functions in centrosomal attachment of the gamma-tubulin ring complex. *Mol. Biol. Cell*. 19:115–125.

Fong, K.W., S.Y. Hau, Y.S. Kho, Y. Jia, L. He, and R.Z. Qi. 2009. Interaction of CDK5RAP2 with EB1 to track growing microtubule tips and to regulate microtubule dynamics. *Mol. Biol. Cell*. 20:3660–3670.

Fry, A.M., P. Meraldi, and E.A. Nigg. 1998. A centrosomal function for the human Nek2 protein kinase, a member of the NIMA family of cell cycle regulators. *EMBO J.* 17:470–481.

George, N.M., C.E. Day, B.P. Boerner, R.L. Johnson, and N.E. Sarvetnick. 2012. Hippo signaling regulates pancreas development through inactivation of Yap. *Mol. Cell. Biol.* 32:5116-5128

Giusti, C., E. Tresse, M.F. Luciani, and P. Golstein. 2009. Autophagic cell death: Analysis in Dictyostelium. *Biochim. Biophys. Acta - Mol. Cell Res.* 1793:1422–1431.

Gräf, R., C. Daunderer, and I. Schulz. 2004. Molecular and functional analysis of the dictyostelium centrosome. *Int. Rev. Cytol.* 241:155–202.

Graser, S., Y.-D. Stierhof, and E.A. Nigg. 2007. Cep68 and Cep215 (Cdk5rap2) are required for centrosome cohesion. *J. Cell Sci.* 120:4321–4331.

Guo, C., S. Tommasi, L. Liu, J.K. Yee, R. Dammann, and G. Pfeifer. 2007. RASSF1A Is Part of a Complex Similar to the Drosophila Hippo/Salvador/Lats Tumor-Suppressor Network. *Curr. Biol.* 17:700–705.

Habedanck, R., Y.-D. Stierhof, C.J. Wilkinson, and E.A. Nigg. 2005. The Polo kinase Plk4 functions in centriole duplication. *Nat. Cell Biol.* 7:1140–1146.

Halder, G., and R.L. Johnson. 2011. Hippo signaling: growth control and beyond. *Development*. 138:9–22.

Harper, J.W., G.R. Adami, N. Wei, K. Keyomarsi, and S.J. Elledge. 1993. The p21 Cdk-interacting protein Cip1 is a potent inhibitor of G1 cyclin-dependent kinases. *Cell*. 75:805–816.

Harvey, K.F., C.M. Pfleger, and I.K. Hariharan. 2003. The Drosophila Mst ortholog, hippo, restricts growth and cell proliferation and promotes apoptosis. *Cell*. 114:457–467.

Hassan, M.J., M. Khurshid, Z. Azeem, P. John, G. Ali, M.S. Chishti, and W. Ahmad. 2007. Previously described sequence variant in CDK5RAP2 gene in a Pakistani family with autosomal recessive primary microcephaly. *BMC Med. Genet.* 8:58–64.

Heallen, T., M. Zhang, J. Wang, M. Bonilla-Claudio, E. Klysik, R.L. Johnson, and J.F. Martin. 2011. Hippo pathway inhibits Wnt signaling to restrain cardiomyocyte proliferation and heart size. *Science*. 332:458–461.

Hergovich, A., R.S. Kohler, D. Schmitz, A. Vichalkovski, H. Cornils, and B.A. Hemmings. 2009. The MST1 and hMOB1 Tumor Suppressors Control Human Centrosome Duplication by Regulating NDR Kinase Phosphorylation. *Curr. Biol.* 19:1692–1702.

Hong, J.H., E.S. Hwang, M.T. McManus, A. Amsterdam, Y. Tian, R. Kalmukova, E. Mueller, T. Benjamin, B.M. Spiegelman, P. a Sharp, N. Hopkins, and M.B. Yaffe. 2005. TAZ, a transcriptional modulator of mesenchymal stem cell differentiation. *Science*. 309:1074–1078.

Huang, J., S. Wu, J. Barrera, K. Matthews, and D. Pan. 2005. The Hippo signaling pathway coordinately regulates cell proliferation and apoptosis by inactivating Yorkie, the Drosophila Homolog of YAP. *Cell*. 122:421–434.

Hung, L.Y., C.J. Tang, and T.K. Tang. 2000. Protein 4.1 R-135 interacts with a novel centrosomal protein (CPAP) which is associated with the gamma-tubulin complex. *Mol. Cell. Biol.* 20:7813–7825.

Issa, L., N. Kraemer, C.H. Rickert, M. Sifringer, O. Ninnemann, G. Stoltenburg-Didinger, and A.M. Kaindl. 2013a. CDK5RAP2 expression during murine and human brain development correlates with pathology in primary autosomal recessive microcephaly. *Cereb. Cortex*. 23:2245–2260.

Issa, L., K. Mueller, K. Seufert, N. Kraemer, H. Rosenkotter, O. Ninnemann, M. Buob, A.M. Kaindl, and D.J. Morris-Rosendahl. 2013b. Clinical and cellular features in patients with primary autosomal recessive microcephaly and a novel CDK5RAP2 mutation. *Orphanet J. Rare Dis.* 8:59–73.

Janetopoulos, C., and R.A. Firtel. 2008. Directional sensing during chemotaxis. *FEBS Lett.* 582:2075–2085.

Johnston, G.C., J.A. Prendergast, and R.A. Singer. 1991. The Saccharomyces cerevisiae MYO2 gene encodes an essential myosin for vectorial transport of vesicles. *J. Cell Biol.* 113:539–551.

Kaindl, A.M. 2014. Autosomal recessive primary microcephalies (MCPH). *Eur. J. Paediatr. Neurol.* 18:547–548.

Kango-Singh, M. 2002. Shar-pei mediates cell proliferation arrest during imaginal disc growth in Drosophila. *Development*. 129:5719–5730.

Keryer, G., B. Di Fiore, C. Celati, K.F. Lechtreck, M. Mogensen, A. Delouve, P. Lavia, M. Bornens, and A. Tassin. 2003. Part of Ran is associated with AKAP450 at the

centrosome : Involvement in microtubule-organizing Aactivity. *Mol. Biol. Cell.* 14:4260–4271.

Khaire, N., R. Müller, R. Blau-Wasser, L. Eichinger, M. Schleicher, M. Rief, T.A. Holak, and A.A. Noegel. 2007. Filamin-regulated F-actin assembly is essential for morphogenesis and controls phototaxis in Dictyostelium. *J. Biol. Chem.* 282:1948–1955.

Khurana, B., T. Khurana, N. Khaire, and A.A. Noegel. 2002. Functions of LIM proteins in cell polarity and chemotactic motility. *EMBO J.* 21:5331–5342.

Kitagawa, D., I. Vakonakis, N. Olieric, M. Hilbert, D. Keller, V. Olieric, M. Bortfeld, M.C. Erat, I. Flöckiger, P. Gönczy, and M.O. Steinmetz. 2011. Structural basis of the 9-fold symmetry of centrioles. *Cell.* 144:364–375.

Kobayashi, T., and B.D. Dynlacht. 2011. Regulating the transition from centriole to basal body. *J. Cell Biol.* 193:435–444.

Kraemer, N., L. Issa, S.C.R. Hauck, S. Mani, O. Ninnemann, and A.M. Kaindl. 2011. What's the hype about CDK5RAP2? *Cell. Mol. Life Sci.* 68:1719–1736. d

Lancaster, M. A, M. Renner, C.A. Martin, D. Wenzel, L.S. Bicknell, M.E. Hurles, T. Homfray, J.M. Penninger, A.P. Jackson, and J. A. Knoblich. 2013. Cerebral organoids model human brain development and microcephaly. *Nature.* 501:373–379.

Lavado, A., Y. He, J. Paré, G. Neale, E.N. Olson, M. Giovannini, and X. Cao. 2013. Tumor suppressor Nf2 limits expansion of the neural progenitor pool by inhibiting Yap/Taz transcriptional coactivators. *Development.* 140:3323–34.

Lee, K.P., J.H. Lee, T.S. Kim, T.H. Kim, H.D. Park, J.S. Byun, M.C. Kim, W.I. Jeong, D.F. Calvisi, J.M. Kim, and D.S. Lim. 2010. The Hippo-Salvador pathway restrains hepatic oval cell proliferation, liver size, and liver tumorigenesis. *Proc. Natl. Acad. Sci. U. S. A.* 107:8248–8253.

Lee, S., and K. Rhee. 2010. CEP215 is involved in the dynein-dependent accumulation of pericentriolar matrix proteins for spindle pole formation. *Cell Cycle.* 9:774–783.

Lei, Q.Y., H. Zhang, B. Zhao, Z.Y. Zha, F. Bai, X.H. Pei, S. Zhao, Y. Xiong, and K.L. Guan. 2008. TAZ promotes cell proliferation and epithelial-mesenchymal transition and is inhibited by the hippo pathway. *Mol. Cell. Biol.* 28:2426–36.

Leidel, S., M. Delattre, L. Cerutti, K. Baumer, and P. Gönczy. 2005. SAS-6 defines a protein family required for centrosome duplication in C. elegans and in human cells. *Nat. Cell Biol.* 7:115–125.

Leidel, S., and P. Gönczy. 2003. SAS-4 is essential for centrosome duplication in C. elegans and is recruited to daughter centrioles once per cell cycle. *Dev. Cell.* 4:431–439.

Lizarraga, S.B., S.P. Margossian, M.H. Harris, D.R. Campagna, A.P. Han, S. Blevins, R. Mudbhary, J.E. Barker, C.A. Walsh, and M.D. Fleming. 2010. Cdk5rap2 regulates centrosome function and chromosome segregation in neuronal progenitors. *Development*. 137:1907–1917.

Lu, L., Y. Li, S.M. Kim, W. Bossuyt, P. Liu, Q. Qiu, Y. Wang, G. Halder, M.J. Finegold, J.-S. Lee, and R.L. Johnson. 2010. Hippo signaling is a potent in vivo growth and tumor suppressor pathway in the mammalian liver. *Proc. Natl. Acad. Sci. U. S. A.* 107:1437–1442.

Malchow, D., B. Nägele, H. Schwarz, and G. Gerisch. 1972. Membrane-bound cyclic AMP phosphodiesterase in chemotactically responding cells of Dictyostelium discoideum. *Eur. J. Biochem.* 28:136–142.

Mardin, B.R., C. Lange, J.E. Baxter, T. Hardy, S.R. Scholz, A.M. Fry, and E. Schiebel. 2010. Components of the Hippo pathway cooperate with Nek2 kinase to regulate centrosome disjunction. *Nat. Cell Biol.* 12:1166–1176.

Mayor, T., U. Hacker, Y.D. Stierhof, and E.A. Nigg. 2002. The mechanism regulating the dissociation of the centrosomal protein C-Nap1 from mitotic spindle poles. *J. Cell Sci.* 115:3275–3284.

Megraw, T.L., J.T. Sharkey, and R.S. Nowakowski. 2011. Cdk5rap2 exposes the centrosomal root of microcephaly syndromes. *Trends Cell Biol.* 21:470–480.

Mori, M., R. Triboulet, M. Mohseni, K. Schlegelmilch, K. Shrestha, F.D. Camargo, and R.I. Gregory. 2014. Hippo signaling regulates microprocessor and links cell-density-dependent miRNA biogenesis to cancer. *Cell*. 156:893–906.

Müller, R., C. Herr, S.K. Sukumaran, N.N. Omosigho, M. Plomann, T.Y. Riyahi, M. Stumpf, K. Swaminathan, M. Tsangarides, K. Yiannakou, R. Blau-Wasser, C. Gallinger, M. Schleicher, W. Kolanus, and A.A. Noegel. 2013. The cytohesin paralog Sec7 of Dictyostelium discoideum is required for phagocytosis and cell motility. *Cell Commun. Signal.* 11:54–70.

Neitzel, H., L.M. Neumann, D. Schindler, A. Wirges, H. Tönnies, M. Trimborn, A. Krebsova, R. Richter, and K. Sperling. 2002. Premature chromosome condensation in humans associated with microcephaly and mental retardation: a novel autosomal recessive condition. 70.

Nigg, E. A, L. Cajánek, and C. Arquint. 2014. The centrosome duplication cycle in health and disease. *FEBS Lett.*

Nigg, E.A., and J.W. Raff. 2009. Centrioles, Centrosomes, and Cilia in Health and Disease. *Cell*. 139:663–678.

Nishioka, N., K. Inoue, K. Adachi, H. Kiyonari, M. Ota, A. Ralston, N. Yabuta, S. Hirahara, R.O. Stephenson, N. Ogonuki, R. Makita, H. Kurihara, E.M. Morin-Kensicki, H. Nojima, J. Rossant, K. Nakao, H. Niwa, and H. Sasaki. 2009. The Hippo signaling pathwaycomponents Lats and Yap pattern Tead4 activity to distinguish mouse trophectoderm from inner cell mass. *Dev. Cell*. 16:398–410.

Novorol, C., J. Burkhardt, K.J. Wood, A. Iqbal, C. Roque, N. Coutts, A.D. Almeida, J. He, C.J. Wilkinson, and W.A Harris. 2013. Microcephaly models in the developing zebrafish retinal neuroepithelium point to an underlying defect in metaphase progression. *Open Biol.* 3:130065.

Pagnamenta, A.T., J.E. Murray, G. Yoon, E. Sadighi Akha, V. Harrison, L.S. Bicknell, K. Ajilogba, H. Stewart, U. Kini, J.C. Taylor, D. a Keays, A.P. Jackson, and S.J.L. Knight. 2012b. A novel nonsense CDK5RAP2 mutation in a Somali child with primary microcephaly and sensorineural hearing loss. *Am. J. Med. Genet. A*. 158A:2577–82.

Pantalacci, S., N. Tapon, and P. Léopold. 2003. The Salvador partner Hippo promotes apoptosis and cell-cycle exit in Drosophila. *Nat. Cell Biol.* 5:921–7.

Pelletier, L., E. O'Toole, A. Schwager, A.A. Hyman, and T. Müller-Reichert. 2006. Centriole assembly in Caenorhabditis elegans. *Nature*. 444:619–623.

Piel, M., P. Meyer, A. Khodjakov, C.L. Rieder, and M. Bornens. 2000. The respective contributions of the mother and daughter centrioles to centrosome activity and behavior in vertebrate cells. *J. Cell Biol.* 149:317–330.

Pulvers, J.N., J. Bryk, J.L. Fish, M. Wilsch-Bräuninger, Y. Arai, D. Schreier, R. Naumann, J. Helppi, B. Habermann, J. Vogt, R. Nitsch, A. Tóth, W. Enard, S. Pääbo, and W.B. Huttner. 2010. Mutations in mouse Aspm (abnormal spindle-like microcephaly associated) cause not only microcephaly but also major defects in the germline. *Proc. Natl. Acad. Sci. U. S. A.* 107:16595–16600.

Raper, B.K.B. 1935. *D. discoideum*, a new species of slime mould from decaying forest leaves. *J. Agr. Res.* 50:135-147

Reinders, Y., I. Schulz, R. Gra, and A. Sickmann. 2006. Identification of Novel Centrosomal Proteins in Dictyostelium discoideum by Comparative Proteomic Approaches *J. Prot. Res*. 5:589–598.

Rohlfs, M., R. Arasada, P. Batsios, J. Janzen, and M. Schleicher. 2007. The Ste20-like kinase SvkA of Dictyostelium discoideum is essential for late stages of cytokinesis. *J. Cell Sci.* 120:4345–4354.

Song, H., K.K. Mak, L. Topol, K. Yun, J. Hu, L. Garrett, Y. Chen, O. Park, J. Chang, R.M. Simpson, C.Y. Wang, B. Gao, J. Jiang, and Y. Yang. 2010. Mammalian Mst1 and Mst2

kinases play essential roles in organ size control and tumor suppression. *Proc. Natl. Acad. Sci. U. S. A.* 107:1431–1436.

Steinert, M., and K. Heuner. 2005. Dictyostelium as host model for pathogenesis. *Cell. Microbiol.* 7:307–314.

Strmecki, L., D.M. Greene, and C.J. Pears. 2005. Developmental decisions in Dictyostelium discoideum. *Dev. Biol.* 284:25–36.

Strnad, P., and P. Gönczy. 2008. Mechanisms of procentriole formation. *Trends Cell Biol.* 18:389–396. doi:10.1016/j.tcb.2008.06.004.

Studier, F.W., and B.A. Moffatt. 1986. Use of bacteriophage T7 RNA polymerase to direct selective high-level expression of cloned genes. *J. Mol. Biol.* 189:113–130.

Tan, C. A, S. Topper, C. Ward Melver, J. Stein, A. Reeder, K. Arndt, and S. Das. 2014. The first case of CDK5RAP2-related primary microcephaly in a non-consanguineous patient identified by next generation sequencing. *Brain Dev.* 36:351–355

Tapon, N., K.F. Harvey, D.W. Bell, D.C.R. Wahrer, T. a Schiripo, D. a Haber, and I.K. Hariharan. 2002. salvador Promotes both cell cycle exit and apoptosis in Drosophila and is mutated in human cancer cell lines. *Cell.* 110:467–478.

Tian, W., J. Yu, D.R. Tomchick, D. Pan, and X. Luo. 2010. Structural and functional analysis of the YAP-binding domain of human TEAD2. *Proc. Natl. Acad. Sci. U. S. A.* 107:7293–7298.

Torija, P., A. Robles, and R. Escalante. 2006. Optimization of a large-scale gene disruption protocol in Dictyostelium and analysis of conserved genes of unknown function. *BMC Microbiol.* 6:75–81.

Udan, R.S., M. Kango-Singh, R. Nolo, C. Tao, and G. Halder. 2003. Hippo promotes proliferation arrest and apoptosis in the Salvador/Warts pathway. *Nat. Cell Biol.* 5:914–920.

Ueda, M., M. Schliwa, and U. Euteneuer. 1999. Unusual centrosome cycle in Dictyostelium: correlation of dynamic behavior and structural changes. *Mol. Biol. Cell*. 10:151–160.

Van Haastert, P.J.M., and D.M. Veltman. 2007. Chemotaxis: navigating by multiple signaling pathways. *Sci. STKE*. 2007:pe40–42.

Wakefield, J.G., S. Bonaccorsi, and M. Gatti. 2001. The drosophila protein asp is involved in microtubule organization during spindle formation and cytokinesis. *J. Cell Biol.* 153:637–648.

Wallraff, E., and H.G. Wallraff. 1997. Migration and bidirectional phototaxis in Dictyostelium discoideum slugs lacking the actin cross-linking 120 kDa gelation factor. *J. Exp. Biol.* 200:3213–3220.

Wang, X., Y.P. Ching, W.H. Lam, Z. Qi, M. Zhang, and J.H. Wang. 2000. Identification of a common protein association region in the neuronal Cdk5 activator. *J. Biol. Chem.* 275:31763–31769.

Wang, Z., T. Wu, L. Shi, L. Zhang, W. Zheng, J.Y. Qu, R. Niu, and R.Z. Qi. 2010. Conserved motif of CDK5RAP2 mediates its localization to centrosomes and the Golgi complex. *J. Biol. Chem.* 285:22658–22665.

Willard, S.S., and P.N. Devreotes. 2006. Signaling pathways mediating chemotaxis in the social amoeba, Dictyostelium discoideum. *Eur. J. Cell Biol.* 85:897–904.

Wilmeth, L.J., S. Shrestha, G. Montaño, J. Rashe, and C.B. Shuster. 2010. Mutual dependence of Mob1 and the chromosomal passenger complex for localization during mitosis. *Mol. Biol. Cell.* 21:380–392.

Xiong, H., F. Rivero, U. Euteneuer, S. Mondal, S. Mana-Capelli, D. Larochelle, A. Vogel, B. Gassen, and A.A. Noegel. 2008. Dictyostelium Sun-1 connects the centrosome to chromatin and ensures genome stability. *Traffic.* 9:708–24.

Zhang, H., C.Y. Liu, Z.Y. Zha, B. Zhao, J. Yao, S. Zhao, Y. Xiong, Q.Y. Lei, and K.L. Guan. 2009a. TEAD transcription factors mediate the function of TAZ in cell growth and epithelial-mesenchymal transition. *J. Biol. Chem.* 284:13355–13362.

Zhang, X., D. Liu, S. Lv, H. Wang, X. Zhong, B. Liu, B. Wang, J. Liao, J. Li, G.P. Pfeifer, and X. Xu. 2009b. CDK5RAP2 is required for spindle checkpoint function. *Cell Cycle.* 8:1206–1216.

Zhao, B., L. Li, and K.L. Guan. 2010. Hippo signaling at a glance. *J. Cell Sci.* 123:4001–4006.

Zhao, B., X. Wei, W. Li, R.S. Udan, Q. Yang, J. Kim, J. Xie, T. Ikenoue, J. Yu, L. Li, P. Zheng, K. Ye, A. Chinnaiyan, G. Halder, Z.C. Lai, and K.L. Guan. 2007. Inactivation of YAP oncoprotein by the Hippo pathway is involved in cell contact inhibition and tissue growth control. *Genes Dev.* 21:2747–2761.

Zhou, D., C. Conrad, F. Xia, J.S. Park, B. Payer, Y. Yin, G.Y. Lauwers, W. Thasler, J.T. Lee, J. Avruch, and N. Bardeesy. 2009. Mst1 and Mst2 maintain hepatocyte quiescence and suppress hepatocellular carcinoma development through inactivation of the Yap1 Oncogene. *Cancer Cell.* 16:425–438.

7. Erklärung

Ich versichere, dass ich die von mir vorgelegte Dissertation selbständig angefertigt, die benutzten Quellen und Hilfsmittel vollständig angegeben und die Stellen der Arbeit- einschließlich Tabellen und Abbildungen-, die anderen Werke im Wortlaut oder dem Sinn nach entnommen sind, in jedem Einzelfall als Entlehnung kenntlich gemacht habe; dass diese Dissertation noch keiner anderen Fakultät oder Universität zur Prüfung vorgelegen hat; dass sie- abgesehen von unten angegebenen beantragten Teilpublikationen- noch nicht veröffentlicht ist, sowie, dass ich eine Veröffentlichung vor Abschluss des Promotionsverfahrens nicht vornehmen werde. Die Bestimmungen dieser Promotionsordnung sind mir bekannt. Die von mir vorgelegte Dissertation ist von Prof. Dr. Angelika A. Noegel betreut worden.

Köln, den

Salil Kalarikkal Sukumaran

8. Curriculum vitae

Personal Data

Name:	Salil Kalarikkal Sukumaran
Date of birth:	23.05.1982
Place of birth:	Kerala , India
Sex:	männlich
Nationality:	India
Address:	Luxemburger-Str. 426, 50937 Köln
E-Mail Address:	**salilkalarikkal@gmail.com**

Educational Background

2011 to present	Doctoral studies Institut for Biochemistry I Medical Faculty University of Cologne
June 2007 – Dec 2007	Post M.Sc in Plant Genetic Engineering, Madurai Kamaraj University, India
June 2002 – April 2004	Master of Science in Industrial Biotechnology, Bharathiar University, India
June 1999 – April 2002	Bachelor of Science in Zoology, Calicut University, India

Languages Known	Englisch : IELTS grade 7.5/10 Malayalam : Native speaker

Fellowship and Grants

Jan 2011 – Sept 2013	CECAD scholarship for doctoral studies, University of Cologne
June 2010 – Dec 2010	Fellowship from IGS-DHD graduate school, University of Cologne

Publication

Müller R, Herr C, **Sukumaran S**, Omosigho N, Plomann M, Riyahi T, Stumpf M, Swaminathan K, Tsangarides M, Yiannakou K, Blau-Wasser R, Gallinger C, Schleicher M, Kolanus W and Noegel A. 2013. The cytohesin paralog Sec7 of Dictyostelium discoideum is required for phagocytosis and cell motility. *Cell communication and signaling*. 11:54-70.

Lebenslauf

Persönliche Daten

Name:	Salil Kalarikkal Sukumaran
Geburtsdatum:	23.05.1982
Geburtsort:	Kerala , India
Geschlecht:	männlich
Staatsangehörigkeit:	India
Anschrift:	Luxemburger-Str. 426, 50937 Köln
E-Mail Adresse:	**salilkalarikkal@gmail.com**

Schulische Ausbildung/Studium

2011 bis jetzt	Doktorand/Wissenschaftlicher Mitarbeiter Institut für Biochemie I Medizinische Fakultät Universität zu Köln
June 2007 – Dec 2007	Post M.Sc in Plant Genetic Engineering, Madurai Kamaraj University, India
June 2002 – April 2004	Master of Science in Industrial Biotechnology, Bharathiar University, India
June 1999 – April 2002	Bachelor of Science in Zoology, Calicut University, India

Sprachkenntnisse	Englisch : IELTS grade 7.5/10 Malayalam : Muttersprache

Fellowship und Zuschüsse

Jan 2011 – Sept 2013	CECAD scholarship for doctoral studies, Universität zu Köln
June 2010 – Dec 2010	IGS-DHD fellowship, Universität zu Köln

Publikation

Müller R, Herr C, **Sukumaran S**, Omosigho N, Plomann M, Riyahi T, Stumpf M, Swaminathan K, Tsangarides M, Yiannakou K, Blau-Wasser R, Gallinger C, Schleicher M, Kolanus W and Noegel A. 2013. The cytohesin paralog Sec7 of Dictyostelium discoideum is required for phagocytosis and cell motility. *Cell communication and signaling*. 11:54-70.